Copyright Warning & Restrictions

The copyright law of the United States (Title 17, United States Code) governs the making of photocopies or other reproductions of copyrighted material.

Under certain conditions specified in the law, libraries and archives are authorized to furnish a photocopy or other reproduction. One of these specified conditions is that the photocopy or reproduction is not to be "used for any purpose other than private study, scholarship, or research." If a, user makes a request for, or later uses, a photocopy or reproduction for purposes in excess of "fair use" that user may be liable for copyright infringement,

This institution reserves the right to refuse to accept a copying order if, in its judgment, fulfillment of the order would involve violation of copyright law.

Please Note: The author retains the copyright while the New Jersey Institute of Technology reserves the right to distribute this thesis or dissertation

Printing note: If you do not wish to print this page, then select "Pages from: first page # to: last page #" on the print dialog screen

NJIT New Jersey's Science & Technology University

The Van Houten library has removed some of the personal information and all signatures from the approval page and biographical sketches of theses and dissertations in order to protect the identity of NJIT graduates and faculty.

ABSTRACT

HYDRODYNAMIC EFFECTS OF AN ARCH-SHAPED FIBER OPTIC PROBE IN A DISSOLUTION TESTING APPARATUS 2

by

Yiran Zhang

Dissolution testing is widely used in the pharmaceutical industry to evaluate newly developed drug formulations and as a quality control method to insure that solid dosage forms have consistent dissolution property. Typically, samples are manually drawn from the dissolution vessel prior to analysis. An approach to overcome the limitations of manual sampling consists in the use of sampling probes, such as fiber optic probes, permanently inserted in the dissolution medium and continually sampling the drug concentration in it as the solid dosage form dissolves. Despite their advantages, permanently inserted fiber optic probes can alter the normal fluid flow within the vessel and produce different dissolution testing results.

In this study, the hydrodynamic effects introduced by an arch-shaped fiber optic probe in a USP Dissolution Testing Apparatus 2 are studied by: (1) conducting dissolution tests, with and without the probe, using Prednisone tablets fixed at nine different locations at the bottom of the vessel and comparing the dissolution profiles obtained using statistical tools; and (2) experimentally determining the velocity profiles in the vessel, with and without the probe, using Particle Image Velocimetry (PIV) and quantifying changes in the flow velocities on selected horizontal iso-surfaces.

The results show that the arch shaped fiber optic probe does have a baffling effect on the hydrodynamics in the dissolution vessel. This effect results in changes in the velocities in the fluid flow, and therefore in changes in the dissolution rate of the tablets undergoing testing. The baffle effect is observed mainly in the region where the probe is

inserted. However, this perturbation is also found to reach the region below the impeller and to change the velocity profile there, resulting in differences in dissolution profiles when the tablets are fixed at positions that are downstream of the probe and within the low velocity region below the impeller.

On the other hand, the hydrodynamic effect generated by the probe does not appear to be particularly strong. In most dissolution testing runs, the changes in dissolution profile are not large enough to fail the tests, according to the FDA criteria (f_1 and f_2 values). The PIV measurements additionally show that the baffle effect is not strong enough to break the overall flow pattern, or to affect the region around the impeller, which is dominated by the main flow generated by the impeller.

It can be concluded that the hydrodynamic effects generated by the arch-shaped fiber optic probe are real and observable, resulting in slightly modification of the fluid flow in the dissolution vessel and therefore in detectable differences in the dissolution profiles. However, these effects are limited and do not typically lead to dissolution testing failures.

HYDRODYNAMIC EFFECTS OF AN ARCH-SHAPED FIBER OPTIC PROBE IN A DISSOLUTION TESTING APPARATUS 2

by
Yiran Zhang

A Thesis
Submitted to the Faculty of
New Jersey Institute of Technology
in Partial Fulfillment of the Requirements for the Degree of
Master of Science in Pharmaceutical Engineering

Otto H. York Department of Chemical, Biological and Pharmaceutical Engineering

May 2012

APPROVAL PAGE

HYDRODYNAMIC EFFECTS OF AN ARCH-SHAPED FIBER OPTIC PROBE IN A DISSOLUTION TESTING APPARATUS 2

Yiran Zhang

Dr. Piero M. Armenante, Thesis Advisor — Date
Distinguished Professor of Chemical Engineering, NJIT

Dr. Norman Loney, Committee Member — Date
Professor of Chemical Engineering, NJIT

Mr. Gerard Bredael, Committee Member — Date
Associate Principal Scientist, Merck & Co., Inc.

BIOGRAPHICAL SKETCH

Author: Yiran Zhang

Degree: Master of Science

Date: May 2012

Undergraduate and Graduate Education:

- Master of Science in Pharmaceutical Engineering,
  New Jersey Institute of Technology, Newark, NJ, 2012

- Bachelor of Engineering in Pharmaceutical Engineering,
  Southeast University, Nanjing, P. R. China, 2010

Major: Pharmaceutical Engineering

This thesis is dedicated to my parents 陆敏 and 张钢平 who have been my constant source of inspiration. They give me the drive and discipline to tackle any task with enthusiasm and determination.

ACKNOWLEDGMENT

During the eight months I have worked for this thesis, I have been helped tremendously by a great number of people. It is a pleasure to convey my gratitude to them all in my humble acknowledgment.

In the first place, I would like to record my gratitude to Dr. Piero Armenante for his consistent guidance throughout this research work as well as encouragement and motivation. This thesis would not be possible without his immense knowledge and enthusiasm. I also gratefully acknowledge Dr. Norman Loney and Mr. Gerard Bredael for participating in my committee, and I am also very thankful for their time, considerations and helps.

I would also like to thank Merck & Co., Inc for sponsoring this research project.

My sincere thanks to Mr. George H. Barnes and Mr. Shawn W. Yetman for their tech support, and my warm thanks to Dr. Shilan Motamedvaziri, Ms. Shruti Parekh, and Mr. Nonjaros Chomcharn for their kind support and guidance for my project. This work would not exist without them teaching me the techniques used in the research in the first place.

Finally, I would like to express my deepest gratitude towards my parents Min Lu and Gangping Zhang, and my beloved one Ying Feng for their enormous moral support. I am also thankful to all my friends who were important for the successful completion of my thesis, especially to my friend and roommate Yichun Ma for all the rides to the lab he offered, as well as expressing my apology that I could not mention them all personally one by one.

TABLE OF CONTENTS

Chapter	Page
1 INTRODUCTION	1
1.1 Background	1
1.2 Objectives of This Work	4
2 EXPERIMENTAL APPARATUS, MATERIALS AND METHODS	6
2.1 Dissolution Tests	6
2.1.1 Dissolution Apparatus	6
2.1.2 Dissolution Test Materials	14
2.1.3 Dissolution Test Method	15
2.1.4 Dissolution Test Data Analysis	18
2.2 Particle Image Velocimetry (PIV)	21
2.2.1 PIV Apparatus	21
2.2.2 PIV Method	23
3 RESULTS	28
3.1 Results of Dissolution Tests	28
3.1.1 Calibration Results for Prednisone Tablets	28
3.1.2 Dissolution Profiles of Centrally Located (Position 1) Tablets	30
3.1.3 Dissolution Profiles of 10 °off-Center Located (Positions 2, 3, 4, 5) Tablets	32
3.1.4 Dissolution Profiles of 20 °off-Center Located (Positions 6, 7, 8, 9) Tablets	38
3.2 Results of PIV Measurement	44

TABLE OF CONTENTS
(Continued)

Chapter **Page**

3.2.1 Velocity Vectors ……...……..…….…..... 44

3.2.2 Velocity Profiles on Iso-Surfaces ……..……...…..... 47

3.2.3 Sums of Squared Deviations of the Velocity Profiles ……..... 55

4 DISCUSSION ……..…….…….…... 57

4.1 Dissolution Tests ……. 57

4.2 PIV Measurements …….. 59

5 CONCLUSIONS ……..…….. 62

APPENDIX A DERIVATION OF EQUATION 2.1 …...……. 64

APPENDIX B DISSOLUTION PROFILES USING CONCENTRATION RATIO VS. TIME …...…..……... 68

APPENDIX C TABLES OF DISSOLUTION TESTING RESULTS ……... 81

REFERENCES ……... 95

LIST OF TABLES

Table		Page
2.1	Operating Conditions for Dissolution Experiments with Prednisone Tablets	18
3.1	Calibration Data for Prednisone Tablets ……..…….	29
3.2	Statistical Values of Three Runs with Position 1 Tablets ……..	32
3.3	Statistical Values of Three Runs with Position 2 Tablets …….…….	37
3.4	Statistical Values of Three Runs with Position 3 Tablets …….……..……..	37
3.5	Statistical Values of Three Runs with Position 4 Tablets ……..……..…….	37
3.6	Statistical Values of Three Runs with Position 5 Tablets …….……...…….	37
3.7	Statistical Values of Three Runs with Position 6 Tablets …….……..…..…….	42
3.8	Statistical Values of Three Runs with Position 7 Tablets …….……..…..…….	42
3.9	Statistical Values of Three Runs with Position 8 Tablets …….……..……..….	42
3.10	Statistical Values of Three Runs with Position 9 Tablets ……..…..…….	42
3.11	Average Standard Deviations of PIV Measurements in Three Regions for the Standard System ……	48
3.12	Sums of Squared Deviations……...……	56
4.1	Average f_1 and f_2 Values of Dissolution Profiles for Each Tablet Position ……....	58

LIST OF FIGURES

Figure		Page
1.1	Three types of UV Fiber Optic Probes ……..	3
2.1	(a) Distek 5100 Bathless Dissolution Apparatus (b) USP Dissolution Testing Apparatus 2: paddle impeller and glass vessel ……..	6
2.2	(a) Front view of USP Dissolution Testing Apparatus 2 vessel (b) Bottom view of USP Dissolution Testing Apparatus 2 vessel …….....	8
2.3	Arch shaped fiber optic probe and vessel cover ……	9
2.4	Dimensions of arch fiber optic probe ……..……...…	9
2.5	(a) Front view of the probe in dissolution testing vessel (b) Side view of the probe in dissolution testing vessel (c) Bottom view of the probe in dissolution testing vessel……...	12
2.6	Setup of de-aeration process for dissolution medium ……..……...	14
2.7	(a) Top view of the bottom of the dissolution vessel with nine different tablet positions in testing system (b) The front view of the dissolution vessel with three different tablet positions (0°, 10°, 20°) in standard system ……..	16
2.8	Schematic of laboratory PIV experimental set-up …….	22
2.9	Schematic of the four sections (in grey) studied using PIV ……...	25
2.10	Nine iso-surfaces chosen for PIV measurements ……...	26
3.1	Calibration curve and regression for Prednisone tablets ……	29
3.2	Dissolution profiles of three runs with Position 1 tablets ……..	31
3.3	Dissolution profiles of three runs with Position 2 tablets ……..……...	33
3.4	Dissolution profiles of three runs with Position 3 tablets ……..……...	34
3.5	Dissolution profiles of three runs with Position 4 tablets ……..……...	35
3.6	Dissolution profiles of three runs with Position 5 tablets ……..……...	36

LIST OF FIGURES
(Continued)

Figure		Page
3.7	Dissolution profiles of three runs with Position 6 tablets ……..……...	39
3.8	Dissolution profiles of three runs with Position 7 tablets ……..……...	40
3.9	Dissolution profiles of three runs with Position 8 tablets ……..……...	41
3.10	Dissolution profiles of three runs with Position 9 tablets ……..……...	42
3.11	PIV velocity vectors map for the standard system ……..……...……...	45
3.12	PIV velocity vectors maps for all four sections in the testing system ……...…...	46
3.13	PIV measurements for radial velocities on iso-surfaces above the impeller …….	49
3.14	PIV measurements for axial velocities on iso-surfaces above the impeller ……..	50
3.15	PIV measurements for radial velocities on iso-surfaces around the impeller ……	51
3.16	PIV measurements for axial velocities on iso-surfaces around the impeller……..	52
3.17	PIV measurements for radial velocities on iso-surfaces below the impeller……..	54
3.18	PIV measurements for axial velocities on iso-surfaces below the impeller…..…	55

CHAPTER 1

INTRODUCTION

1.1 Background

Dissolution testing is widely used in the pharmaceutical industry, both as a tool to evaluate, *in vitro*, newly developed solid formulations, and as a quality control technique to insure that the manufactured tablets/capsules have consistent dissolution property. The USP Dissolution Testing Apparatus 2 is the device most commonly used in dissolution testing for oral dosage forms. Typically, dissolution testing consists of dropping the dosage form in the dissolution vessel containing the dissolution medium, stirred by a paddle, manually removing liquid samples over time, and then bringing the samples either to a UV spectrometer for determination of the analytic concentration, or to a HPLC for UV or fluorescence detection after separation. This manual operation has a number of disadvantages:

1. Labor intensiveness. At least one trained individual is needed to take samples over the whole testing period, and extra time is needed to analyze the samples afterwards.
2. Operator's errors. The operator has to carefully follow standard operating procedure (SOP) to avoid introducing errors. Still human errors cannot be totally eliminated.
3. Limited dissolution data. Usually less than 10 samples are taken over the whole testing period. The drug release curve cannot be plotted smoothly based on such small number of data points.

An approach to overcome the limitations of manual sampling consists in the use of sampling probes permanently inserted in the dissolution medium and continually sampling the drug concentration in it as the solid dosage form dissolves. Fiber optic probes are one of the most important classes of probes. The application of fiber optic

probes in dissolution testing has been studied in past decades since early study was done by Josefson (1988). The application was considered to be able to change the traditional way of sampling and overcome the disadvantages mentioned above (Liu, et al., 2008). Labor intensiveness can be significantly reduced by eliminating manual sampling and analyzing procedure. Accuracy and consistency of data are increased by eliminating operator's errors and analyst-to-analyst variation. A real-time drug release level can be determined in-situ or in the vessels without sample removal. Many more data points can be collected and more accurate dissolution profiles can be generated than with manual sampling.

Despite of all these advantages, the use of fiber optic probes also has limitations. One of them is the effect to hydrodynamics in the dissolution vessel. The presence of any permanently inserted probe can alter, in principle, the normal fluid flow within the vessel. Although the probe is typically small, it can act as a baffle in a perfectly symmetrical system. This loss of symmetry, and the introduction of the probe, which acts as a small baffle, can result in changes in velocity profile and shear rates, which can cause variations in dissolution testing results when compared to system that do not incorporate such as device. Therefore, research has been conducted to validate this technique to insure that it is compliant with regulatory requirements (Gary, 2003; Mirza, et al., 2009). Possible changes in the dissolution performance variation should be studied carefully before replacing the current methodology with this technique.

Being a relatively new technology in dissolution testing, no standards exist for fiber optic probes. In addition, there are different types of probes, and this adds complexity to the issue. Based on the shape and the location where they are placed in the

vessel, fiber optic probes can be categorized into three types, as shown Figure 1.1: 1) shaft probes, which are fixed in a hollow shaft and placed at the center of the vessel; 2) rod probes, essentially a solid rod dipped in the vessel with a detection window in the traditional sampling location defined by United States Pharmacopeia (USP); and 3) arch-shaped probes, which have an arch shape and a detection gap at the bottom of the probe located at the traditional USP sampling location (Lu et al., 2003). UV light is able to get into the dissolution medium from one side of the gap and travels to the other side. Therefore light absorption data can be obtained. This system also has other advantages, such as small displacement volume, simple light path, and reduced bubble and particulate accumulation (Inman et al., 2001). In this study, an arch-shaped probe was used to be tested in the USP Dissolution Apparatus 2 to determine possible changes in the flow pattern introduced by the presence of the probe.

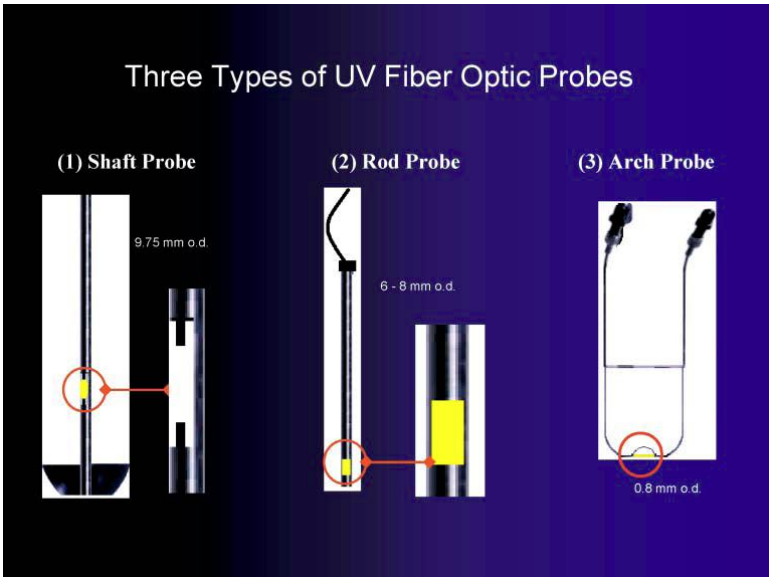

Figure 1.1 Three types of UV Fiber Optic Probes.(Lu et al., 2003)

The USP Dissolution Apparatus 2 has been widely used in the pharmaceutical industry for decades, since this test was first officially introduced almost 30 years ago

(Cohen et al., 1990). However, previous studies done by Baxter et al. (2005) and Bai et al. (2007) have shown that as a small unbaffled vessel with hemispherical bottom, this apparatus is associated with complex hydrodynamic conditions. As a perfectly symmetrical mixing system, the USP Apparatues 2 is very sensitive to any deviation from symmetry, such as the introduction of the arch shaped fiber optic probe.

A literature review of studies on hydrodynamic effect of fiber optic probes showed that investigation has been done by several groups. Schatz et al. (2000) reported no significant difference in dissolution result using shaft probe. Martin (2003) and Lu et al. (2003) reported noticeable difference using rod probe, and Inman et al. (2001), Inman (2003), and Lu et al. (2003) all reported minimal or small difference using the arch-shaped probe. However, these studies on arch shaped probes were limited by limited amount of data and lack of a more sophisticated experimental methodology.

1.2 Objectives of This Work

Therefore, the overall objective of this study was to quantify the hydrodynamic effects of the arch shaped fiber optic probe in USP Dissolution Testing Apparatus 2. To do so, two different methodologies were used in this study. In order to study solely the hydrodynamic changes introduced by the arch-shaped probe and its effect on the dissolution profiles, efforts were made to eliminate any other factors that could also affect the test results. As shown in previous study on the USP Dissolution Apparatus 2 (Bai et al., 2007), the exact location of the dissolving tablet introduces significant variations in the flow and in the shear stress experienced by the tablet, which, in turn, can affect the dissolution process and the dissolution profiles. Therefore, in this study, dissolution tests

were conducted in the presence and in the absence of the arch-shaped fiber optic probe using tablets fixed in place at 9 different locations at the bottom of the USP Apparatus 2 dissolution vessel, i.e., with tablets located 10 °or 20 °off-center and at different positions with respect to the probe. Statistical tools were then used to evaluate and compare the results at each tablet position.

In addition, in order to find the root cause of possible hydrodynamic effects of the probe on the dissolution profiles, velocity measurements were made under different conditions using Particle Image Velocimetry (PIV). PIV was used to visualize and quantify the flow velocity field in the vessel. This approach also allowed a comparison to be made between changes in the dissolution profiles and variations in the flow field that could be attributed to the presence or absence of the probe.

CHAPTER 2

EXPERIMENTAL APPARATUS, MATERIALS AND METHODS

2.1 Dissolution Tests

2.1.1 Dissolution Apparatus

Dissolution testing experiments were conducted in a USP Dissolution Testing Apparatus 2. The dissolution test system was a Distek 5100 Bathless Dissolution Apparatus (Figure 2.1a) from Distek Inc., North Brunswick, NJ. The agitation system was a two-blade paddle impeller mounted on a shaft and connected to the motor in the Distek system. Unbaffled, cylindrical, hemisphere-bottomed glass vessels with maximum capacity of 1 L were used as the dissolution vessels. In the standard system, the vessel was covered by a plastic vessel lid with two openings for sampling. The agitation system, the vessel and the lid are shown in Figure 2.1b.

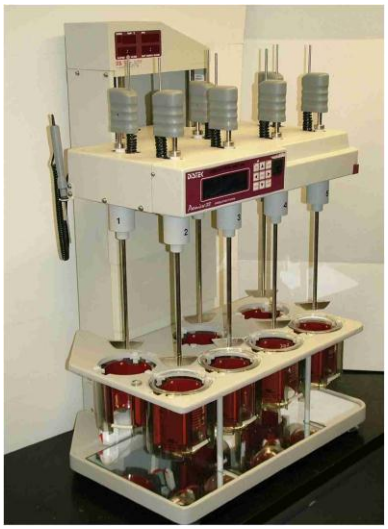

(a)

(b)

Figure 2.1 (a) Distek 5100 Bathless Dissolution Apparatus **(b)** USP Dissolution Testing Apparatus 2: paddle impeller and glass vessel.

The dimensions of the vessel and the impeller were measured by a caliper, and were found to be as follows: vessel internal diameter, 100.16 mm; shaft diameter, 9.52 mm; length of the top edge of the blade, 74.10 mm; length of the bottom edge of the blade, 42.00 mm; height of the blade, 19.00 mm; and thickness of the blade, 4.00 mm. The impeller clearance off the vessel bottom was 25 mm, as mandated by the USP (2008). When the vessel was filled with 500 mL of dissolution media, the corresponding liquid height, as measured from the bottom of the vessel, was 78.6 mm. The geometry of the vessel with the probe and the agitation system in place and containing 500 mL of dissolution media is shown in Figure 2.2.

The fiber optic sampling probe tested in this study was an arch shaped metal probe provided by the Merck Company. The probe consisted of two sections of a thin (0.8 mm) vertical tubing bent at their bottom to bring their ends near each other horizontally so that they were separated by a small gap (2 mm), as shown in Figure 2.3. The two pieces of tubing were kept in position by two horizontal metal braces. The fiber optic cable ran inside the tubing. Although not used for this purpose in this work, the probe is intended to measure the light attenuation as a light beam travels in the gap when the probe was inserted in a the medium in which a tablet is dissolving. When connected to UV spectrometer, UV light would go through the detecting gap and get partially absorbed by the dissolution solution. Therefore the UV absorbance data of the solution can be obtained continuously. The figure also shows the specially made plastic vessel lid with a long slot that was used to support the probe and keep it in place. Additional dimensions of the fiber optic probe were measured by caliper and are shown in Figure 2.4.

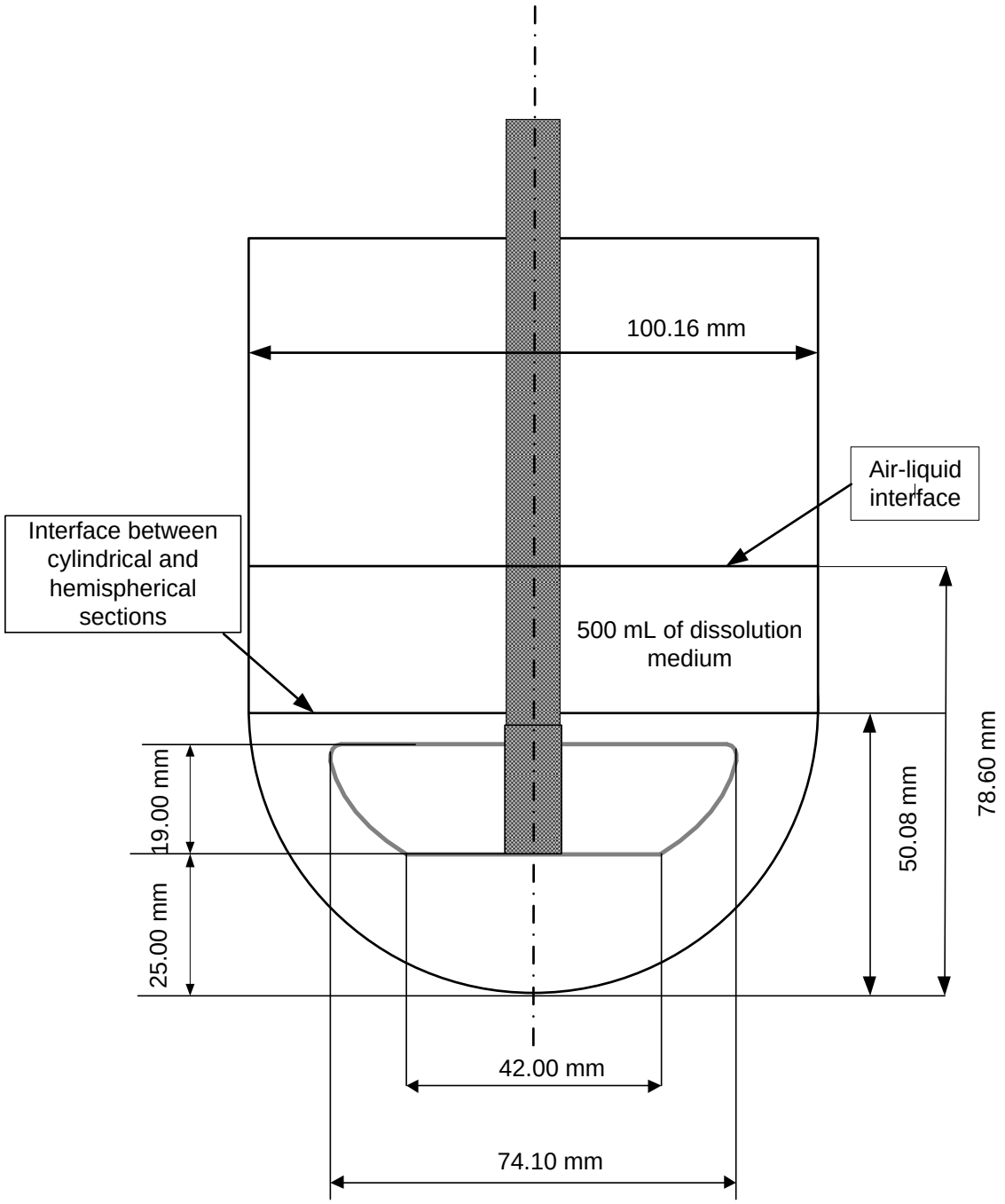

Figure 2.2 (a) Front view of USP Dissolution Testing Apparatus 2 vessel.

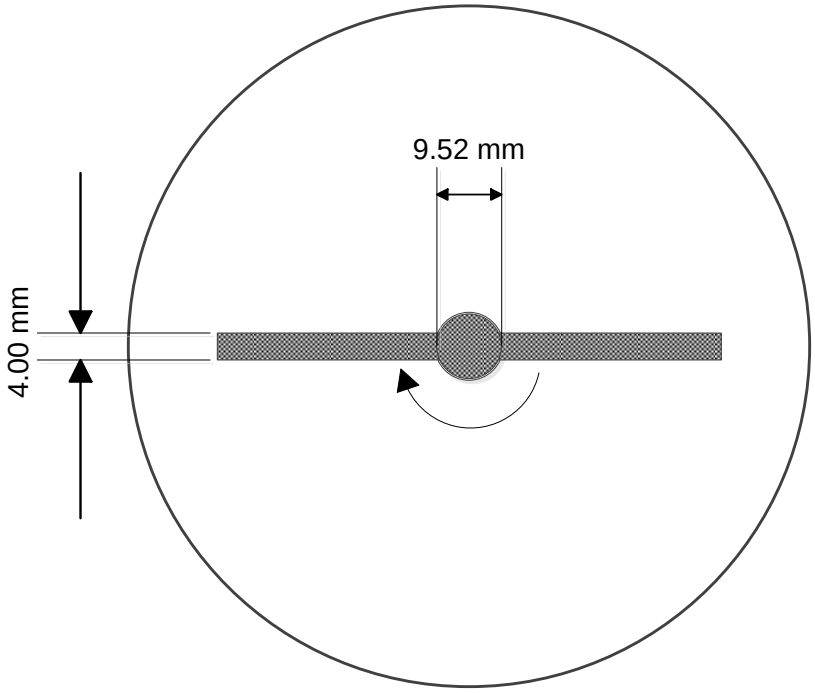

Figure 2.2 (b) Bottom view of USP Dissolution Testing Apparatus 2 vessel (Continued).

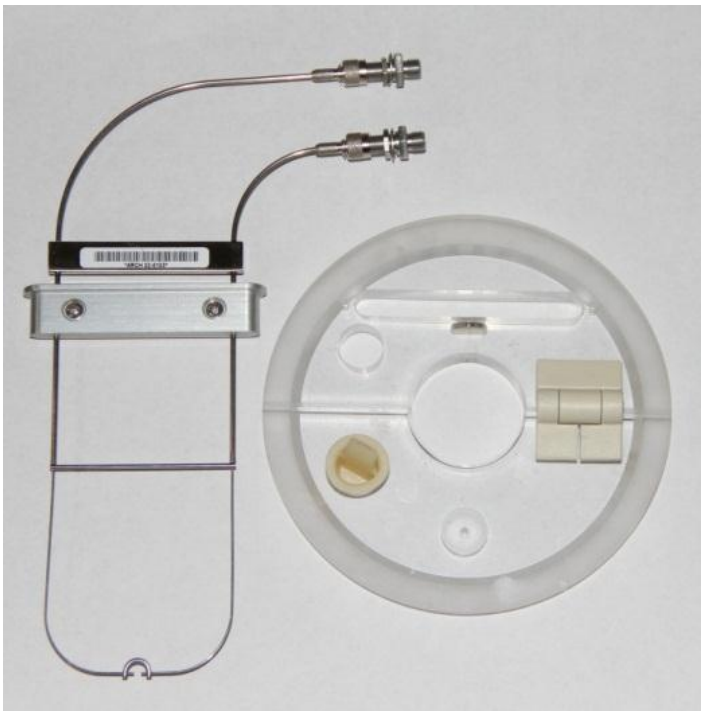

Figure 2.3 Arch shaped fiber optic probe and vessel cover.

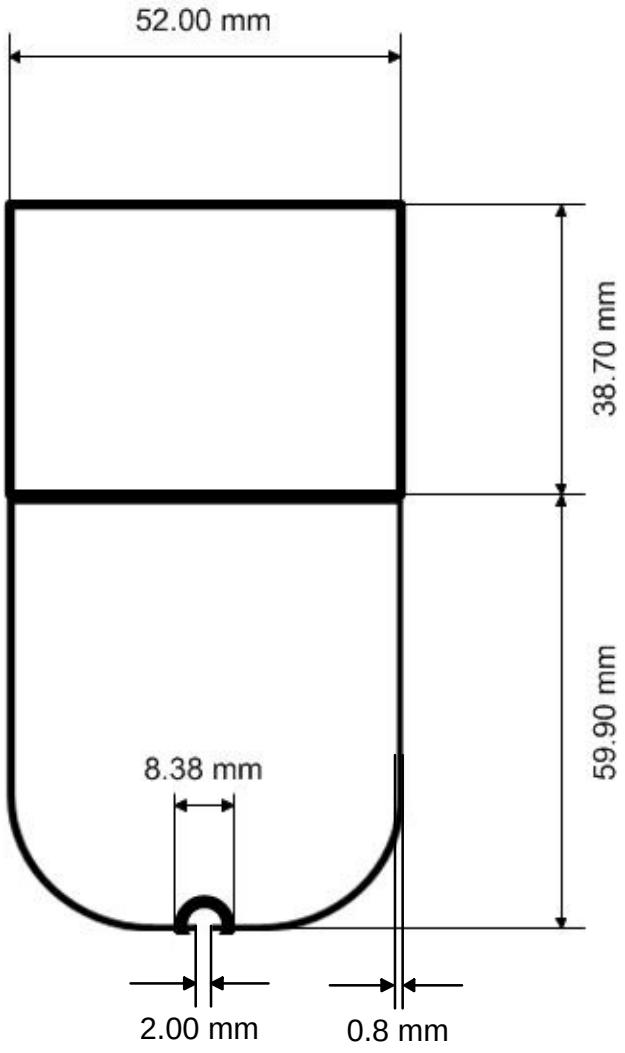

Figure 2.4 Dimensions of arch fiber optic probe.

As specified in the USP, liquid samples taking manually during a dissolution test should be taken within a required zone in the dissolution medium, i.e., horizontally midway between the impeller shaft and the vessel wall, and vertically midway between the top edge of the impeller and the surface of the dissolution medium. In the case of the fiber optic probe, the detecting gap at the bottom of the probe was where the samples should be taken. Therefore, the probe would be installed properly so that the detecting

gap stays in the sampling zone during dissolution tests. The detailed location of the probe after its installation in the vessel is shown in Figure 2.5.

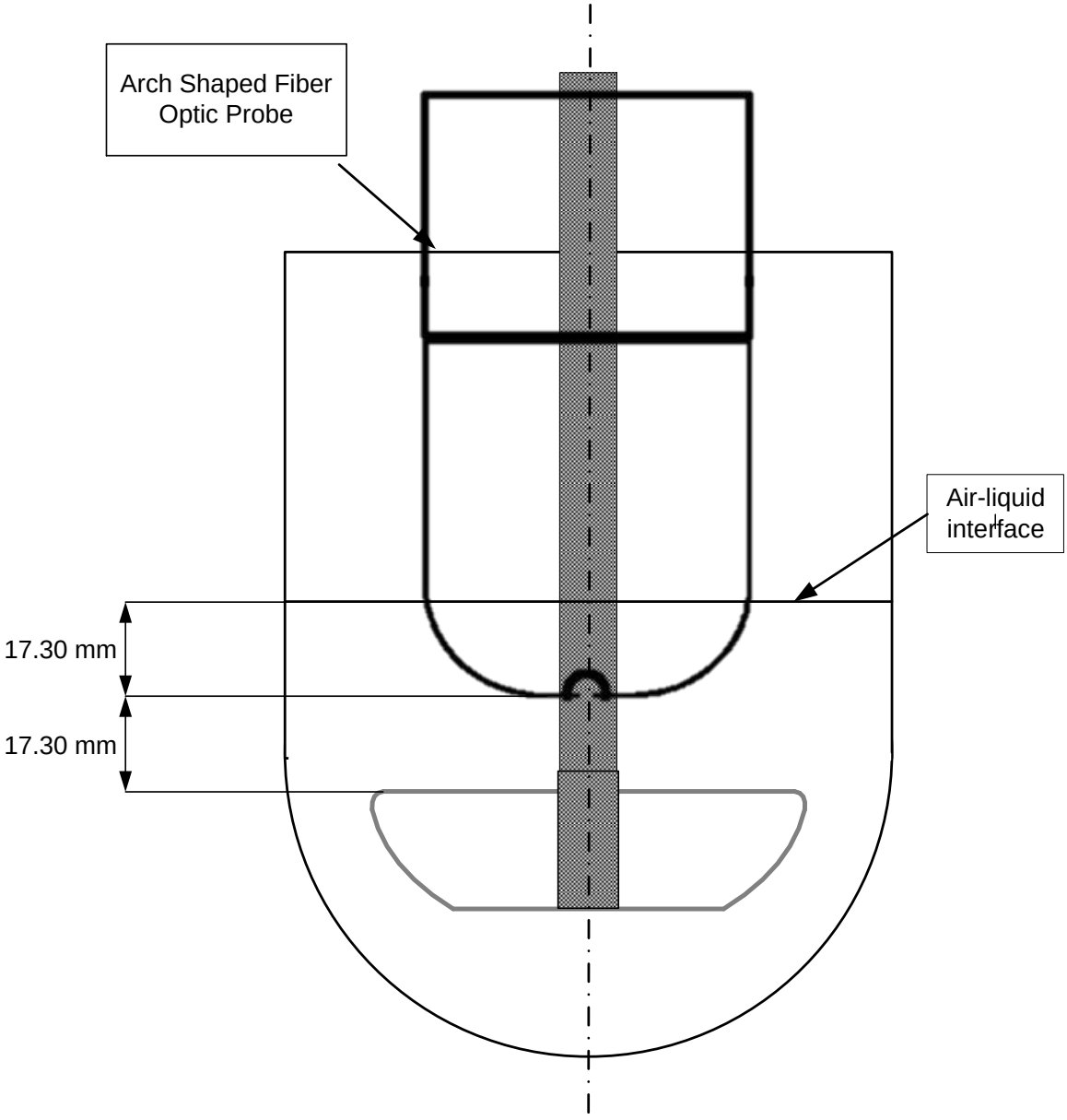

Figure 2.5 (a) Front view of the probe in dissolution testing vessel.

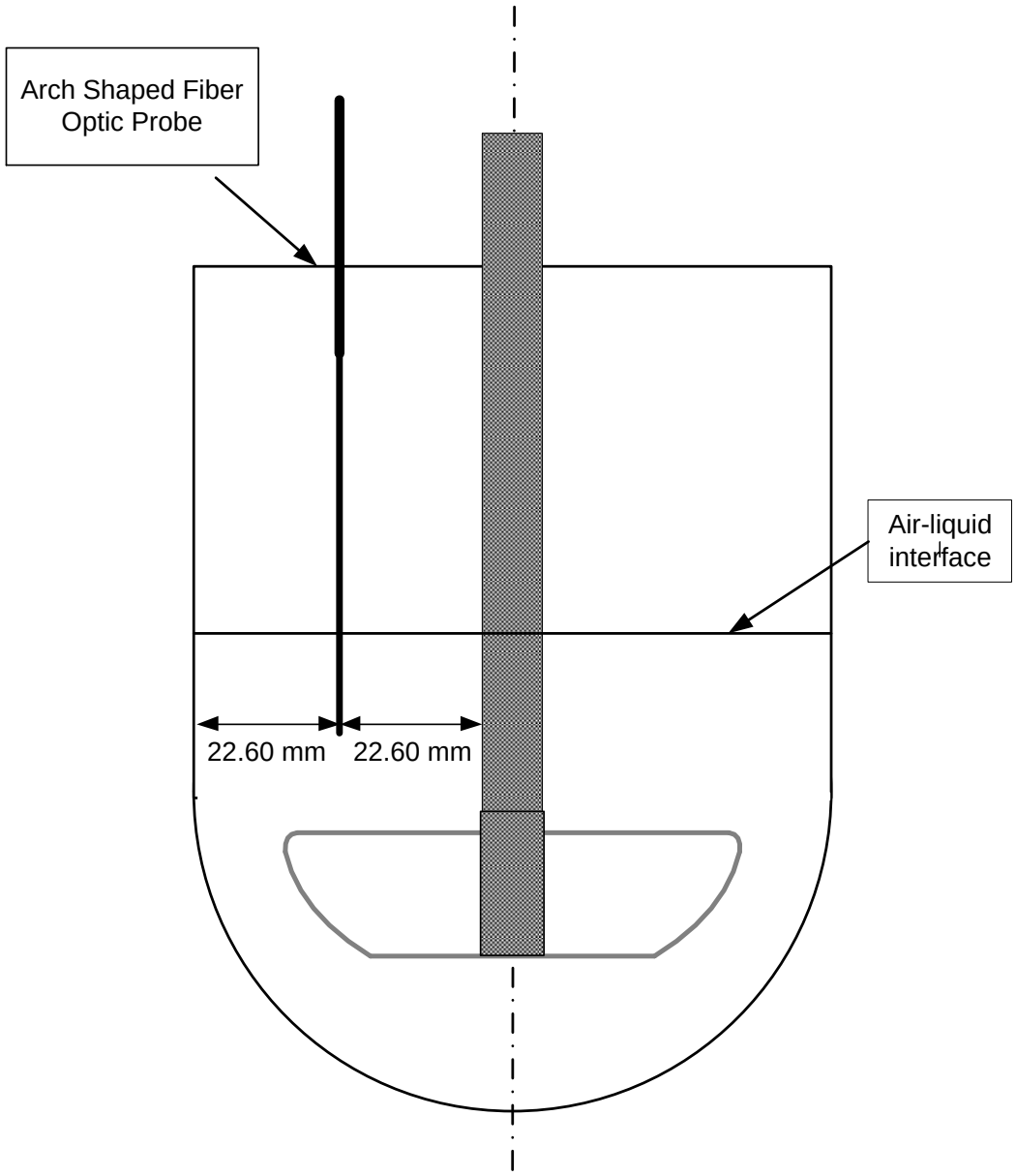

Figure 2.5 (b) Side view of the probe in dissolution testing vessel (Continued).

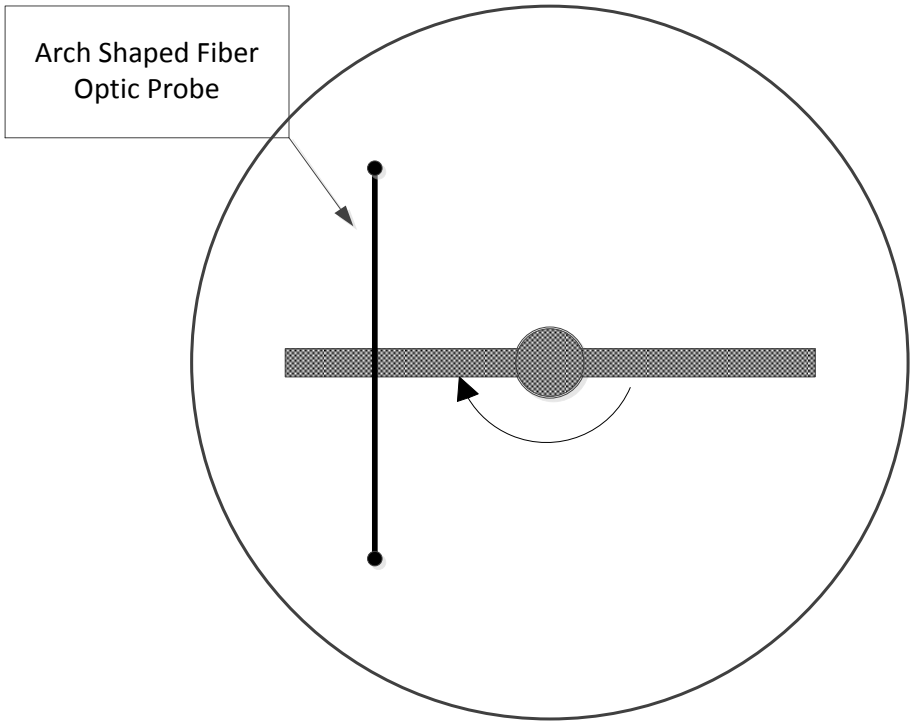

Figure 2.5 (c) Bottom view of the probe in dissolution testing vessel (Continued).

In this work, a 10 mL syringe and 2 mm cannula were used to take samples manually from dissolution testing solution, also a disposable PVDF 0.45 µm filter was attached to remove possible solid particles that could have entered the sample. A spectrophotometer (Cole Parmer S2100UV+) was used to obtain UV absorption data from the samples.

2.1.2 Dissolution Test Materials

Disintegrating tablets, i.e., 10 mg Prednisone tablets (NCDA #2), kindly donated by Dr. Zongming Gao, Food and Drug Administration (FDA), Division of Pharmaceutical Analysis, Center for Drug Evaluation and Research, St. Louis, MO, were used in this study for dissolution testing experiments. An exceedingly small amount of a commercial

acrylic glue was used to fix the tablet at a particular location on the bottom of the dissolution vessel.

The medium used for dissolution tests was de-aerated distilled water. The medium was de-aerated before using, according to the method developed by Moore (1996) following the USP requirement (USP, 2008) (Figure 2.6). Accordingly, the medium was placed in carboy tank, which was then connected to a vacuum pump. Vacuum was applied for 30 minutes while all other valves in the system were closed. This stock solution was used as needed (typically in 500 mL aliquots per test).

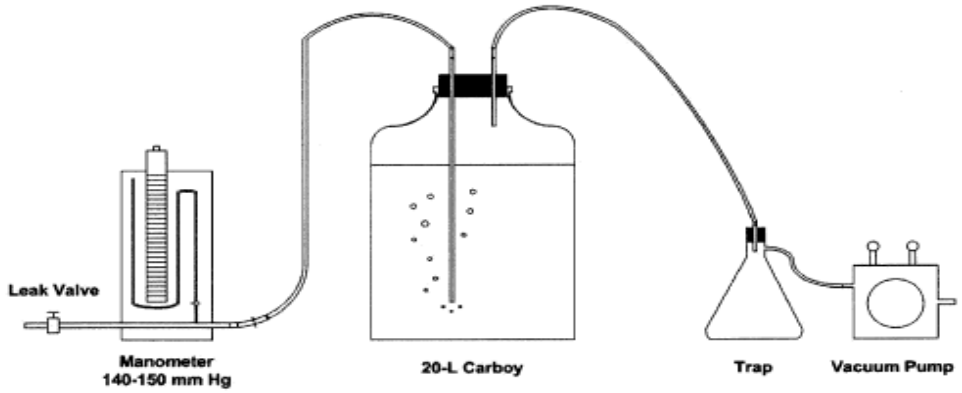

Figure 2.6 Setup of de-aeration process for dissolution medium. (USP, 2008)

2.1.3 Dissolution Test Method

The procedure for the dissolution test was based on the USP requirement (USP, 2008). However changes were made due to the fact that the tablets were fixed on the bottom of the vessel, instead of being dropped into the medium.

In each side-by-side experiment, two tablets were tested simultaneously using different setup of apparatus, i.e., the testing system with the fiber optic probe inserted, and standard system without the probe. The effect of minor geometrical variations between vessels was eliminated by randomly choosing glass vessels in each experiment.

The tablets were attached at the same predefined position on the vessel bottom with a very small bead of commercial glue before the experiment starts. Since the testing system was non-symmetrical, nine positions on the vessel bottom were examined, as shown in Figure 2.7(a). Position 1 in this figure represents the center of the vessel bottom. Positions 2-5 were on an inner circle 10 ° off-center from the vessel vertical centerline. Positions 6-9, were on an outer circle 20 ° off-center from the vessel vertical centerline (Figure 2.6(b)). These angles were taken from the center of the sphere comprising the hemispherical vessel bottom, and measured starting from the vertical centerline to the point of interest, (e.g., the angle would be zero for the central point below the impeller). These positions were spaced 90 ° apart from each other. As for standard system, though it is symmetrical, data from nine points were obtained to pair with the data from the testing system. For each point, three runs were performed at different times.

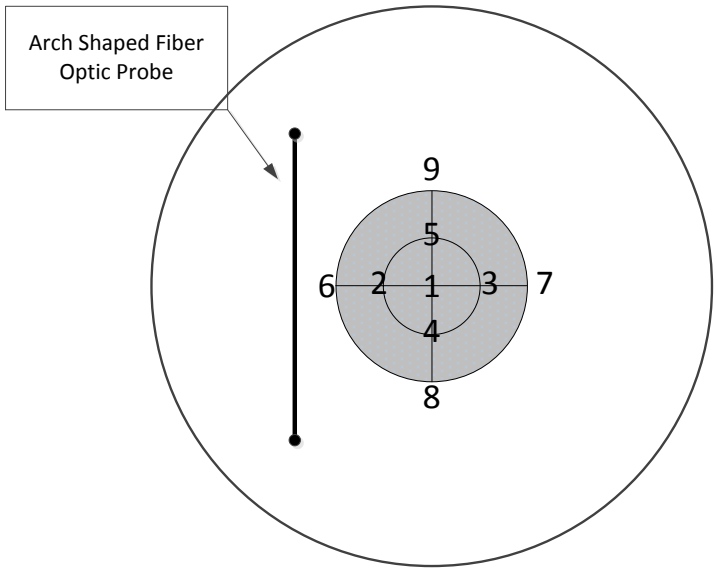

Figure 2.7 (a) Top view of the bottom of the dissolution vessel with nine different tablet positions in testing system**.**

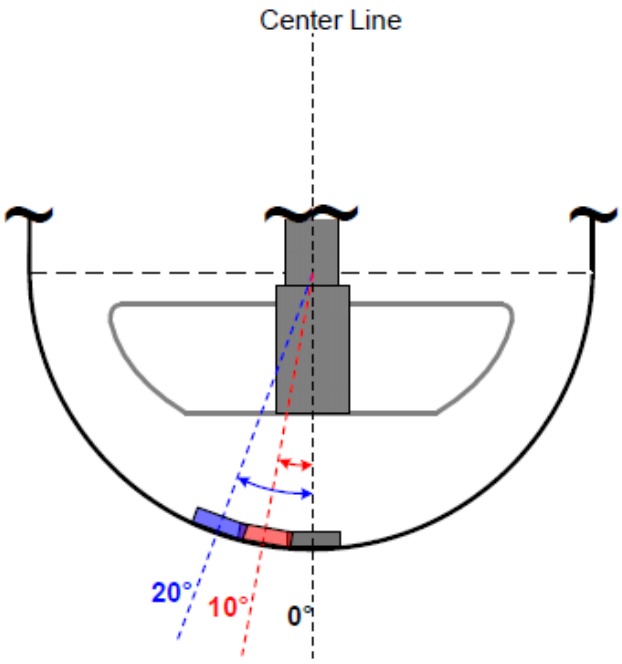

(b)

Figure 2.7 (b) The front view of the dissolution vessel with three different tablet positions (0 °, 10 °, 20 °) in standard system (Continued).

Before each experiment, all key geometrical measurements were checked (impeller clearance, impeller position, etc.). After the vessels with the attached tablets were properly placed in the Distek system, 500 mL de-aerated distilled water, previously preheated to 37.5 ^{o}C, were poured gently to each of the two vessels. A plastic funnel was used to keep water running down along the wall in order to minimize gas introduction and dissolution of the tablet before the test started. The agitation, previously set at 50 rpm, was turned on immediately after pouring the dissolution medium, the probe was inserted to its predefined place in the testing system, and a stopwatch was started simultaneously. The first pair of samples was taken immediately after starting the agitation. These samples were defined as the samples of time t=0. The time interval between samples was 5 minutes. The experiment lasted 45 minutes and ten samples were taken for each system.

The temperature was maintained at 37 ^{o}C throughout the whole experiment by the temperature controller built in the Distek system.

In order to keep the results from the two systems comparable, the same conventional sampling procedure was used in both systems, in despite of the fact that the fiber optic probe was able to take samples continuously. Samples were taken by removing 10 mL aliquots by the combination of syringe, filter and cannula. The volume of medium removed by sampling was not replaced, in accordance to the USP procedure (USP, 2008). The sampling position was within the USP specified sampling zone, i.e., horizontally located midway between the impeller shaft and the vessel wall, and vertically midway between the top edge of the impeller and the surface of the dissolution medium. The initial 2 ml of each sample was discarded, and the remaining was moved to a sample vial for further analysis.

Analysis of samples was carried out using 1 cm quartz cells placed in a UV spectrophotometer measuring absorbance at USP specified wavelength, i.e., 242 nm for Prednisone (the approximate wavelength of maximum absorbance). A blank data was taken for reference, by measuring the absorbance of only the dissolution medium, i.e., de-aerated distilled water. Before putting the sample solution into the quartz cell, the cell was rinsed with the same solution twice.

The absorbance data was converted to concentration of Prednisone by a calibrated absorbance vs. concentration curve for Prednisone. To plot the calibration curve, a series of standard solutions of Prednisone was made by fully dissolving a Prednisone tablet (10 mg) into the dissolution medium, and diluting with a known volume of distilled water. UV absorbance data for these solutions were obtained to generate the calibration curve. A

regression was performed to establish the conversion from UV absorbance to Prednisone concentration.

Additional details of the operating conditions are presented in Table 2.1.

Table 2.1 Operating Conditions for Dissolution Experiments with Prednisone Tablets

Dose	10 mg
Medium	500 ml de-aerated, distilled water
Temperature	37 ^{o}C
Agitation Speed	50 rpm
Filter	PVDF 0.45 μm
UV Wavelength (UV Spectroscopy)	242 nm
Standard Tablets	Calibrated Tablets
Time	5 min sampling interval; 45 min total
Sample Volume	10 ml
Sample Replacement	No

2.1.4 Dissolution Test Data Analysis

The UV absorbance data obtained was first converted to Prednisone concentration at certain time, (C_n, mg/ml). Since samples were removed without replacing their volumes, the drug release ratio (m_D/m_T), i.e. the amount of drug in solution at any time t out of the total initial amount of drug in the tablet was calculated using the following equation to compensate the removal of samples:

$$\frac{m_D(t_n)}{m_T} = \frac{C_n}{C^*}\left(1 - \frac{n\Delta V}{V}\right) + \frac{\Delta V}{V}\sum_{i=0}^{n-1}\frac{C_i}{C^*} \tag{2.1}$$

Where $m_D(t_n)$ is the mass of dissolved Prednisone at time n, m_T is the label claimed mass of the tablet, C_n is the Prednisone concentration in the sample at time t_n, C* is the concentration of Prednisone tablet fully dissolved into 500ml dissolution medium, V is the initial volume of dissolution medium (500 ml), ΔV is the volume of each sample (10 ml). The detailed derivation of Equation 2.1 is shown in Appendix A.

Since a sample was initially taken at t= 0 (zeroth sample). So the 10th sample in the dissolution test (including the initial one) corresponded to n=9 (not n=10), i.e., n=0, 1, 2, 3, 4, 5, 6, 7, 8, and 9 (10 samples taken every 5 minutes, starting at time $t=t_o=0$ min, and ending at time t9=45 minutes).

The dissolution profiles for each experiment obtained with the testing system were compared to the profile from its paired standard system in order to determine whether these dissolution curves were statistically similar to each other. These drug release data was plotted against time (min) and evaluated by the following methods.

A paired Student's t-test was used to obtain the probability of the null hypothesis that the two sets of data came from the same underlying population, i.e., that the probability the dissolution profiles from the two systems were statistically the same. The equations for the paired Student's t-test are

$$t = \frac{(\overline{X_D} - \mu_0)}{S_D/\sqrt{n}} \tag{2.2}$$

$$DF=n-1 \tag{2.3}$$

where $\overline{X_D}$ is the sample mean (in this case the average of the differences between curves), μ_0 the population mean (in this case the constant from which to test whether the average of the difference is different, i.e., μ_0=0 here), S_D is the sample standard deviation (in this case the standard deviation of the differences between curves), *DF* is degree of freedom and *n* is sample size. Once a t and *DF* is determined, the probability (T-value) can be found using a table of values from Student's t-distribution (Dunnett and Sobel, 1954)

The significant level was chosen to be 0.05, i.e., if the T-value obtained was smaller than 0.05, the null hypothesis was rejected; the two groups of data were considered statistically from different systems.

In addition, to quantify the similarity/difference of two groups of dissolution profiles, the FDA-recommended approach was used. This approach consists of using two model-independent methods based on the similarity factor (f_1) and difference factor (f_2) proposed by Moore and Flanner (Moore and Flanner, 1996):

$$f_1 = \frac{\sum_{t=1}^{n}\left|R_t - T_t\right|}{\sum_{t=1}^{n} R_t} \times 100 \tag{2.4}$$

$$f_2 = 50\log_{10}\{[1+(\frac{1}{n})\sum_{t=1}^{n}(R_t - T_t)^2]^{-0.5} \times 100\} \quad (2.5)$$

where R_t is the reference assay at time *t,* i.e., the results from the standard system. T_t is the test assay at the same time, i.e., the paired results from the testing system, and *n* is the number of points. The f_1 factor measures the percent error between two curves for all points. The percent error is zero when the test and reference profiles are identical, but increases proportionally with the dissimilarity between the two dissolution profiles. The higher the similarity factor f_1 (which can be in the range of 0 to 100), the higher the average difference between reference and test curves is. The f_2 factor is a logarithmic transformation of the sum-squared error of differences between the test and the reference dissolution profiles over all time points (which can be in the range -α to 100). If this difference is higher than 100, normalization of the data is required. The higher the difference factor f_2, the lower the average difference between reference and test curves (Costa and Lobo, 2001). Public standards have been set by FDA for f_1 and f_2. Accordingly, statistical similarity between the two curves being compared requires that both $0<f_1<15$ and $50<f_2<100$ (FDA, 1997; Baxter et al., 2005).

2.2 Particle Image Velocimetry (PIV)

2.2.1 PIV Apparatus

A Dantec FlowMap 1500 2D Particle Image Velocimetry (PIV) apparatus (Dantec Dynamics A/S, Tonsbakken 16 – 18, DK – 2740 Skovlunde, Denmark) was used to determine the velocity flow field inside both testing system and standard system. The setup of the PIV apparatus is shown in Figure 2.8.

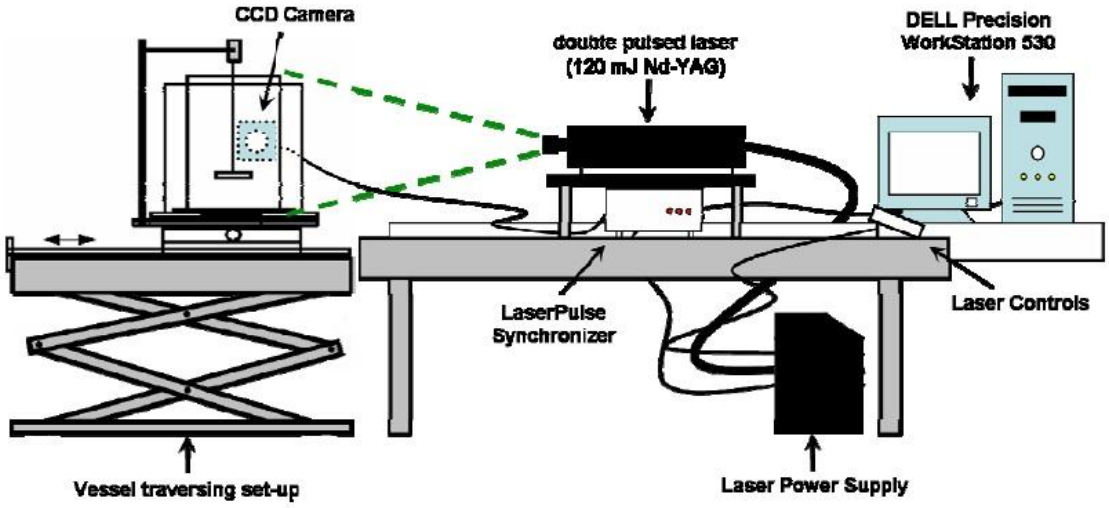

Figure 2.8 Schematic of laboratory PIV experimental set-up.

The dissolution vessel used in the PIV experiment was placed in a Plexiglas tank filled with water in order to minimize refractive effects at the curved surface of the vessel wall. The agitation was provided by an electric motor connected to an external controller that kept it 50 rpm. The shaft and impeller in the experiment were specially made in black, in order to minimize the reflection of the laser light impinging on them.

The light source of the PIV system was produced by a double pulsed 120 mJ Nd-Yag laser (New Wave Research model Solo 120 15 Hz, Fremont, CA, USA), consisting of two infrared laser heads combined in a single package with a second harmonic generator and two discrete power supplies. The laser source came from a Class IV laser, which emitted 532 nm wavelengths light. The laser produced two pulsed infrared laser beams which passed through an optical arrangement of lenses to generate a laser light sheet. The laser light sheet was shot through the dissolution apparatus with seed particles in the medium. These particles were used to follow the fluid flow and scatter the laser light for fluid velocity measurements. In the experiments performed, the seed particles were silver-coated hollow borosilicate glass spheres (Dantec Measurement Technology

USA, Mahwah, NJ, USA) with a density of 1.4 g/cm3, sizes ranged from 2 to 20 μm, and mean particle size of 10 μm. The laser light scattered by these particles was captured by a digital camera (Dantec Dynamics HiSense PIV/PLIF camera model C4742-53-12NRB), which was installed perpendicularly against the laser light sheet. The digital camera contained a light filter to eliminate visible light and only capture the laser light. The laser and the digital camera were connected to a synchronizer (LASERPULSE Synchronizer, TSI model 610034), which was then in turn connected to a computer (DELL Precision WorkStation 530) for control and data analysis.

All these components were controlled by dedicated software (FlowManager 4.71) which collected pairs of digitized images of illuminated particles in the dissolution apparatus from the CCD camera (with the two images in each pair being collected at a small but known time interval), which were subdivided into small subsections called interrogation areas. Each pair of frames for a given interrogation areas was then analyzed using cross-correlation to determine the spatial x- and y-displacement that maximized the cross-correlation function for that interrogation area. The resulting displacement vector obtained by dividing the x- and y- displacements by the time interval was taken as the fluid velocity in that interrogation area.

2.2.2 PIV Method

Both the testing system and the standard system were used in the PIV experiments. In each experiment, the velocity profiles on only one-half of top portion of the longitudinal section of the vessel could be determined since the laser light sheet was blocked by the shaft. Since the testing system (with probe inserted) was non-symmetrical, four lengthwise cross-sections of the testing system, 90 ° apart from each other, were studied.

Using the position numbering of tablets described in Figure 2.7(a), the four sections were named using the 10 ° and 20 ° tablet positions that lie on the section, i.e., Section 2-6 (i.e., the section intersecting tablet Positions 2 and 6), Section 3-7, Section 4-8, and Section 5-9, as shown in Figure 2.9 (gray parts show the sections studied).

In each PIV experiments, two pairs of images of the dissolution apparatus were taken at a time interval of 1 ms. 300 pairs in total were taken at a time interval of 600 ms between each pair. Image masks were defined and applied to all images to reject outside regions as well as the impeller and shaft regions of the apparatus in the image, in order to reduce the error in cross correlation. After the correlation was performed for every pair, the statistical average was taken out of the 300 pairs to obtain the velocity profile on the section under investigation. The profile then went through moving-range validation and average filter to obtain the final velocity vector map for further analysis. (FlowMap PIV Installation & User's guide, 2000)

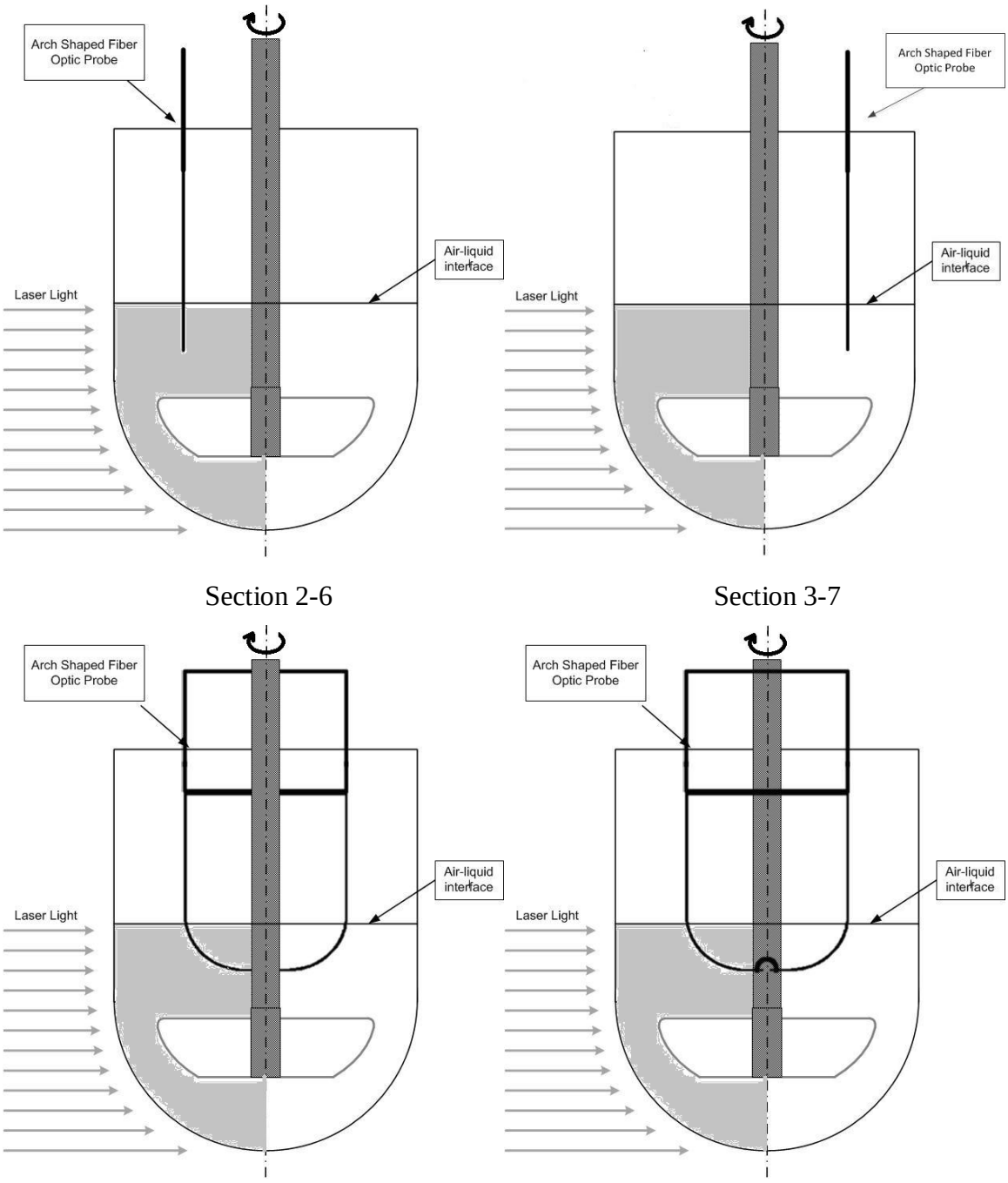

Figure 2.9 Schematic of the four sections (in grey) studied using PIV.

The liquid velocity at any point in the vessel has three components. The first velocity component is radial and acts in a direction perpendicular to the shaft of the impeller. The second component is axial and acts in a direction parallel with the shaft.

The third component is tangential and acts in a direction tangent to a circular path around the shaft. In this study, only the axial and radial components were investigated.

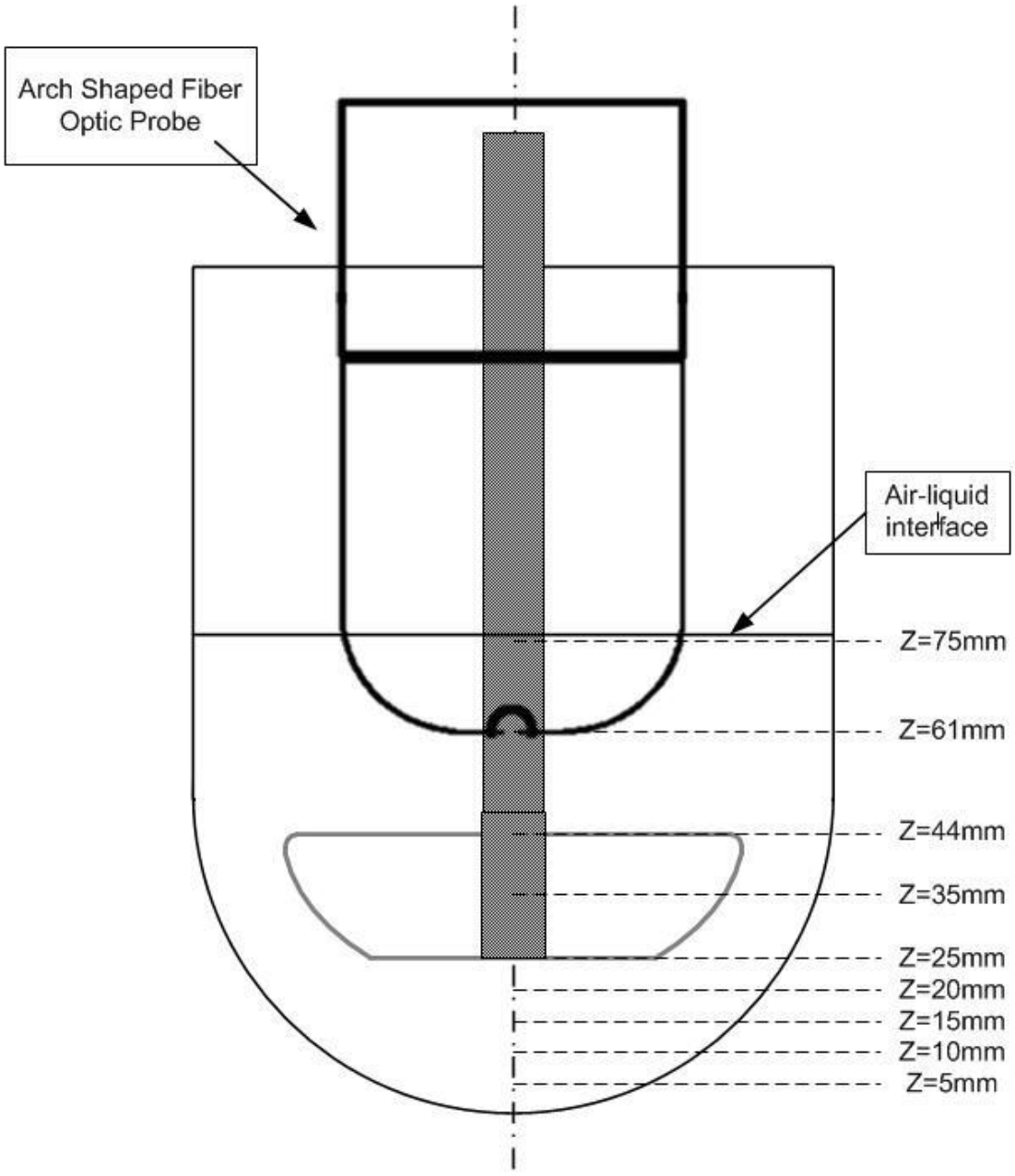

Figure 2.10 Nine iso-surfaces chosen for PIV measurements.

To fully quantify the fluid flow in the dissolution apparatus, nine horizontal surfaces (iso-surfaces) were selected inside the vessel, as shown in Figure 2.10. The

bottom of the vessel was defined as z=0 mm. Four iso-surfaces were chosen below the impeller (z=20mm, 15mm, 10mm and 5mm). Three were chosen in the impeller region: the top edge of the impeller, i.e., z=44mm, the middle of the impeller, i.e., z=35mm, and the bottom edge of the impeller, i.e., z=25mm. Two were chosen above the impeller, i.e., in the medium surface region, i.e., at z=75mm and at the bottom of the probe, i.e., at z=61mm. The radial and axial velocities on these iso-surfaces were extracted, plotted and analyzed.

Sums of squared deviations were calculated to compare the velocity profiles on the four sections of the testing system to those of the standard system. The equation used for this purpose is:

$$S = \sum \frac{(U - U_0)^2}{U_{tip}} \tag{2.6}$$

where U is the velocity of the testing system and U_0 is the corresponding velocity of the standard system at the same data point. By summing up all squared deviations in each of the three regions, i.e., below the impeller, around the impeller and above the impeller, as well as in the whole section, the hydrodynamic effect generated by the fiber optic probe could be identified and quantified.

CHAPTER 3

RESULTS

As discussed in Chapter 2, this study was focused on the quantification of the hydrodynamic effects introduced by the presence of a fiber optic probe in a USP Apparatus 2 by comparing the dissolution profiles obtained in the testing system and the standard system, and by visualizing the flow velocity vectors in the two systems using PIV measurements and quantitatively analyzing the velocities on nine iso-surfaces.

3.1 Results of Dissolution Tests

The dissolution profiles of Prednisone at nine different tablet positions (at 0°, 10° and 20°) in both systems were obtained following the method described in Section 2.1. The results were interpreted by plotting the drug release curve, i.e., the drug release ratio m_D/m_T against time (min), for all experimental run. The result were also interpreted by plotting the concentration ratio $C(t_n)/C^*$, i.e., the sample concentration at time n divided by fully dissolved concentration, against time (min). These results are shown in Appendix B.

To eliminate the effect of other variations such as room temperature and humidity, the dissolution profiles of the testing system were only compared with their corresponding profiles of the standard system. Each individual run was studied separately without taken any average. Paired t-test (t), similarity factor (f_1), and difference factor (f_2) were also calculated for each individual run.

3.1.1 Calibration Results for Prednisone Tablets

Calibration was performed following the method described in Chapter 2 Section 2.1.3. This process was initially performed twice to establish the conversion from UV absorbance to Prednisone concentration, and repeated every 3 months, without showing significant change. The results are presented in Table 3.1 and Figure 3.1 for two sets of calibration experiments.

Table 3.1 Calibration Data for Prednisone Tablets

Concentration (mg/ml)	Absorbance 1	Absorbance 2	Average Absorbance
0.05	2	1.947	1.9735
0.025	1.02	0.986	1.003
0.0166	0.68	0.675	0.6775
0.0125	0.536	0.506	0.521
0.01	0.44	0.428	0.434
0.005	0.253	0.243	0.248
0.0033	0.187	0.182	0.1845
0	0.055	0.055	0.055

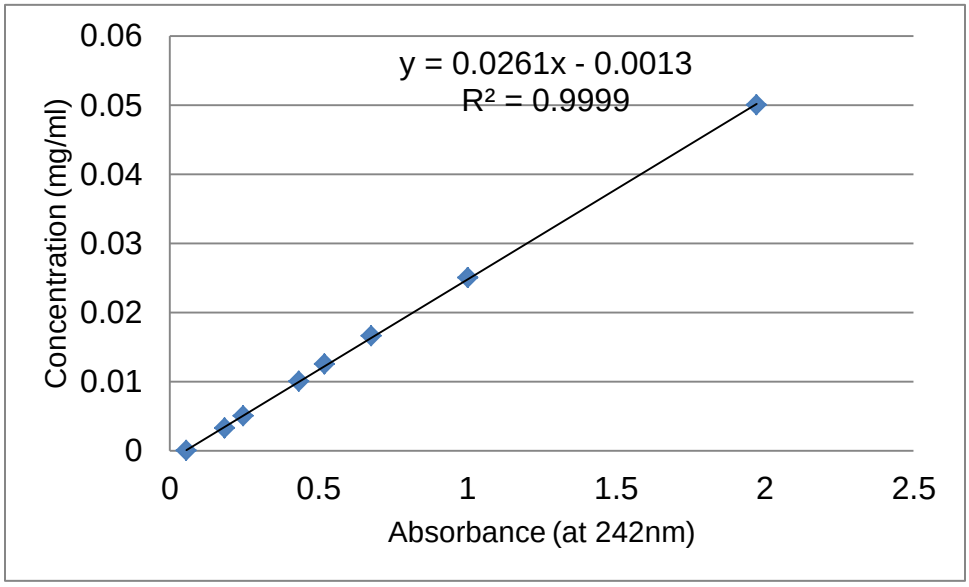

Figure 3.1 Calibration curve and regression for Prednisone tablets.

The difference between the two set of absorbance data was minor, and the R value of the regression was 0.9999. Therefore, a linear relation between UV absorbance and concentration was confirmed. The equation displayed in Figure 3.1 was used to obtain the concentration from absorbance data.

3.1.2 Dissolution Profiles for Centrally Positioned Tablets (Position 1)

The dissolution profiles for centrally positioned Prednisone tablets were obtained using both testing system and the standard system. The experiment with one testing system and one standard system running parallel was repeated three times. The results from these three runs are reported here in terms of drug release ratio m_D/m_T over time, and presented in Figure 3.2. The values of the Similarity Factor f_1 and the Difference Factor f_2 and the paired t-test T values were calculated as described in Section 2.4 and are presented in Table 3.2. The detailed data obtained in this study are shown in Tables C.1, C.2 and C.3 in Appendix C.

The difference between the dissolution profiles for the testing system and the standard system could be easily recognized: the testing system, with the fiber optic probe immersed in the liquid over the entire testing period, generated higher concentrations than the standard system in all three runs. The results of paired t-test showed that the T-values, i.e., the probabilities of the profiles being the same, were lower than the significant level of 0.05. On the other hand, the f1 and f2 values, quantifying the significance of similarity/difference of the dissolution profile of the testing system with respect to the corresponding standard system, were found all within the required FDA range. It should be noticed that in Run 2, both f_1 and f_2 were very close to the FDA limit and the test was just barely passed.

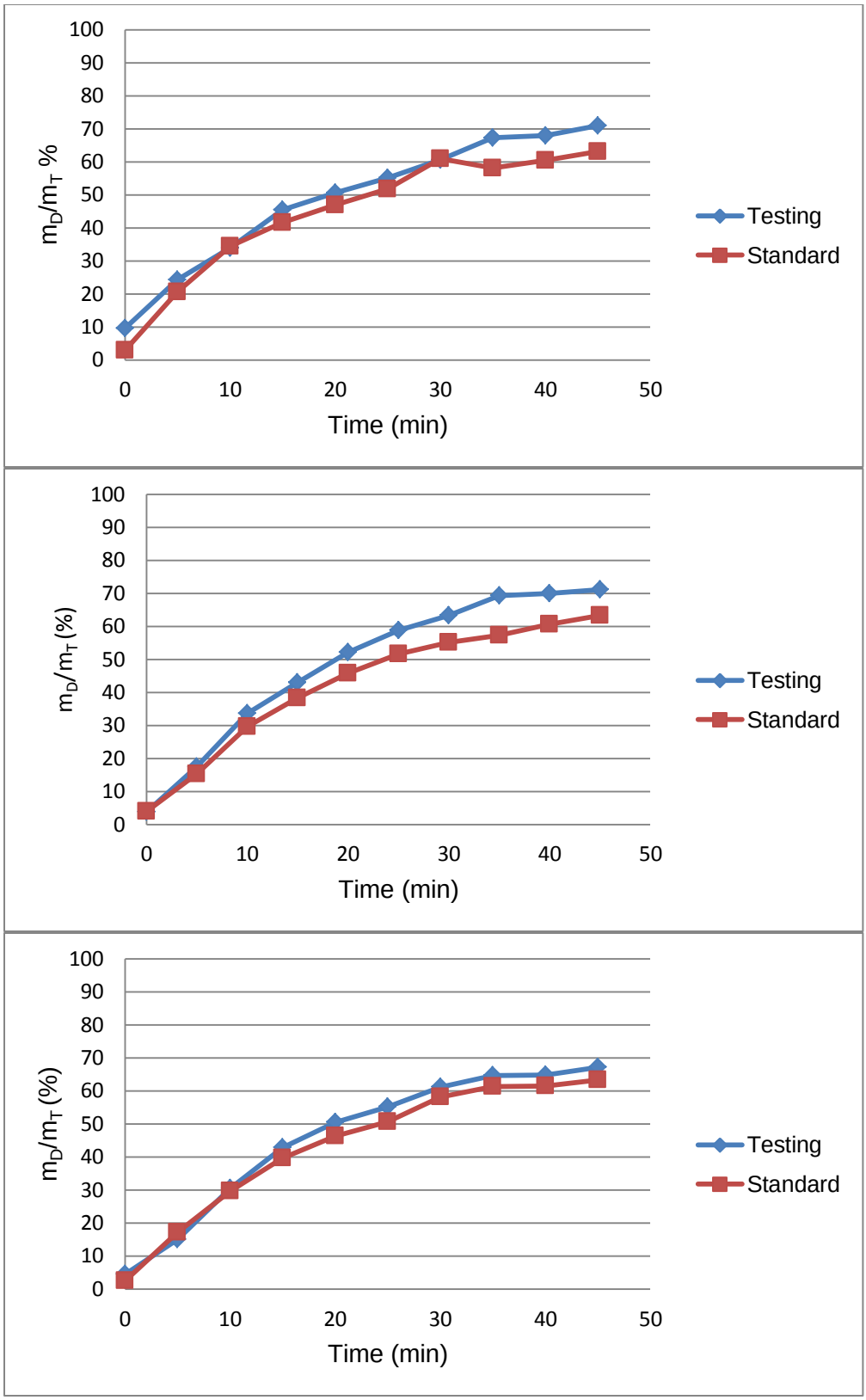

Figure 3.2 Dissolution profiles for three runs with Position 1 tablets.

Table 3.2 Statistical Values of Three Runs with Position 1 Tablets

	Paired T-test (T)	Similarity factor (f_1)	Difference factor (f_2)
Run1	0.005823	9.108	63.266
Run2	0.0001066	14.834	56.342
Run3	0.004491	6.687	72.925
Average		10.209	64.178

3.1.3 Dissolution Profiles for 10 ° Off-Center Tablets (Positions 2, 3, 4, and 5)

The dissolution profiles for 10 ° positioned Prednisone tablets were obtained using both the testing system and the standard system. The results from four positions on the 10 ° off-center circle i.e., Positions 2, 3, 4, and 5 in Figure 2.6 (a) are presented in Figure 3.3, 3.4, 3.5, 3.6, respectively. The corresponding statistics are presented in Table 3.3, 3.4, 3.5, 3.6, respectively, and the detailed data are shown in Tables C.4 to C.15 in Appendix C.

The tendency for the testing system to generate higher dissolution profiles than the standard system was found in all 10 ° off-center positions. The differences between the profiles from the two systems were consistent. On the other hand, the extents of differences were not consistent among the four positions. The most significant difference was found at Position 5, while the least significant one at Position 3.

Paired t-test, f_1 and f_2 calculation confirmed this observation. The probabilities of the profiles being the same were below the significant level of 0.05 for all runs. On the other hand, f_1 and f_2 values indicated that the differences for Position 5 were the largest and those for Position 3 were the smallest. In Run 3 in Position 5, both f_1 and f_2 went out of the FDA limit and dissolution test was failed.

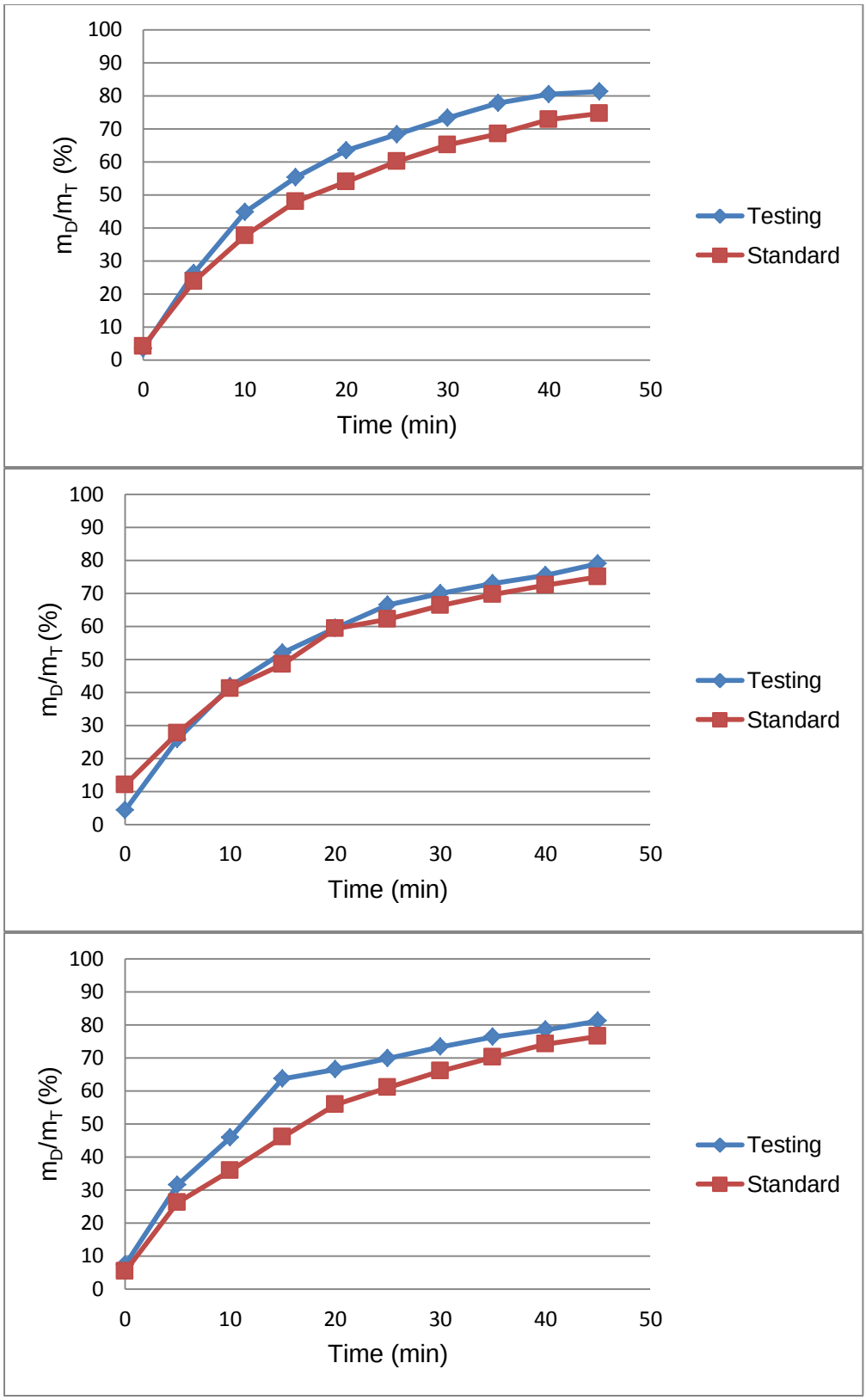

Figure 3.3 Dissolution profiles for three runs with Position 2 tablets.

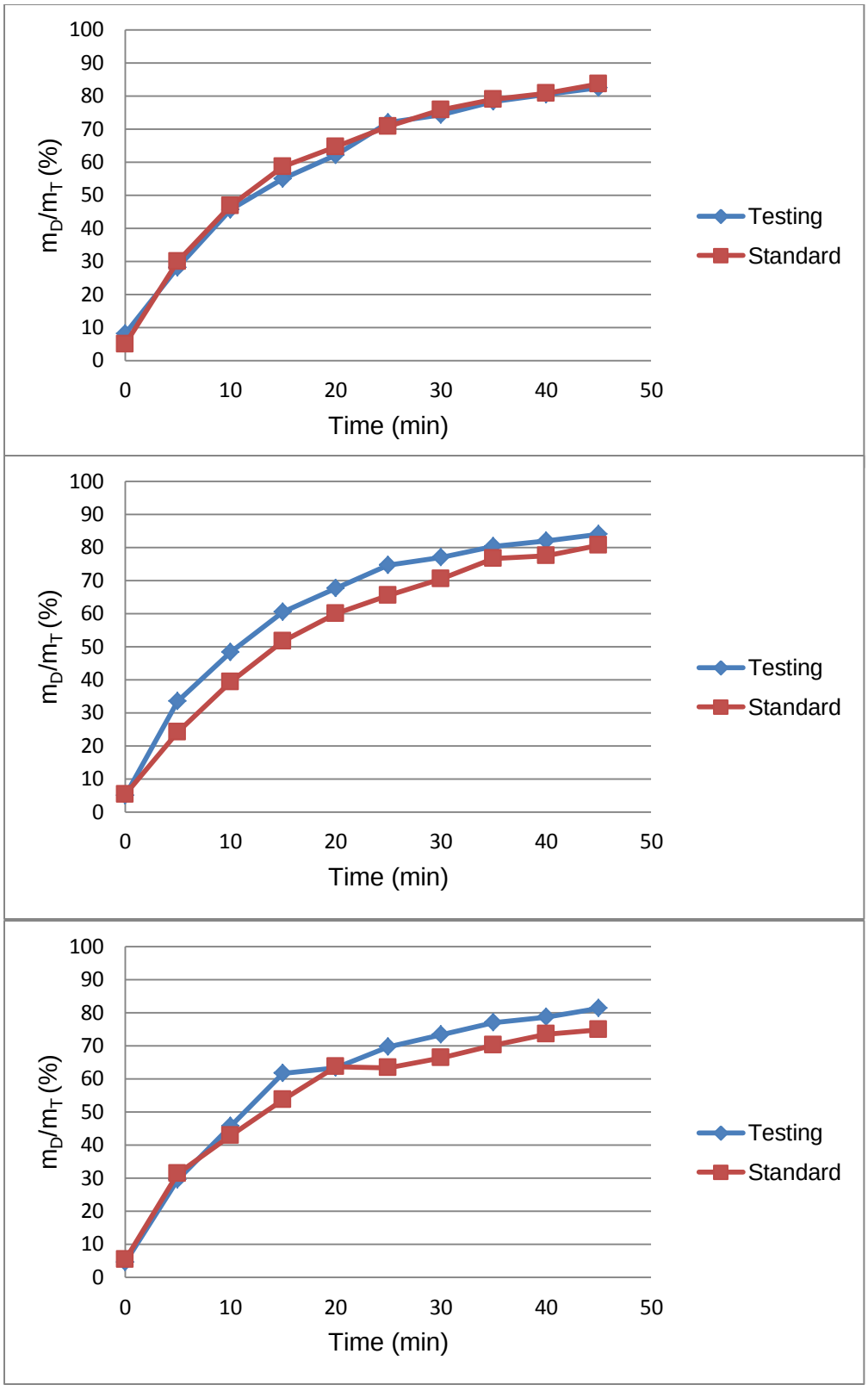

Figure 3.4 Dissolution profiles for three runs with Position 3 tablets.

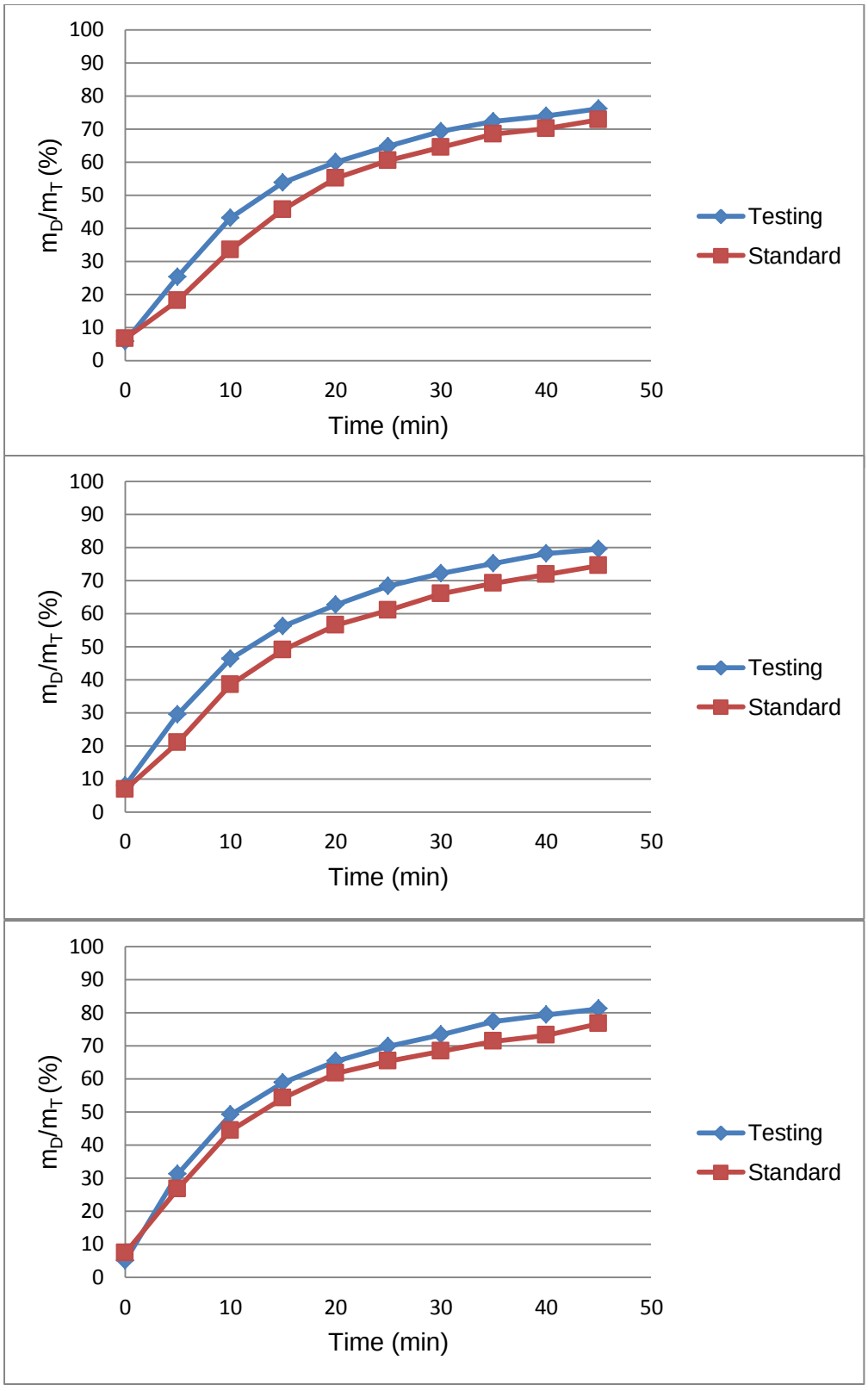

Figure 3.5 Dissolution profiles for three runs with Position 4 tablets.

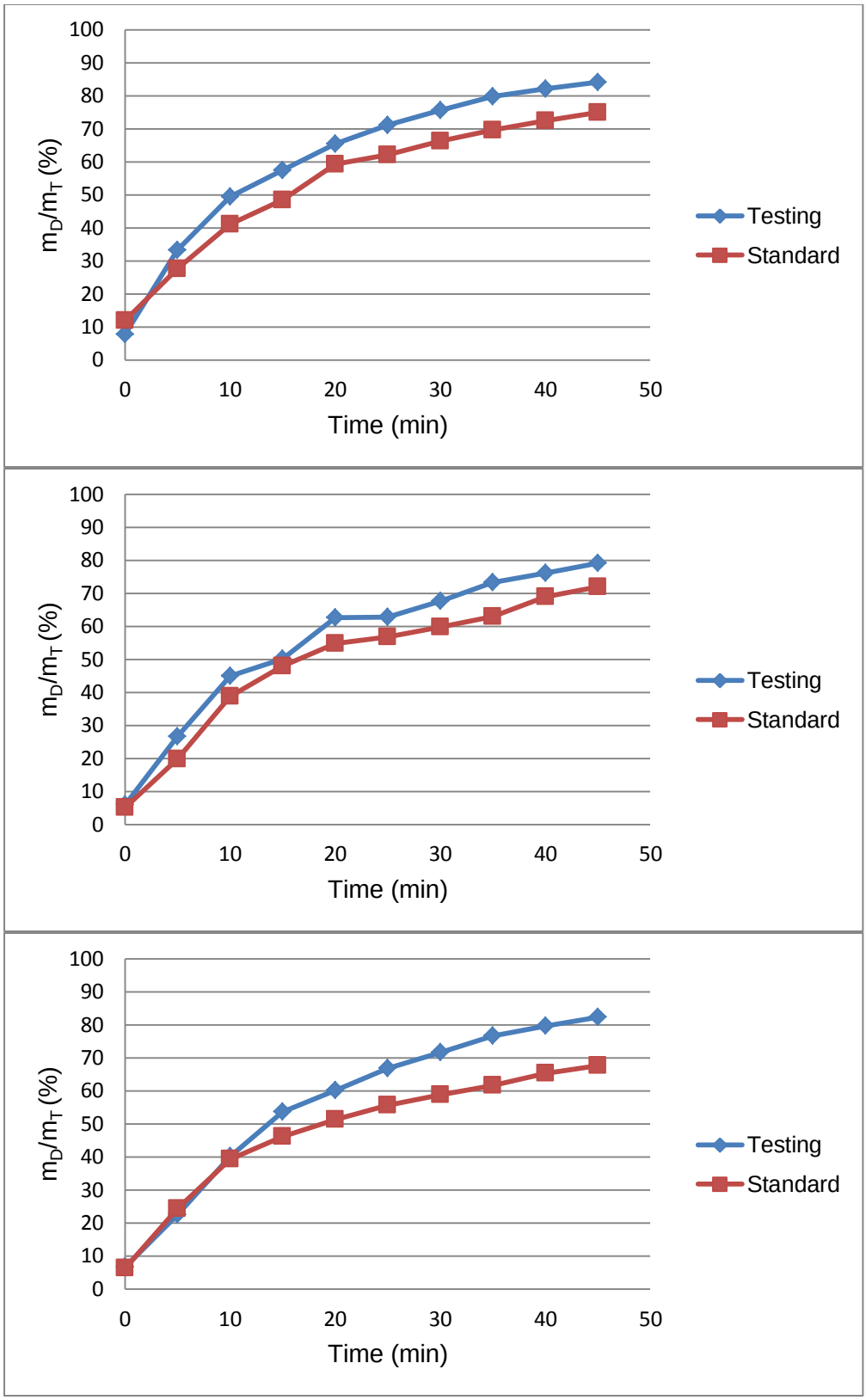

Figure 3.6 Dissolution profiles for three runs with Position 5 tablets.

Table 3.3 Statistical Values of Three Runs with Position 2 Tablets

	Paired T-test (T)	Similarity factor (f_1)	Difference factor (f_2)
Run1	5.491E-06	13.239	55.563
Run2	0.01079	4.721	74.536
Run3	0.0003098	14.723	51.607
Average		10.894	60.569

Table 3.4 Statistical Values of Three Runs with Position 3 Tablets

	Paired T-test (T)	Similarity factor (f_1)	Difference factor (f_2)
Run1	0.019365388	2.320	84.399
Run2	3.214E-05	11.307	56.816
Run3	0.004762	8.352	62.209
Average		7.326	67.808

Table 3.5 Statistical Values of Three Runs with Position 4 Tablets

	Paired T-test (T)	Similarity factor (f_1)	Difference factor (f_2)
Run1	6.599E-05	10.263	60.979
Run2	9.038E-08	11.908	58.175
Run3	8.640E-08	8.131	64.848
Average		10.101	61.334

Table 3.6 Statistical Values of Three Runs with Position 5 Tablets

	Paired T-test (T)	Similarity factor (f_1)	Difference factor (f_2)
Run1	1.835E-07	14.685	53.036
Run2	1.293E-05	12.778	57.119
Run3	0.001954	18.551	47.938
Average		15.338	52.697

3.1.4 Dissolution Profiles for 20 ° Off-Center Tablets (Positions 6, 7, 8, and 9)

The dissolution profiles for the 20 ° off-center Prednisone tablets were obtained using both the testing system and the standard system. The results for the tablets at four positions on the 20 ° off-center circle, i.e.,, for Positions 2, 3, 4, and 5 in Figure 2.6 (a), are presented in Figure 3.7, 3.8, 3.9, 3.10, respectively. The statistics are presented in Tables 3.7, 3.8, 3.9, and 3.10 respectively. The detailed data obtained in this study are shown in Tables C.16 to C.27 in Appendix C.

The difference between dissolution the profiles for the testing system and those for the standard system could still be easily recognized in Position 9, while the differences in Positions 6, 7 and 8 were much less pronounced. In some runs in Position 7 and Position 8, the profiles from the testing system were almost the same or even lower than the standard system.

The results of the paired t-test confirmed this observation. The T-values in Position 8 were much lower than the significant level of 0.05, while larger values were found in other positions. Run 1 in Position 6, Run 2 and Run 3 in Position 7 and Run 2 in Position 8 had T-values larger than 0.05, indicating a higher similarity between the profiles in the testing system and those in the standard system. Also, the f_1 values were highest and f_2 values were lowest for Position 8, suggesting the largest differences in dissolution profiles were found in this position.

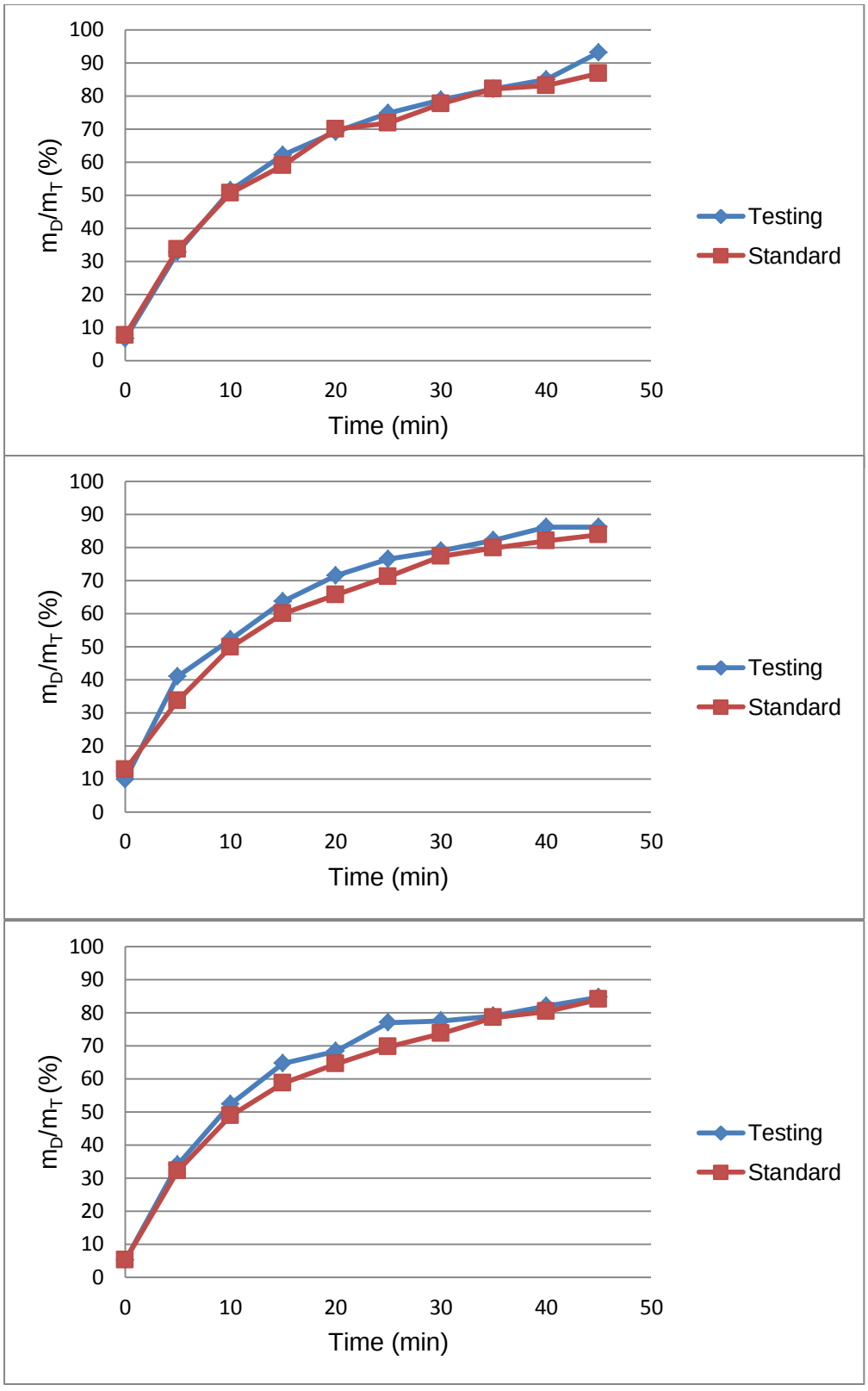

Figure 3.7 Dissolution profiles for three runs with Position 6 tablets.

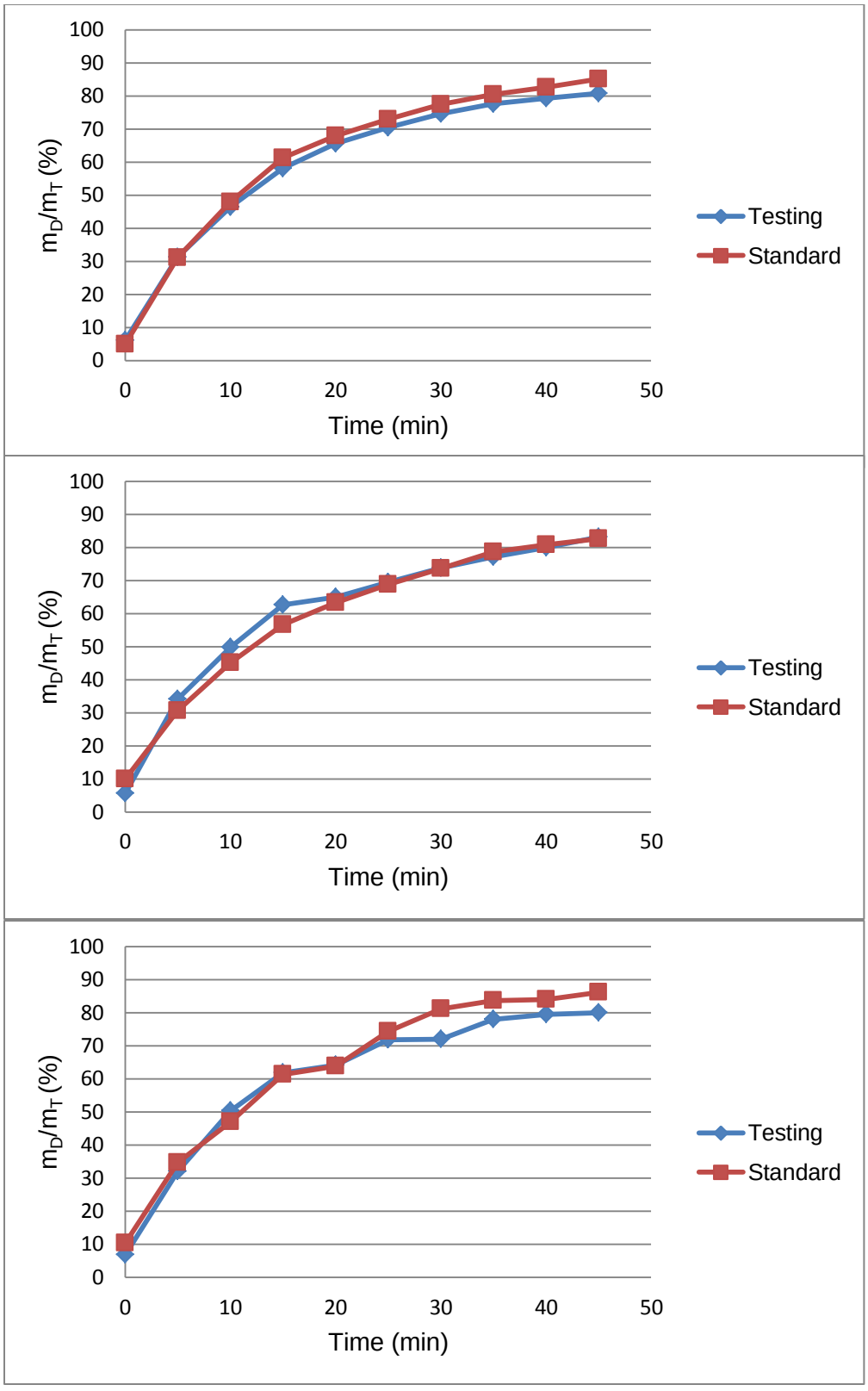

Figure 3.8 Dissolution profiles for three runs with Position 7 tablets.

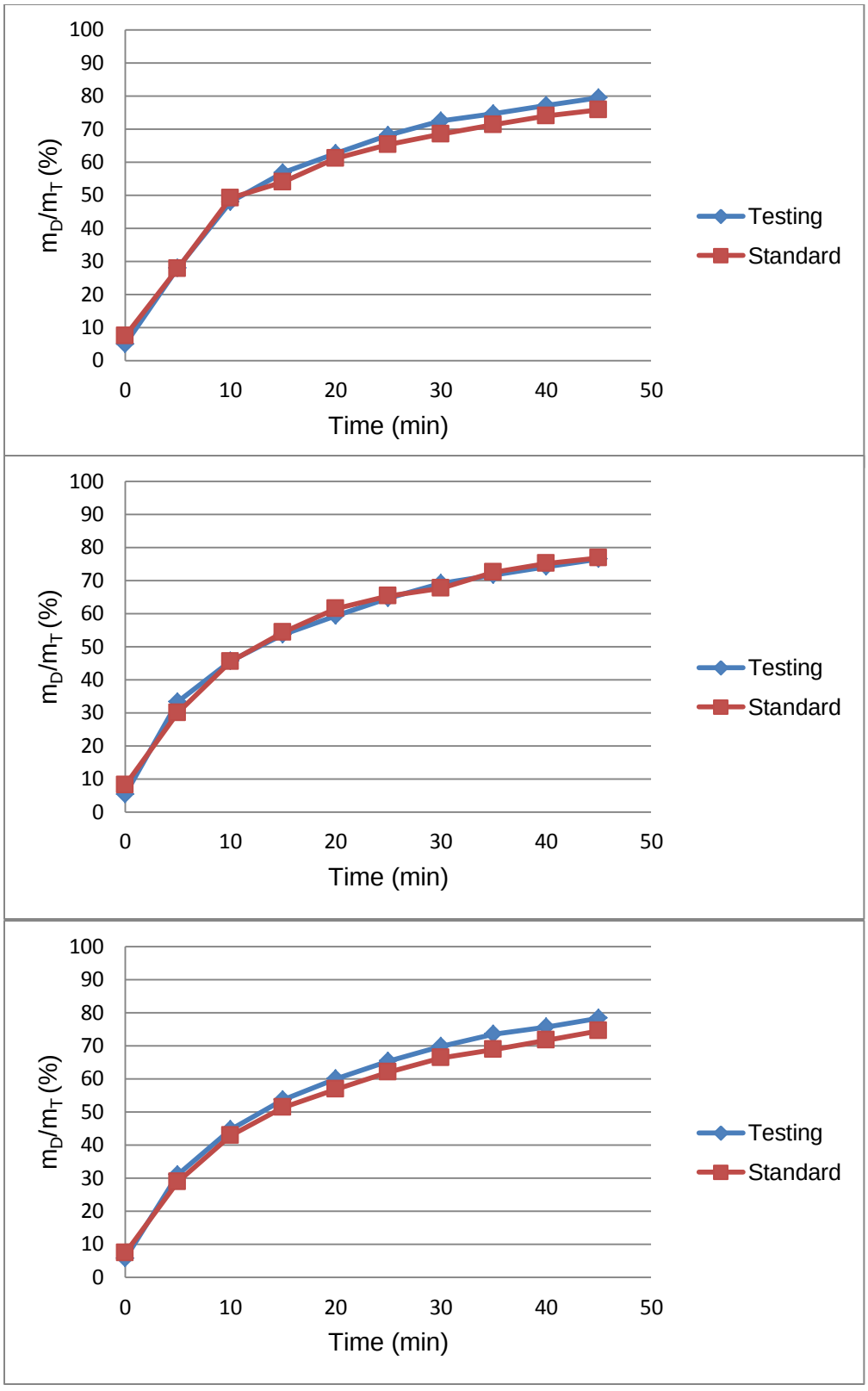

Figure 3.9 Dissolution profiles for three runs with Position 8 tablets.

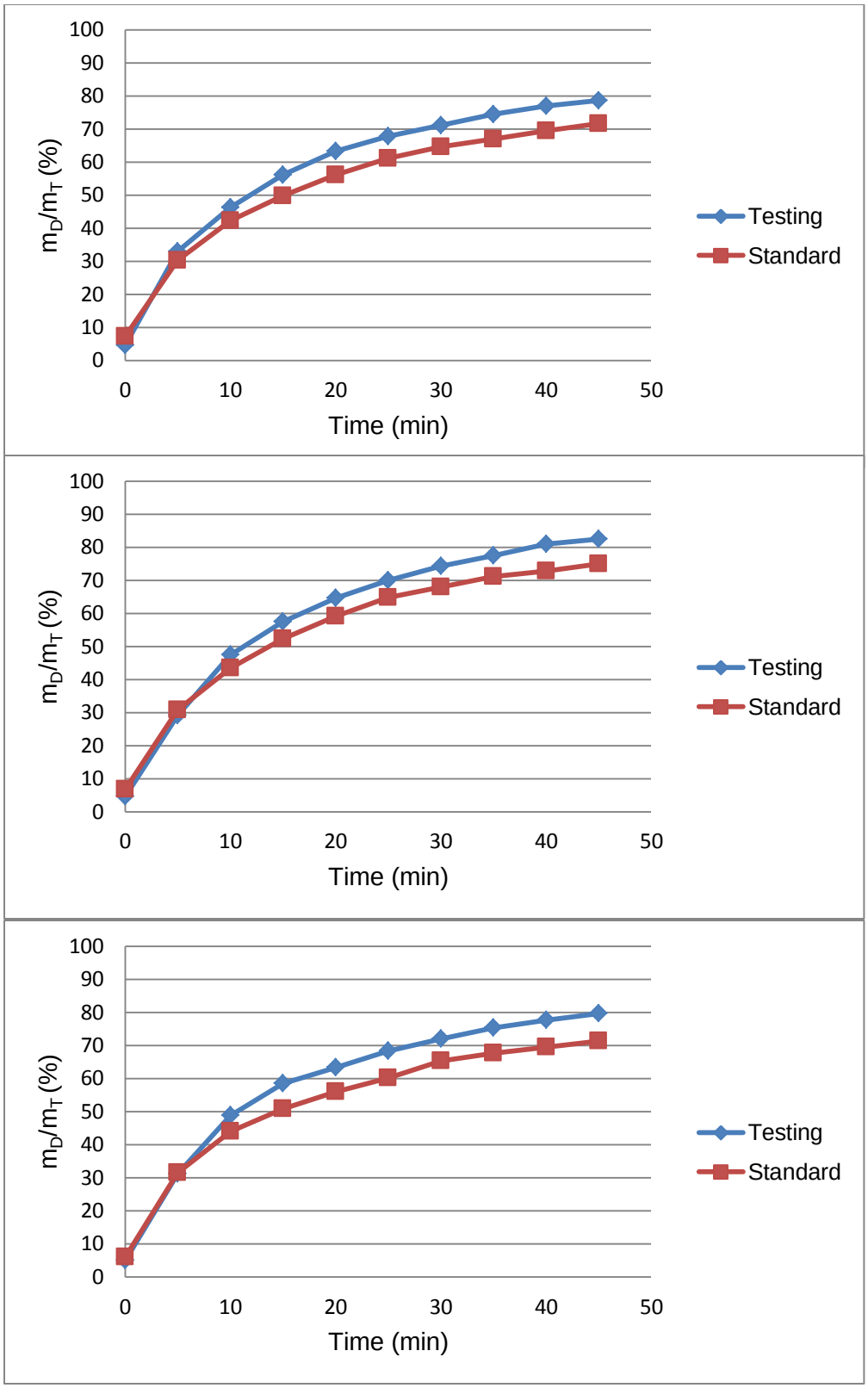

Figure 3.10 Dissolution profiles for three runs with Position 9 tablets.

Table 3.7 Statistical Values of Three Runs with Position 6 Tablets

	Paired T-test (T)	Similarity factor (f_1)	Difference factor (f_2)
Run1	0.07142	2.965	76.814
Run2	0.0002974	5.776	67.902
Run3	0.003185	4.966	69.566
Average		4.569	71.427

Table 3.8 Statistical Values of Three Runs with Position 7 Tablets

	Paired T-test (T)	Similarity factor (f_1)	Difference factor (f_2)
Run1	0.0003626	3.854	76.241
Run2	0.08837	3.404	75.494
Run3	0.05582	5.651	65.872
Average		4.303	72.536

Table 3.9 Statistical Values of Three Runs with Position 8 Tablets

	Paired T-test (T)	Similarity factor (f_1)	Difference factor (f_2)
Run1	0.004357	4.215	76.121
Run2	0.8734	1.996	86.947
Run3	7.659E-06	5.539	72.884
Average		3.917	78.651

Table 3.10 Statistical Values of Three Runs with Position 9 Tablets

	Paired T-test (T)	Similarity factor (f_1)	Difference factor (f_2)
Run1	4.266E-06	10.778	59.650
Run2	0.0005785	9.266	61.419
Run3	0.0001198	11.435	57.574
Average		10.493	59.547

3.2 Results of PIV Measurement

3.2.1 Velocity Vectors

Figure 3.11 and Figure 3.12 show the velocity vectors map in the standard system and for all four sections of the testing system. The vectors in each of the images are scaled with the same scale factor according to their magnitudes. The vectors are color-coded in order of increasing velocity magnitude. The vectors with the lowest velocities are plotted in dark blue, followed by light blue, green, yellow, orange and red, which represents the highest velocities.

The overall flow patterns in all vector maps were similar. The weak, impeller-generated upward and downward flows impacted the vessel wall, forming recirculation loops above and below the impeller. Above the impeller, the circulation loops were dominated by axial velocities. Two regions can be identified below the impeller: the first region is the outer region characterized by recirculation loops formed by the downwards flow produced by the agitation of the impeller and the vessel wall. The second region is the inner region just below the shaft at the center of the vessel bottom. This region was not penetrated by the recirculation loops of the first region, and the flow in this region was very weak. The flow patterns in the standard system were in agreement with those obtained in previous studies (Baxter et al., 2005; Bai and Armenante, 2009), and therefore were considered to be validated.

Despite the similarity between figures, two major differences can be observed. Firstly, in Section 2-6, the recirculation loop above the impeller became more intense, especially in the region where the probe was located. In the other sections in the testing system, the recirculation loops above the impeller were also affected by the presence of

the probe, although not significantly. Secondly, the flow velocities below the shaft, which is the most important region in the vessel since this is where the tablets would stay in actual dissolution tests, were strengthened in Section 2-6 and Section 5-9. Larger radial velocities and more defined and stronger circulations could be found. In contrast, in Section 3-7 and Section 4-8, the velocities in this region remained the same as those in the standard system, or even smaller.

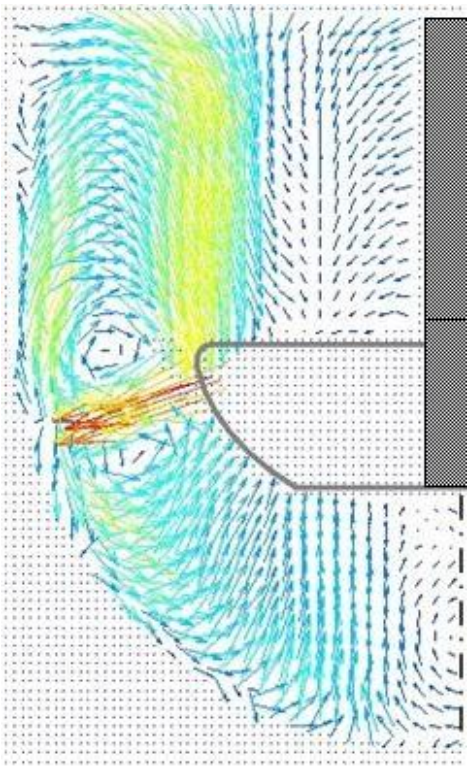

Figure 3.11 PIV velocity vectors map for the standard system.

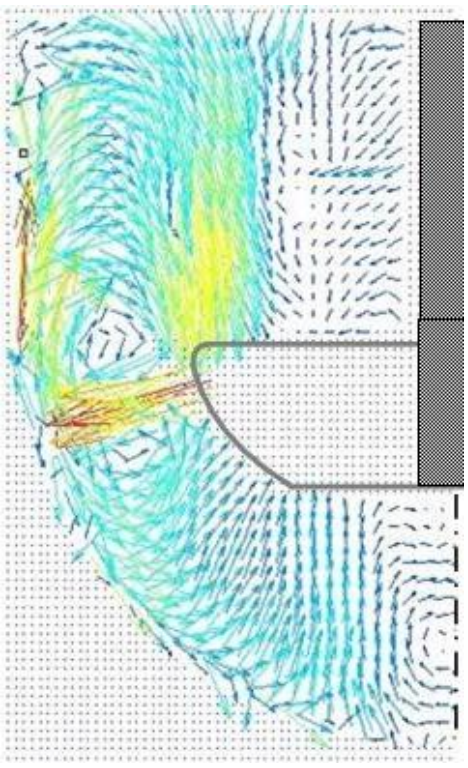

Section 2-6

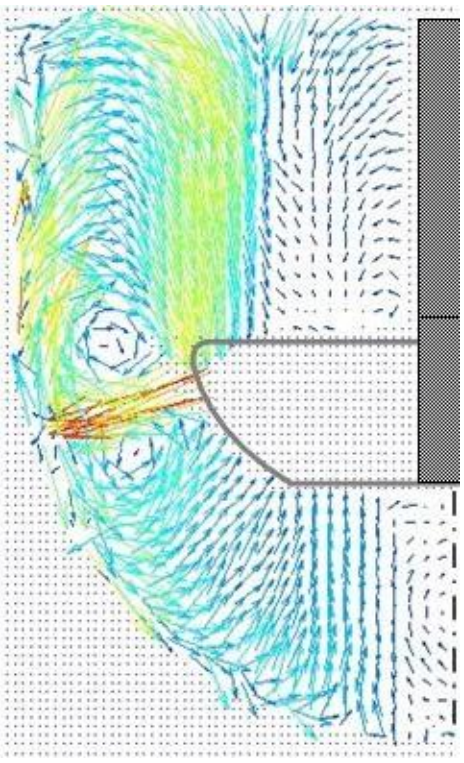

Section 3-7

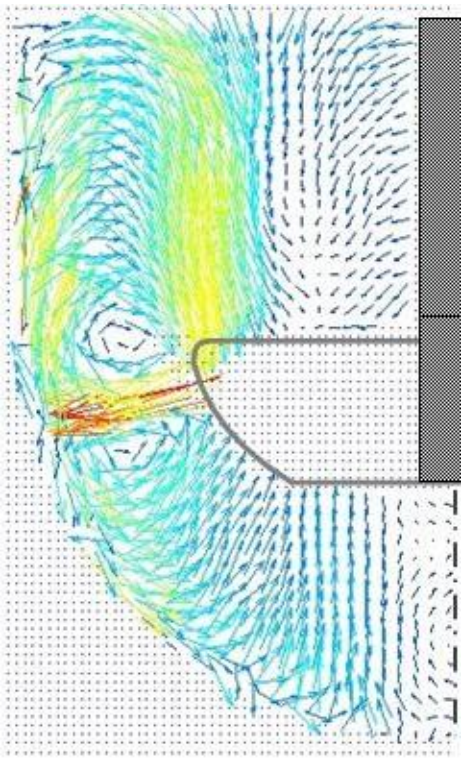

Section 4-8

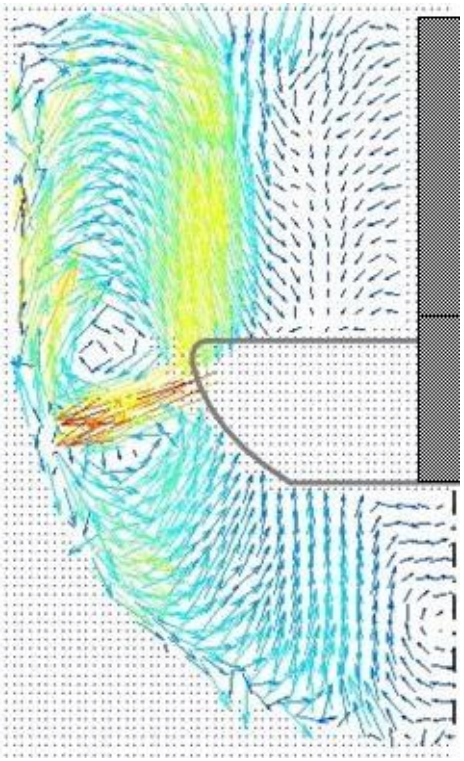

Section 5-9

Figure 3.12 PIV velocity vectors maps for all four sections in the testing system.

3.2.2 Velocity Profiles on Iso-Surfaces

Figures 3.13 through 3.18 show, respectively, the radial and axial velocity profiles on the nine iso-surfaces selected in Section 2.2.2. In these figures, the ordinates represent the normalized fluid velocity U/U_{tip} (scaled by the impeller tip speed, U_{tip}=0.197 mm/s) and the abscissas represent the normalized radial position R/R_0 (scaled using the vessel radius, R_0=50.08 mm). The centrifugal radial velocity and the upwards axial velocity were defined as positive velocity. It should be remarked that the scales in these figures are different.

3.2.2.1 Reproducibility of PIV Measurements. In order to determine the reproducibility of the PIV measurement and to determine the suitability of the instrument to detect differences between velocities in the standard system and in the testing system, 5 identical experiments with the standard system alone were conducted. The standard deviation for each data point was calculated and shown in the figures of velocity profiles in next three sections as error bars on data points for the standard system. The average standard deviations in three regions, i.e., below the impeller, around the impeller and above the impeller, are presented in Table 3.11.

The PIV measurements were found very reproducible in the regions below and above the impeller, while a slightly larger error was found for the velocities around the impeller, because the velocities in this region were affected by the presence of the impeller, therefore the velocities were faster and more turbulent, causing more inconsistency in the velocity data. In further measurements, if the differences in velocities found between the standard system and each section of the testing system were larger

than one standard deviation of that data point, i.e., out of the range of the error bar, the differences were attributed to hydrodynamic effects generated by the fiber optic probe.

Table 3.11 Average Standard Deviations of PIV Measurements in Three Regions for the Standard System

Region	Iso-Surfaces	Average Standard Deviation
Above the Impeller	Z=75 mm, 61 mm	0.002398
Around the Impeller	Z=44 mm, 35 mm, 25 mm	0.004368
Below the Impeller	Z=20 mm, 15 mm, 10 mm 5 mm	0.001962
Overall Average		0.002545

3.2.2.1 Velocity Profiles above the Impeller. Figure 3.13 and Figure 3.14 show, respectively, the radial and axial velocity profiles on the iso-surfaces above the impeller, i.e., Z=75 mm and 61 mm.

The differences of the velocities profiles between different systems can be easily observed in this region. Specifically, in the area where the probe was located, i.e., $0.4<R/R_0<0.7$ in Section 2-6, the impact of the probe was most pronounced. Significant differences were shown in both radial and axial velocities and on both Z=61 mm and Z=75 mm. Also the impact of the probe continued in the region downstream of the probe, i.e., Section 5-9, and as well in Section 4-8. On the other hand, in Section 3-7, from which the probe was farthest away, less noticeable deviation from the standard system was found.

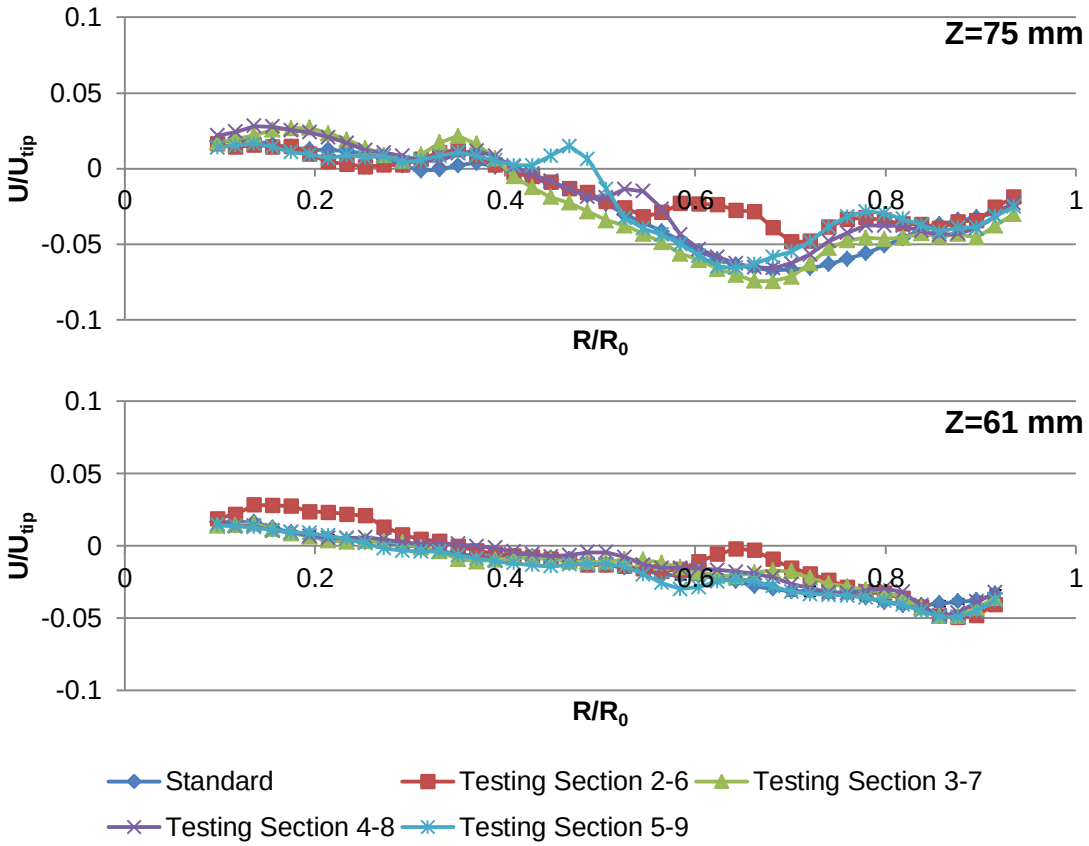

Figure 3.13 PIV measurements for radial velocities on iso-surfaces above the impeller.

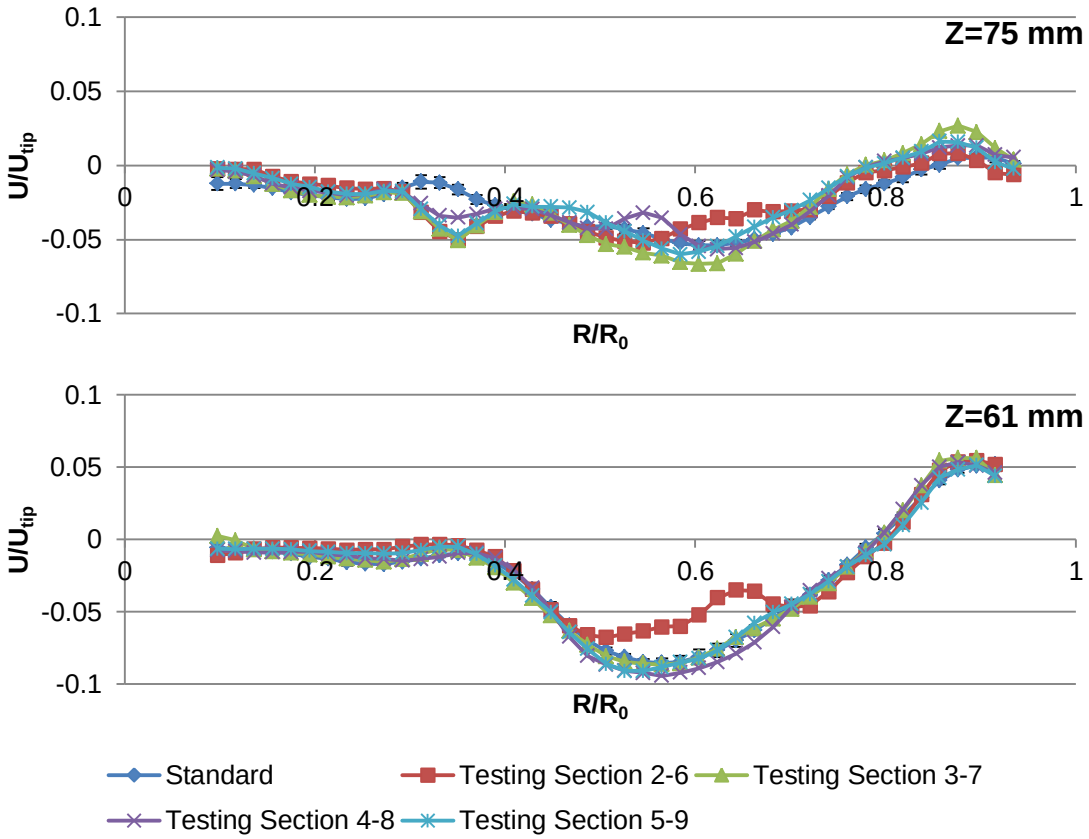

Figure 3.14 PIV measurements for axial velocities on iso-surfaces above the impeller.

3.2.2.2 Velocity Profiles around the Impeller. Figure 3.15 and Figure 3.16 show, respectively, the radial and axial velocity profiles on the iso-surfaces around the impeller, i.e., Z=44 mm, 35 mm and 25 mm.

A larger average standard deviation in this region was obtained (Table 3.11). In the figures, although the differences between runs were found to larger, most data points were within the error range indicated by the error bars. However, several differences cannot be attributed to experimental error. On iso-surface Z=25 mm, Section 2-6 had lower radial velocities near the vessel wall (R/R_0>0.7). On iso-surface Z=35 mm, where the transition between two recirculation loop occurred, all sections showed different flow

velocities compared to the standard system, indicating that the flows were stronger in this zone.

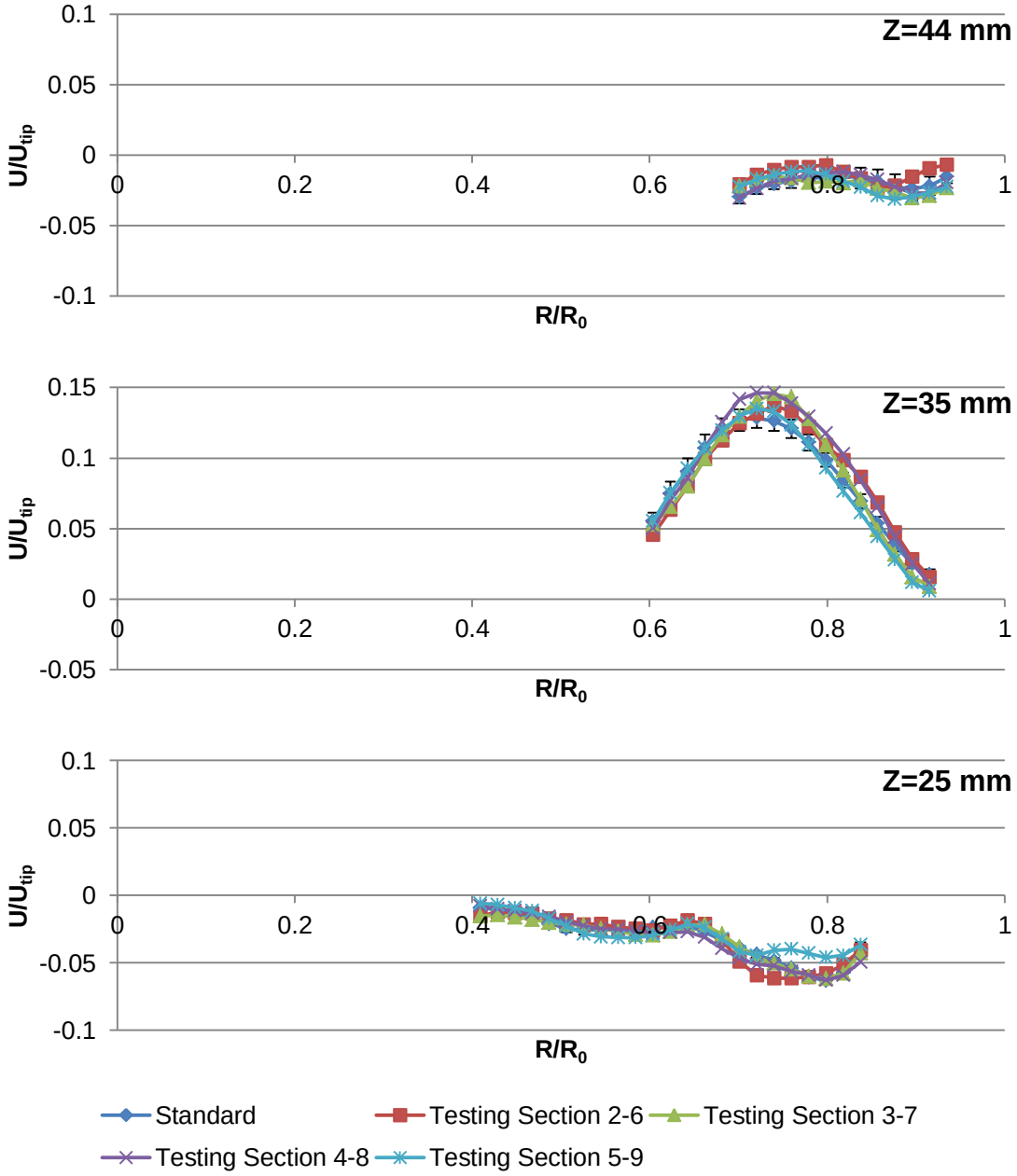

Figure 3.15 PIV measurements for radial velocities on iso-surfaces around the impeller.

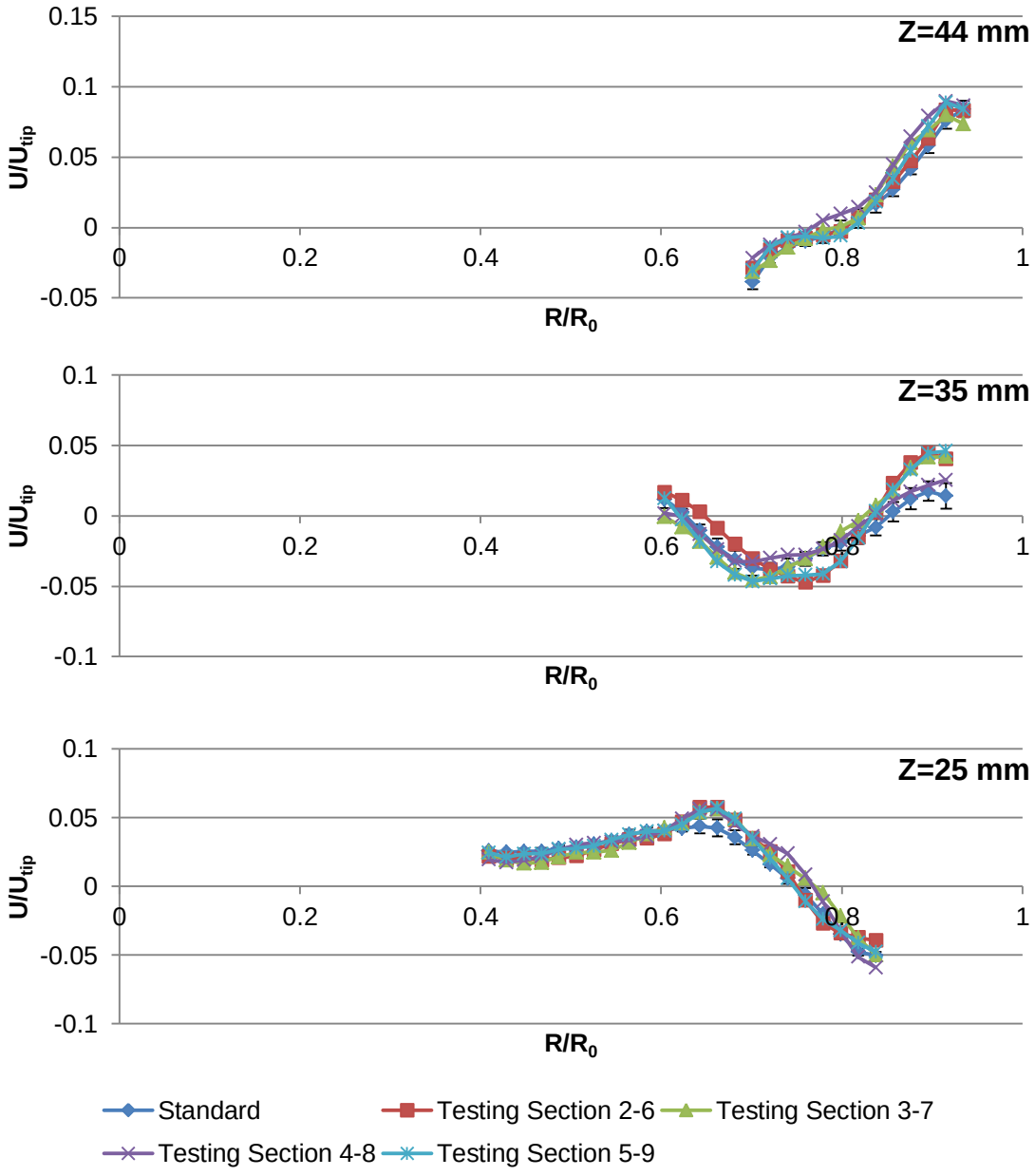

Figure 3.16 PIV measurements for axial velocities on iso-surfaces around the impeller.

3.2.2.3 Velocity Profiles below the Impeller. Figure 3.17 and Figure 3.18 show, respectively, the radial and axial velocity profiles on iso-surfaces below the impeller, i.e., Z=20 mm, 15 mm, 10 mm and 5 mm.

In general, the differences between the velocities were not significant in this region. The largest differences in both radial and axial velocities were found in the upward recirculation zone, i.e., $0.5<R/R_0<0.6$ for Z=20 mm, $0.4<R/R_0<0.5$ for Z=15 mm, $0.5<R/R_0<0.6$ for Z=10 mm, and $0.3<R/R_0<0.4$ for Z=5 mm, and the differences in this zone were obtained for all four sections in the testing system. Also slightly higher radial velocities in Section 2-6 and Section 5-9 were found in the low velocity zone below the shaft ($R/R_0<0.2$ for all four iso-surfaces), which supported the measurement of velocity vectors in Section 3.2.1.

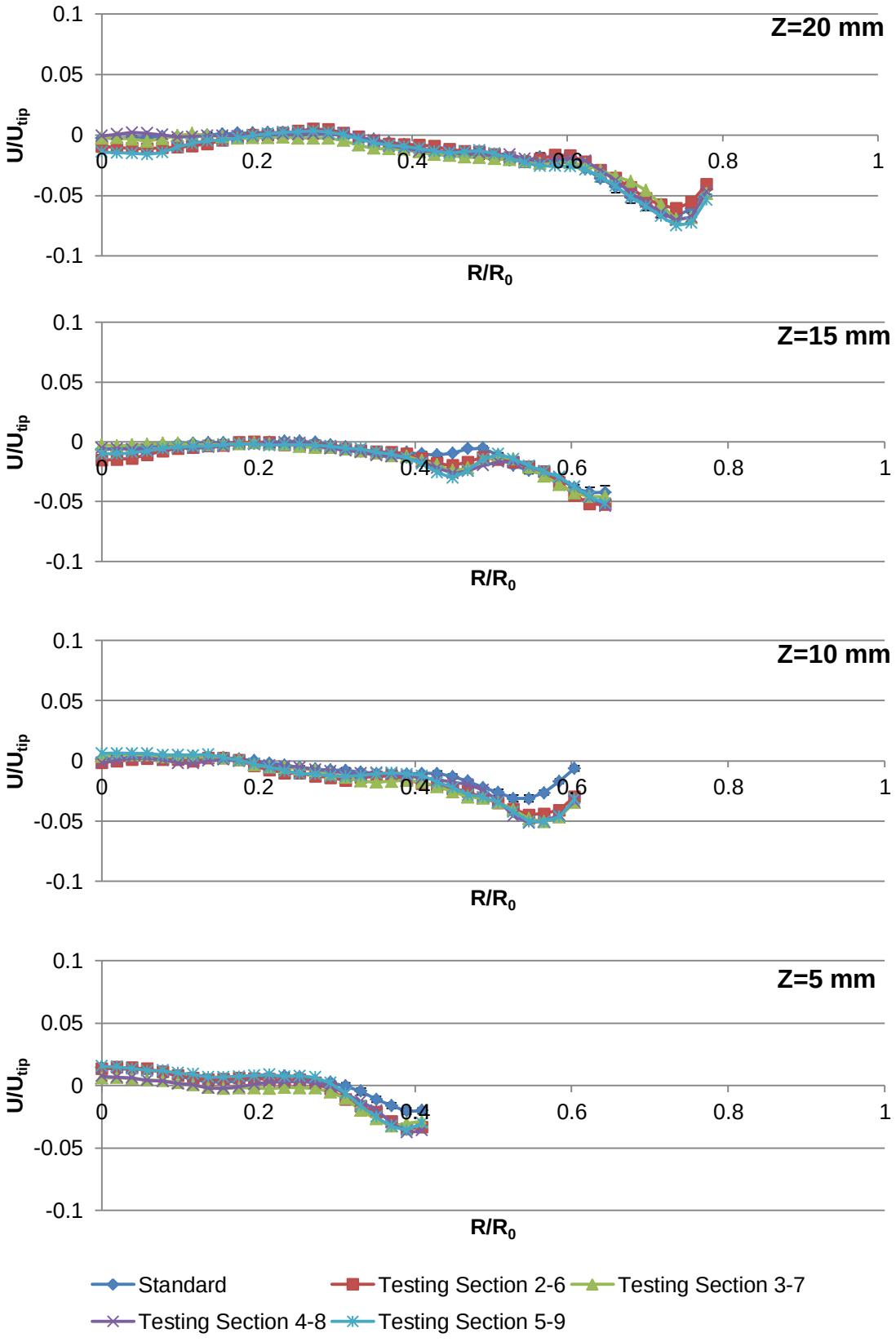

Figure 3.17 PIV measurements for radial velocities on iso-surfaces below the impeller.

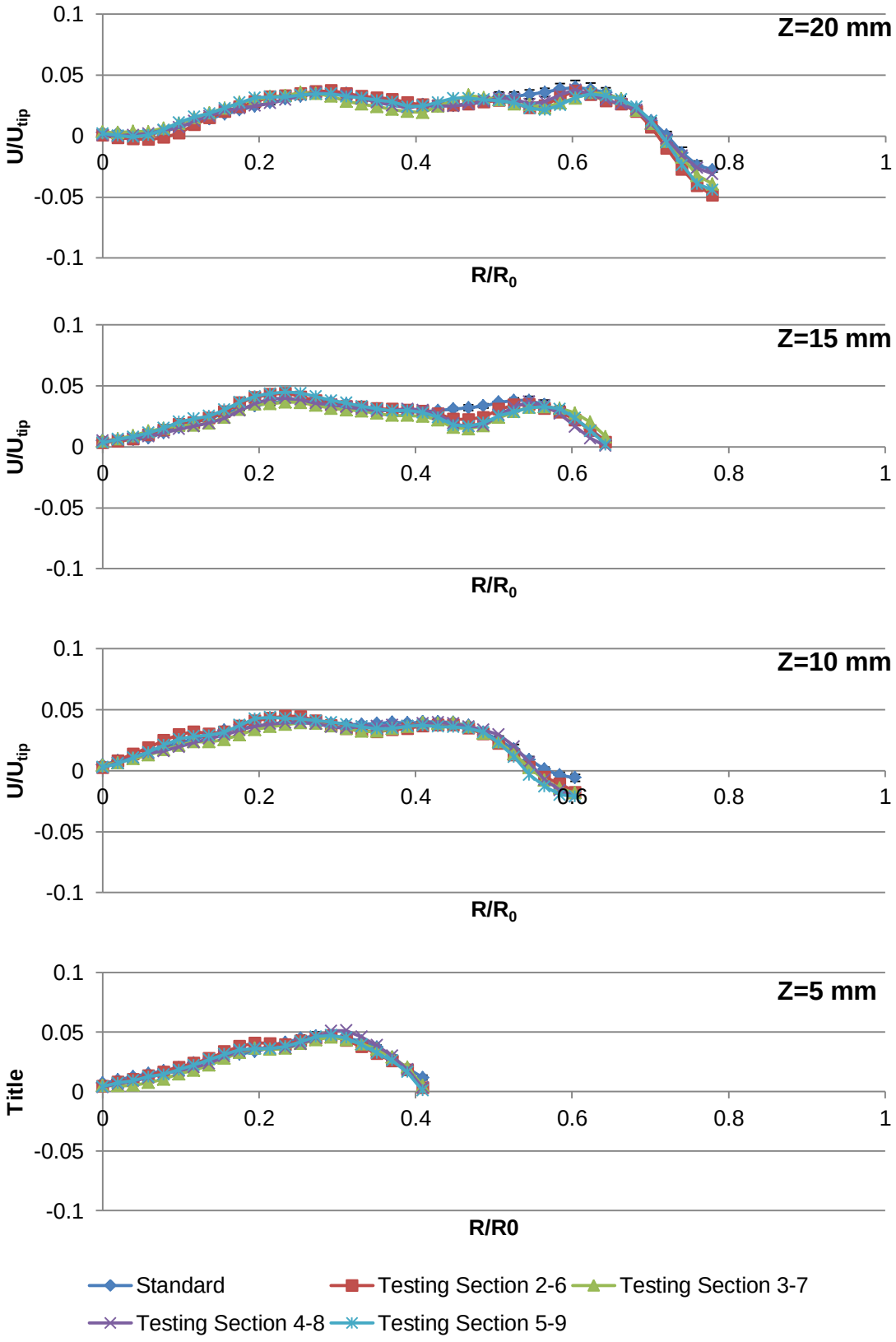

Figure 3.18 PIV measurements for axial velocities on iso-surfaces below the impeller.

3.2.3 Sums of Squared Deviations of the Velocity Profiles

The sums of squared deviation (S value) were calculated for each of the three regions, as described in Section 2.2.2. The results are shown in Table 3.12.

Among the four sections in the testing system, the velocities in Section 2-6 had largest total deviation compared to those in the standard system, due to the significant differences above the impeller where the probe was inserted. This was followed by Section 5-9, where the largest difference can be found in the region below the impeller. The deviations around the impeller were similar for all four sections, indicating again the flow in the region wa dominated by agitation, which was consistent with studies.

Table 3.12 Sums of Squared Deviations

Section	Section 2-6	Section 3-7	Section 4-8	Section 5-9
Above the Impeller	0.028667	0.012550	0.008817	0.013530
Around the Impeller	0.008852	0.007994	0.007503	0.007673
Below the Impeller	0.010987	0.008816	0.008272	0.011343
Total	0.048506	0.029365	0.024592	0.032546

CHAPTER 4

DISCUSSION

4.1 Dissolution Tests

The results of the experiments presented in Chapter 3 Section 3.1 show that the dissolution rates in the testing system were slightly higher than those in the standard system. Even though the differences between the dissolution profiles were not typically too large, they could nevertheless be observed in most runs, regardless of the positions of the tablets. For the majority of the runs, the Student's t-test values were lower than the significant level of 0.05 by one or more order of magnitudes, indicating that the two samples obtained with and without the probe were significantly unlikely to come from the same population, i.e., the testing system and the standard system generated statistically different dissolution results. On the other hand, the similarity factor f_1 and difference factor f_2 for most runs were within the acceptable ranges of, respectively, $0<f_1<15$ and $50<f_2<150$, as required by the FDA, which indicated that the differences were not significant enough to fail the dissolution test. Therefore, the results showed that the fiber optic probe in the system generated a small hydrodynamic effect that increased the dissolution rate of Prednisone tablets. The effect itself was not significant enough to cause failure of the test according to FDA requirement of f_1 and f_2. However, in the industrial practice, this effect would reduce the tolerance of the dissolution test. For example, a tablet that intrinsically dissolves slightly faster than what prescribed according to the standard specifications (but still within the acceptable dissolution testing acceptance range), could get out of spec in a dissolution test in which the fiber optic is

present, and fail the test because of the hydrodynamic effects introduced by the fiber optic probe.

Also, the impact of the hydrodynamic effect was found to be dependent on tablet location. Among both 10 ° off-center positions and 20 ° off-center positions, the positions where tablets were fixed at downstream region of the probe in agitation flow, i.e., Position 5 and 9, tented to generate more significant dissolution profiles differences between the two systems. This trend was also found, though less significantly, in the positions right below the probe, i.e., Position 2 and 6. Compared to other positions, Position 2, 5 and 9 had higher f_1 and lower f_2 values. In some individual runs, they even fell out of requirement range and failed the dissolution tests. The comparisons are shown in Table 4.1. The hydrodynamic effects were more pronounced in the zone where the probe was located and in the region downstream of the probe. This suggests that the probe generates a "baffle effect" in the vessel. As a result, the Prednisone tablets experience a stronger and more turbulent flow than before, hence dissolve faster than tablets at other positions. The flow perturbation was then diluted by the agitation flow, resulted in less significant difference in dissolution profiles of tablets at other positions.

Lastly, by comparing the result for tablet positions on different circles but in the same radial direction, i.e., Position 2 vs. Position 6, Position 3 vs. Position 7, etc., it can be found that 10 ° off-center positions tented to have larger dissolution profile differences between the two systems. This implies that the hydrodynamic effect was also differently pronounced at different off-center locations, in particular, more pronounced when the tablets were closer to the center of the vessel bottom.

Table 4.1 Average f_1 and f_2 Values of Dissolution Profiles for Each Tablet Position

	Position	Similarity factor (f_1)	Difference factor (f_2)
Centered	1	10.209	64.178
10 °off-center	2	10.894	60.569
	3	7.326	67.808
	4	10.101	61.334
	5	15.338	52.697
20 °off-center	6	4.569	71.427
	7	4.303	72.536
	8	3.917	78.651
	9	10.493	59.547

4.2 PIV Measurements

The PIV measurements were consistent with the results from experimental dissolution tests, and showed that the hydrodynamics inside the dissolution vessel was slightly affected by the introduction of the fiber optic probe. According to the velocity vector maps, the general flow pattern in the vessel remained similar in all four sections in the testing system, and it consisted of two recirculation loops and a low-velocity region below the shaft. On the other hand, perturbation in the flow caused by the probe were found above the impeller in Section 2-6, where the probe was located, confirming that the probe did generate a "baffle effect" altering the flow. Also, slight increases in the velocities can be found in the low velocity region in Section 2-6 and Section 5-9. These increases, though minor, may be responsible for a far more significant increase in the dissolution rate of the tablets fixed in those positions, since tablets would directly experience the flow in this region.

Further quantitative study on the nine iso-surfaces selected showed in detail the differences in the velocity profiles between the standard system and the testing system, and between different sections in the testing system.

In the region above the impeller, the most significant difference was observed in Section 2-6, and this was in agreement with the observation from the velocity vector maps. The S values in this region showed the results of the "baffle effect". The probe disturbed the flow going through, generated the largest deviation from the standard system in Section 2-6, and then this flow perturbation was diluted and weakened downstream through Section 5-9, Section 3-7 and Section 4-8, in which gradually smaller S values were found.

In the region around the impeller, despite the slightly larger variation in velocity magnitude due to more turbulent flows, the S values were similar for all sections, indicating that the introduction of the probe did not affect flows in this region, which remained dominated by the impeller.

The region below the impeller was more carefully studied with four iso-surfaces selected, since the dissolution rate of the tablet was expected to be more sensitive to the flow velocity it experienced directly in this region. Section 5-9 was found to have the largest S value, which coincided with the faster dissolution rates of tablets in Position 5 and Position 9. This can be explained that the perturbation generated by the probe above the impeller which reached the region below the impeller at a location further downstream of the probe. Although the perturbation may die down along the recirculation pattern, its effect could still be noticed, especially in contrast with the low velocities baseline below the shaft. This also explained why the effect was more

pronounced for tablets placed 10 ° off-center positions than 20 ° off-center. The central and 10 ° off-center tablet positions were within or partially within the low velocity region under the impeller, while the 20 ° positions were within the upwards recirculation region. Therefore, the baseline velocities were much lower in central and 10 ° off-center positions. As a result, any velocity perturbation in this region was more significant, and greater differences in dissolution rates between the two systems were observed for these tablet positions.

CHAPTER 5

CONCLUSIONS

The hydrodynamic effects of the arch-shaped fiber optic probe in USP Dissolution Testing Apparatus 2 were determined by experimentally comparing the dissolution profiles obtained in the testing system with those in the standard system, and by determining the flow velocities in the two systems via PIV.

Several conclusions can be drawn from this study. The arch shaped fiber optic probe, inserted in the USP-specified sampling zone in the USP Apparatus 2, did have a baffling effect on the hydrodynamics in the dissolution vessel. This effect resulted in a change in the velocities in the fluid flow, and therefore in a change in the dissolution rate of the testing tablet. The baffle effect was observed mainly in the region where the probe was inserted. The flow perturbation that it generated became gradually weaker downstream of the agitation path. This perturbation was also found to reach the region below the impeller and to change the velocity profile there. The effect was most pronounced downstream of the probe within the low velocity region right below the shaft, and this resulted in the most significant difference in dissolution profiles when the tablets were fixed at positions that were downstream of the probe and within the low velocity region.

On the other hand, the hydrodynamic effect generated by the probe was not particularly strong. In most dissolution testing runs, the changes in dissolution profile were not large enough to fail the tests, according to the FDA criteria (f_1 and f_2 values).

The PIV measurements additionally show that the baffle effect was not strong enough to break the overall flow pattern, or to affect the region around the impeller, which was dominated by the agitation flow.

In summary, the hydrodynamic effects generated by the arch-shaped fiber optic probe are real and observable, resulting in slightly modification of the fluid flow in the dissolution vessel and therefore in detectable differences in the dissolution profiles. However, these effects are limited and do not typically lead to dissolution testing failures.

APPENDIX A

DERIVATION OF EQUATION 2.1

In this Appendix, Equation 2.1 in Section 2.1.4 was derived based on the mass balance in the dissolution system.

Table A.1 Medium volume change in dissolution tests

	Initial System	t_o=0	t_1	t_2	t_i	t_n
Volume before taking sample		V	V-ΔV	V-2ΔV	V-iΔV	V-nΔV
		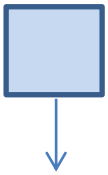 ΔV	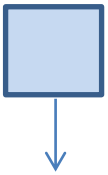 ΔV	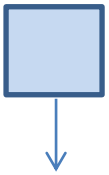 ΔV	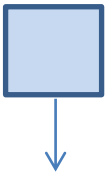 ΔV	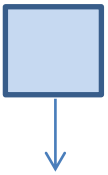 ΔV
Remaining volume after taking sample		V- ΔV	V-2ΔV	V-3ΔV	V-(i+1)ΔV	V-(n+1)ΔV

The drug release ratio needed to be determined:

$$\frac{mass\ of\ drug\ in\ solution\ at\ t}{initial\ mass\ of\ drug\ in\ tablet} = \frac{m_{Dissolved}(t)}{m_{Tablet}} = \frac{m_D(t)}{m_T}$$

i.e., the amount of drug in solution at any time t out of the total initial amount of drug in the tablet.

The initial volume of solution (medium) is V, and each sample has a volume equal to ΔV. Also, the mass of drug initially in the tablet is:

$$m_T = C^* \cdot V \quad \text{i.e.,} \quad C^* = \frac{m_T}{V}$$

In general, at any time t just after taking a sample, the mass balance for the drug removed from the tablet (and transferred to the solution) gives:

$$\begin{pmatrix} \text{mass of drug} \\ \text{removed from tablet} \end{pmatrix} = \begin{pmatrix} \text{mass of drug} \\ \text{left in solution after} \\ \text{sample is taken} \end{pmatrix} + \begin{pmatrix} \text{mass of drug} \\ \text{in current sample} \end{pmatrix} + \begin{pmatrix} \text{mass of drug in all} \\ \text{previous samples} \end{pmatrix}$$

In the presented system, the tablet was dropped in the medium at $t=t_o$, the agitation was immediately started, and a sample was immediately taken (at $t=t_o=0$, corresponding to the initial zeroth sample). This means that for $t=t_o$ (@ t=0) i.e., after the tablet was dropped and the initial sample was taken (and found to have $C=C_0$), the above mass balance gives:

$$\frac{m_D(t_o)}{m_T} = \frac{C_0(V-\Delta V)+C_0\Delta V+0}{C^*V} = \frac{C_0V}{C^*V} = \frac{C_0}{C^*}$$

For $t=t_1$ (corresponding to a sample concentration $C=C_1$) the mass balance gives:

$$\frac{m_D(t_1)}{m_T} = \frac{C_1(V-2\Delta V)+C_1\Delta V+C_0\Delta V}{C^*V} = \frac{C_1(V-\Delta V)+C_0\Delta V}{C^*V}$$

For $t=t_2$ (corresponding to a sample concentration $C=C_2$):

$$\frac{m_D(t_2)}{m_T} = \frac{C_2(V-3\Delta V)+C_2\Delta V+(C_0+C_1)\Delta V}{C*V} = \frac{C_2(V-2\Delta V)+(C_0+C_1)\Delta V}{C*V}$$

For $t=t_i$ (corresponding to a sample concentration $C=C_i$):

$$\frac{m_D(t_1)}{m_T} = \frac{C_i(V-(i+1)\Delta V)+C_i\Delta V+(C_0+C_1+\ldots+C_{i-1})\Delta V}{C*V}$$
$$= \frac{C_i(V-i\Delta V)+(C_0+C_1+\ldots+C_{i-1})\Delta V}{C*V}$$

For $t=t_n$ (corresponding to a sample concentration $C=C_n$):

$$\frac{m_D(t_n)}{m_T} = \frac{C_n(V-(n+1)\Delta V)+C_n\Delta V+(C_0+C_1+\ldots+C_i+\ldots C_{n-1})\Delta V}{C*V}$$
$$= \frac{C_n(V-n\Delta V)+(C_0+C_1+\ldots+C_i+\ldots+C_{n-1})\Delta V}{C*V}$$

Hence, for $t=t_n$ (corresponding to a sample concentration $C=C_n$):

$$\frac{m_D(t_n)}{m_T} = \frac{C_n(V-n\Delta V)}{C*V} + \sum_{i=0}^{n-1}\frac{C_i\Delta V}{C*V}$$

and finally:

$$\frac{m_D(t_n)}{m_T} = \begin{pmatrix} \textit{fraction of drug dissolved at } t_n, \\ \textit{i.e., immediately after nth} \\ \textit{sample was taken} \end{pmatrix} = \frac{C_n}{C^*}\left(1 - \frac{n\Delta V}{V}\right) + \frac{\Delta V}{V}\sum_{i=0}^{n-1}\frac{C_i}{C^*}$$

Remark: in this study a sample was initially taken at $t=t_o=0$ (zeroth sample). This means that the 10th sample (including the initial one) corresponds to n=9 (not n=10), i.e., n=0, 1, 2, 3, 4, 5, 6, 7, 8, and 9 (10 samples taken every 5 minutes, starting at time $t=t_o=0$ min, and ending at time t_9=45 minutes).

APPENDIX B

DISSOLUTION PROFILES USING CONCENTRATION RATIO VS. TIME

In this Appendix, dissolution profiles of Prednisone in both the standard system and the testing system are plotted as concentration ratio $C(t_n)/C^*$ vs. time in Figure B.1 to B.9. And the statistical values of these plots are shown in Table B.1 to B.9

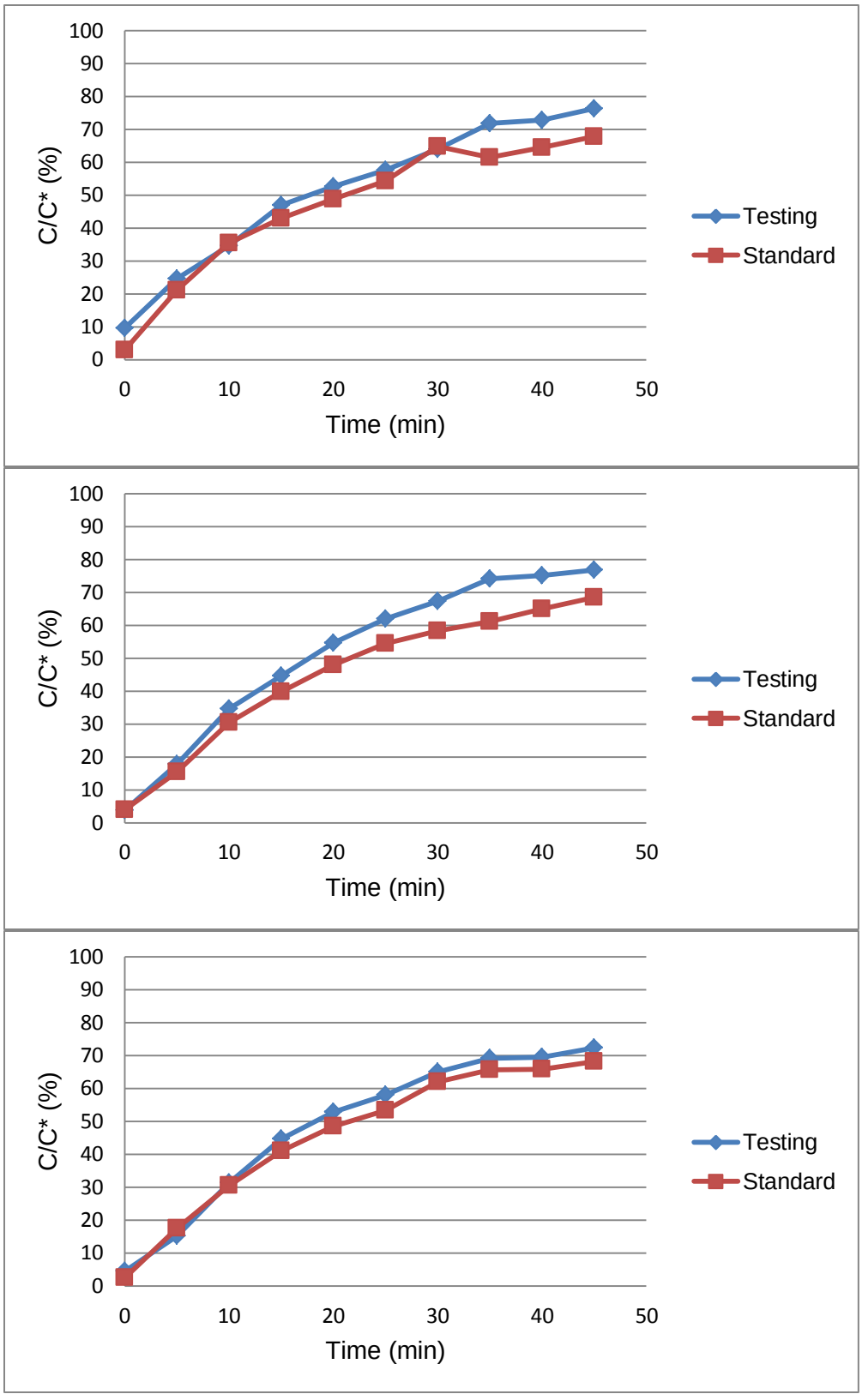

Figure B.1 Dissolution profiles for three runs with Position 1 tablets.

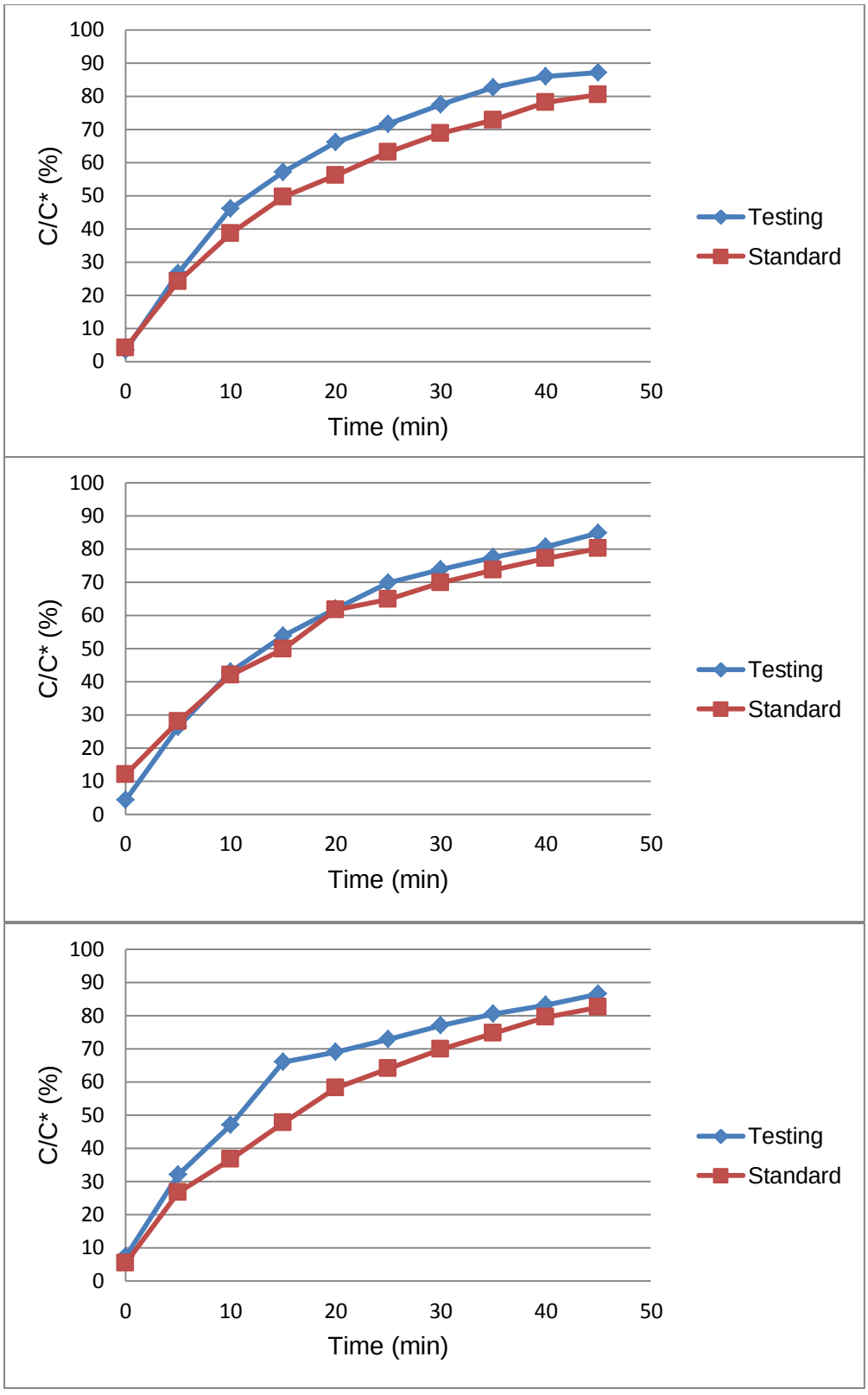

Figure B.2 Dissolution profiles for three runs with Position 2 tablets.

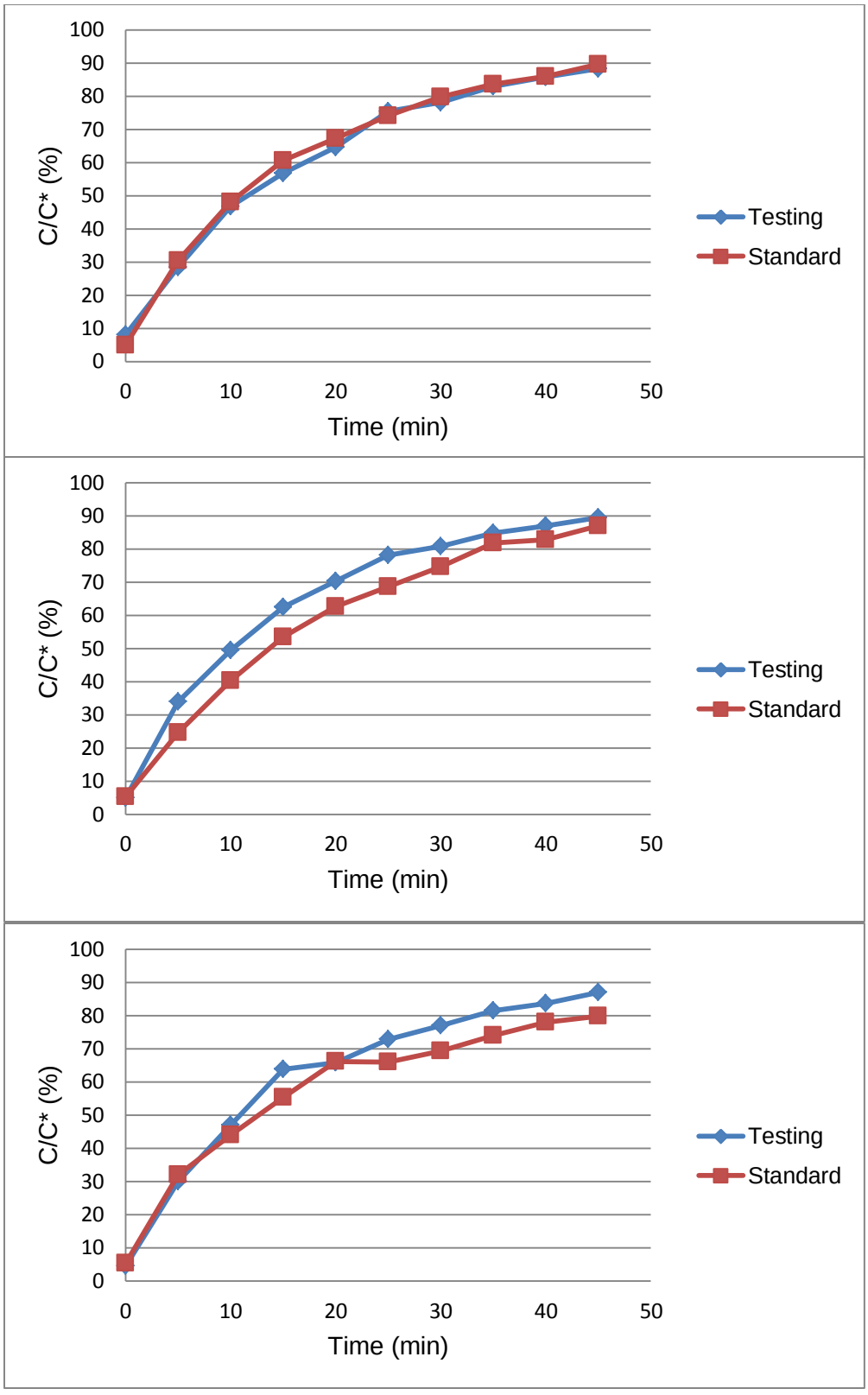

Figure B.3 Dissolution profiles for three runs with Position 3 tablets.

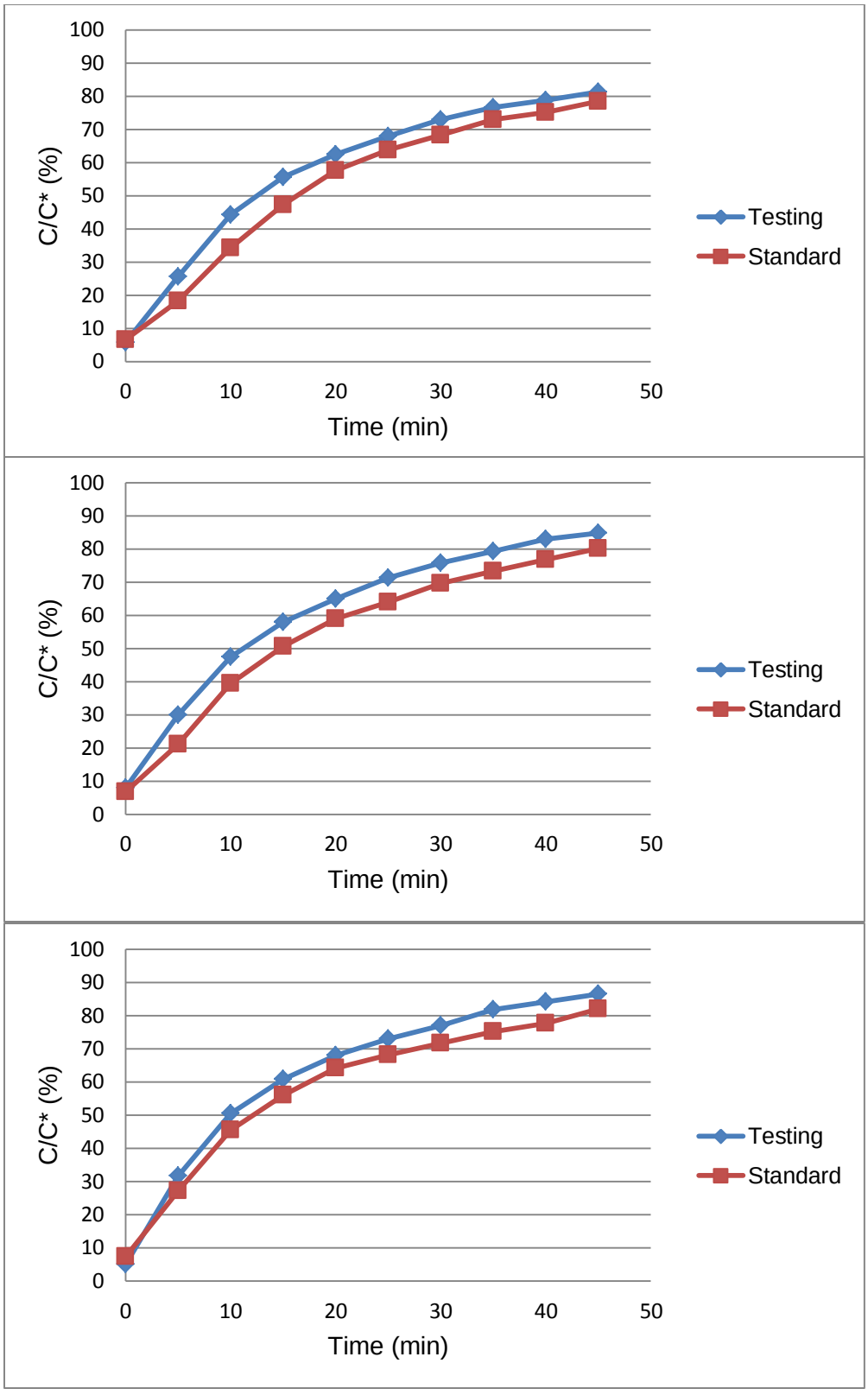

Figure B.4 Dissolution profiles for three runs with Position 4 tablets.

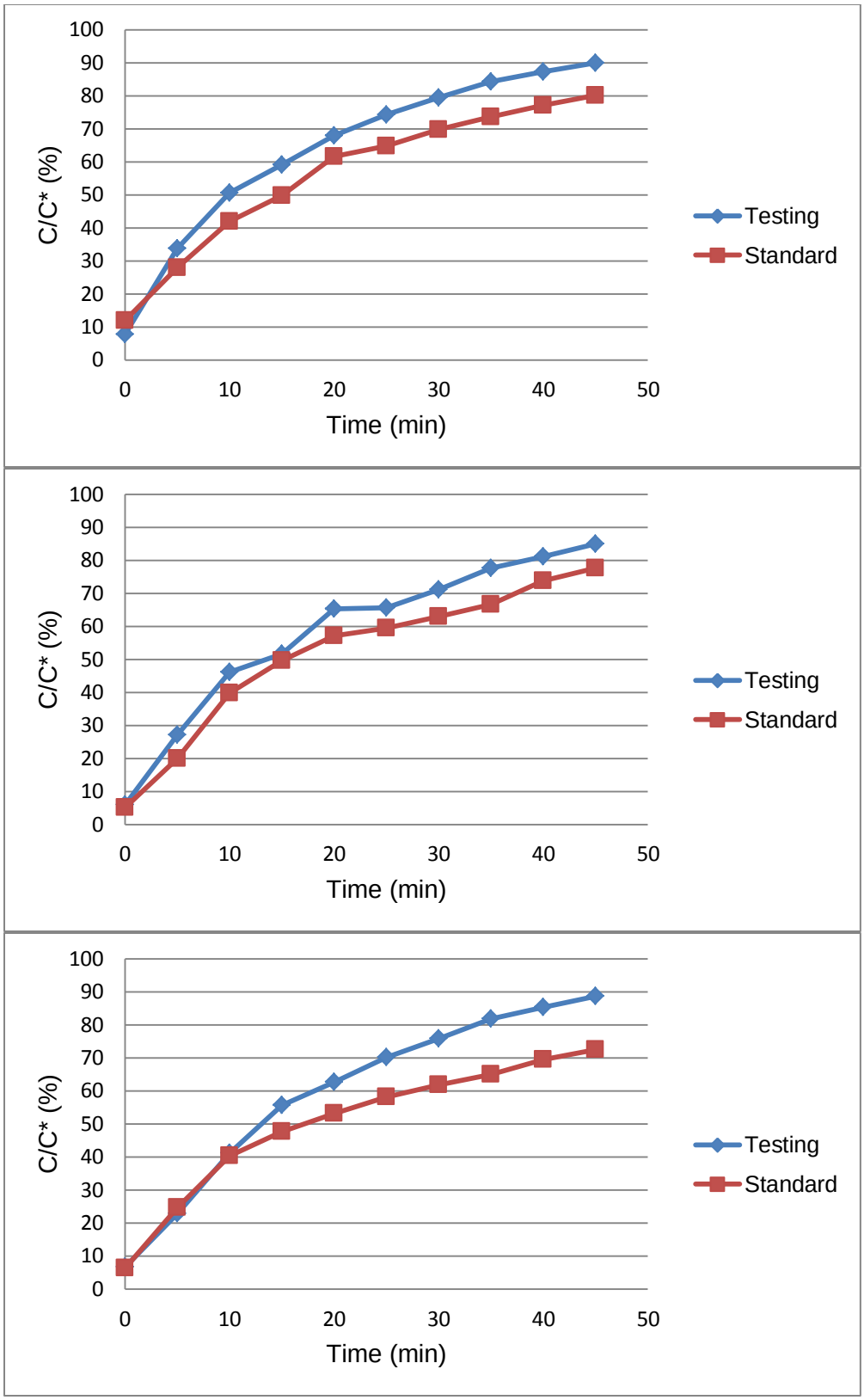

Figure B.5 Dissolution profiles for three runs with Position 5 tablets.

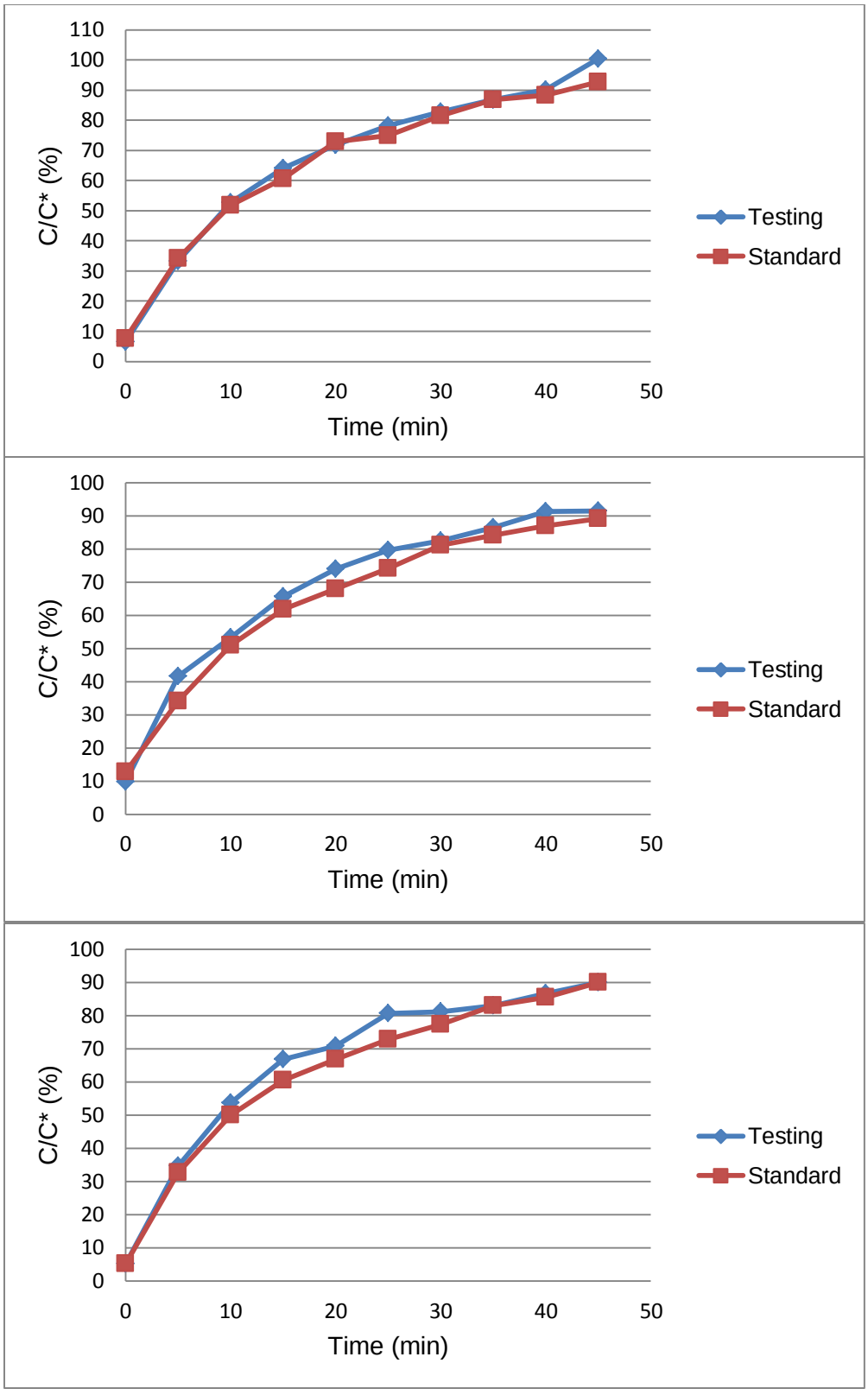

Figure B.6 Dissolution profiles for three runs with Position 6 tablets.

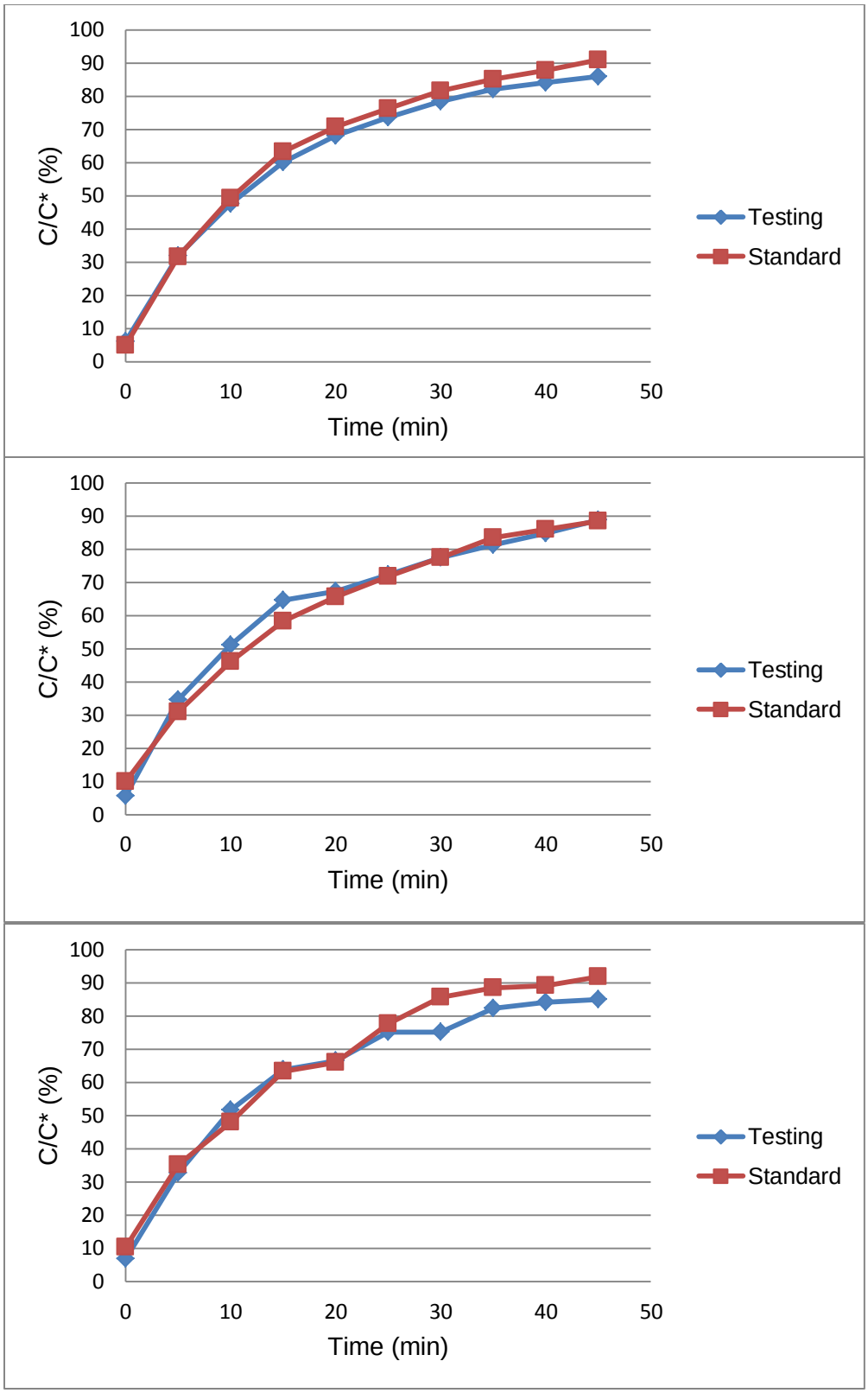

Figure B.7 Dissolution profiles for three runs with Position 7 tablets.

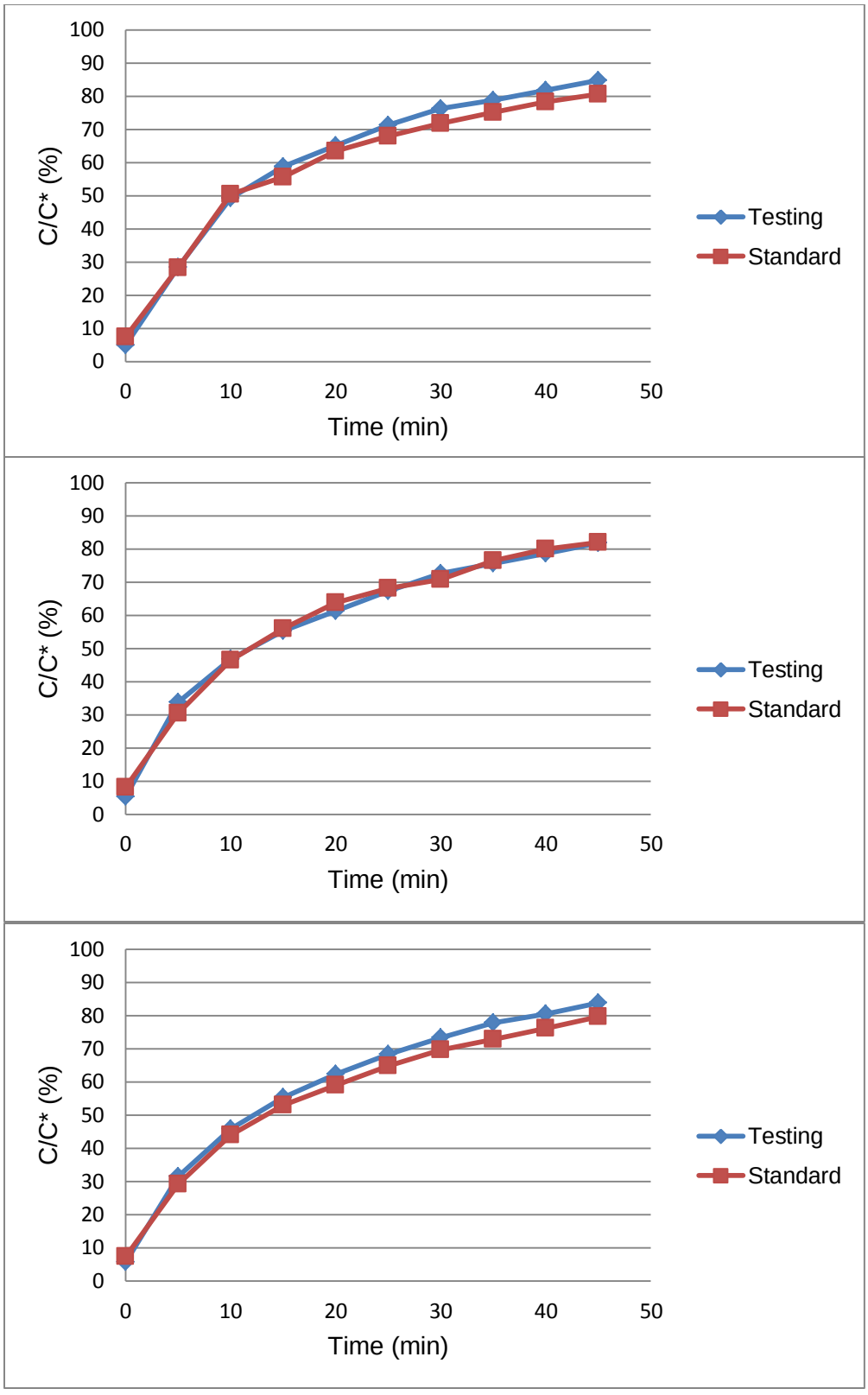

Figure B.8 Dissolution profiles for three runs with Position 8 tablets.

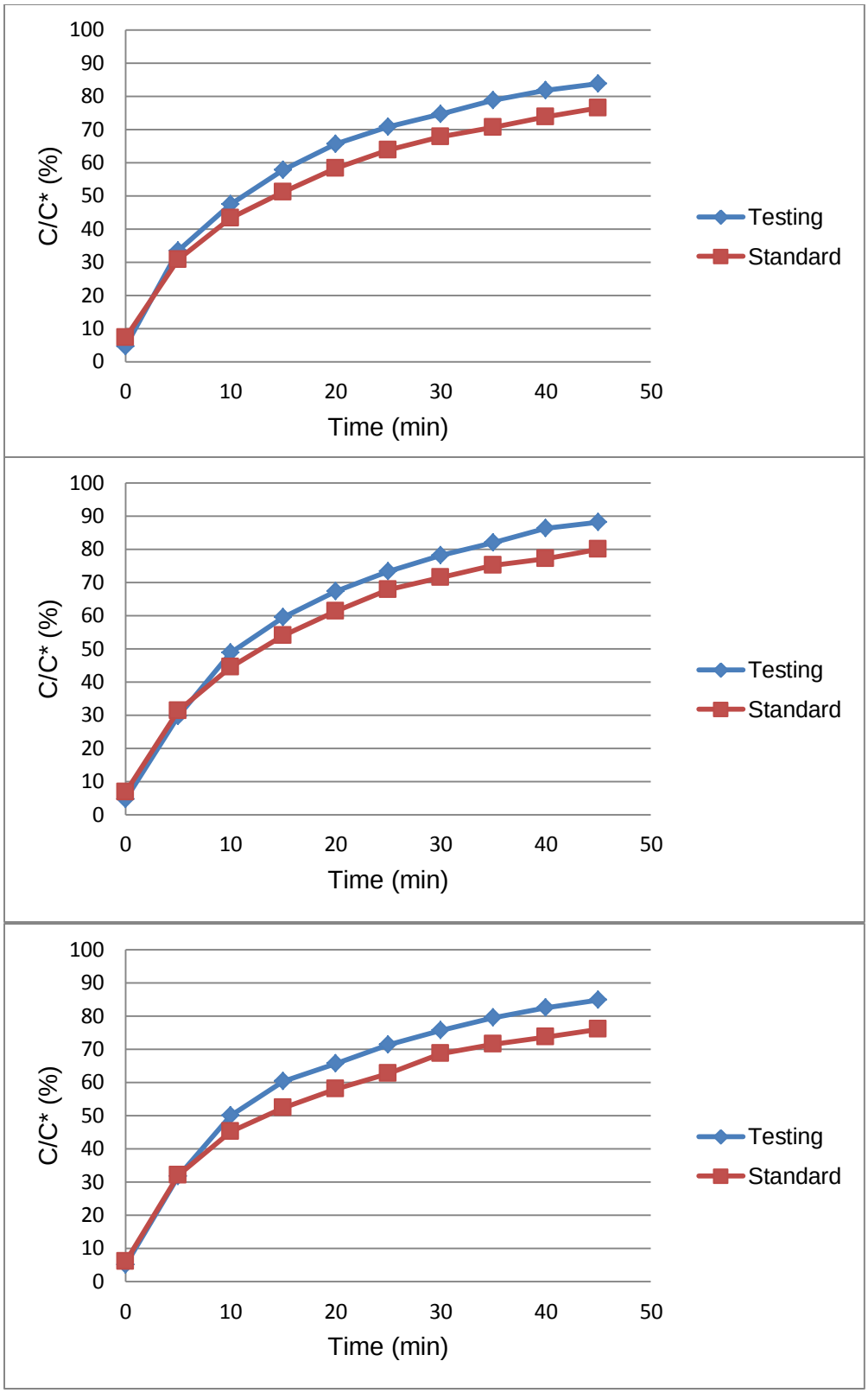

Figure B.9 Dissolution profiles for three runs with Position 9 tablets.

Table B.1 Statistical Values of Three Runs with Position 1 Tablets

	Paired T-test (T)	Similarity factor (f_1)	Difference factor (f_2)
Run1	0.009405	9.370	61.537
Run2	0.000149	14.921	54.870
Run3	0.004398	6.700	71.720
Average		9.727	62.758

Table B.2 Statistical Values of Three Runs with Position 2 Tablets

	Paired T-test (T)	Similarity factor (f_1)	Difference factor (f_2)
Run1	6.67E-06	13.038	54.723
Run2	0.007478	5.109	72.034
Run3	0.000660	13.775	51.404
Average		10.394	58.962

Table B.3 Statistical Values of Three Runs with Position 3 Tablets

	Paired T-test (T)	Similarity factor (f_1)	Difference factor (f_2)
Run1	0.02692	2.339	54.723
Run2	9.62E-05	10.568	72.034
Run3	0.004842	8.629	51.404
Average		5.283	71.049

Table B.4 Statistical Values of Three Runs with Position 4 Tablets

	Paired T-test (T)	Similarity factor (f_1)	Difference factor (f_2)
Run1	0.000672	9.586	60.949
Run2	5.90E-06	11.316	58.095
Run3	0.000348	8.079	63.942
Average		9.629	61.279

Table B.5 Statistical Values of Three Runs with Position 5 Tablets

	Paired T-test (T)	Similarity factor (f_1)	Difference factor (f_2)
Run1	2.71E-07	14.682	52.009
Run2	2.21E-05	12.565	56.245
Run3	0.00199	19.270	46.020
Average		15.213	51.739

Table B.6 Statistical Values of Three Runs with Position 6 Tablets

	Paired T-test (T)	Similarity factor (f_1)	Difference factor (f_2)
Run1	0.07903	3.162	74.030
Run2	0.000500	5.590	67.359
Run3	0.007182	4.665	68.815
Average		4.255	73.399

Table B.7 Statistical Values of Three Runs with Position 7 Tablets

	Paired T-test (T)	Similarity factor (f_1)	Difference factor (f_2)
Run1	0.000411	3.956	74.675
Run2	0.1397	3.412	74.399
Run3	0.05833	5.948	63.676
Average		3.342	76.518

Table B.8 Statistical Values of Three Runs with Position 8 Tablets

	Paired T-test (T)	Similarity factor (f_1)	Difference factor (f_2)
Run1	0.003846	4.452	74.115
Run2	0.8653	2.069	85.805
Run3	1.14E-05	5.624	71.563
Average		3.129	81.241

Table B.9 Statistical Values of Three Runs with Position 9 Tablets

	Paired T-test (T)	Similarity factor (f_1)	Difference factor (f_2)
Run1	4.98E-06	10.890	58.449
Run2	0.003039	9.589	59.729
Run3	0.000595	11.588	56.317
Average		10.417	58.273

APPENDIX C

TABLES OF DISSOLUTION TESTING RESULTS

Dissolution results of Prednisone in both the standard system and the testing system are presented in detail in this Appendix.

Table C.1 Dissolution Profile of Prednisone in Run 1 at Position 1

Time (min)	Standard System			Testing System		
	UV Absorbance	C (mg/mL)	m_D/m_T (%)	UV Absorbance	C (mg/mL)	m_D/m_T (%)
0	0.072	0.00058	2.896	0.123	0.00191	9.552
5	0.211	0.00421	20.673	0.238	0.00491	24.259
10	0.321	0.00708	34.446	0.315	0.00692	33.899
15	0.379	0.00859	41.542	0.409	0.00937	45.416
20	0.424	0.00977	46.917	0.453	0.01052	50.670
25	0.466	0.01086	51.811	0.491	0.01151	55.094
30	0.546	0.01295	60.948	0.540	0.01279	60.671
35	0.521	0.01230	58.066	0.600	0.01436	67.339
40	0.544	0.01290	60.519	0.607	0.01454	68.017
45	0.569	0.01355	63.115	0.635	0.01527	70.920

Table C.2 Dissolution Profile of Prednisone in Run 2 at Position 1

Time (min)	Standard System			Testing System		
	UV Absorbance	C (mg/mL)	m_D/m_T (%)	UV Absorbance	C (mg/mL)	m_D/m_T (%)
0	0.080	0.00079	3.94	0.079	0.00076	3.810
5	0.168	0.00308	15.194	0.186	0.00355	17.494
10	0.283	0.00609	29.597	0.315	0.00692	33.649
15	0.354	0.00794	38.290	0.391	0.00891	42.953
20	0.417	0.00958	45.825	0.468	0.01091	52.166
25	0.467	0.01089	51.656	0.524	0.01237	58.695
30	0.497	0.01167	55.046	0.565	0.01345	63.340
35	0.518	0.01222	57.336	0.618	0.01483	69.210
40	0.548	0.01300	60.549	0.625	0.01501	69.879
45	0.574	0.01368	63.242	0.638	0.01535	71.166

Table C.3 Dissolution Profile of Prednisone in Run 3 at Position 1

Time (min)	Standard System			Testing System		
	UV Absorbance	C (mg/mL)	m_D/m_T (%)	UV Absorbance	C (mg/mL)	m_D/m_T (%)
0	0.068	0.00047	2.374	0.084	0.00089	4.462
5	0.183	0.00348	17.081	0.166	0.00303	14.949
10	0.283	0.00609	29.603	0.290	0.00627	30.479
15	0.364	0.00820	39.523	0.391	0.00891	42.852
20	0.421	0.00969	46.337	0.454	0.01055	50.382
25	0.458	0.01065	50.640	0.494	0.01159	55.033
30	0.524	0.01238	58.167	0.548	0.01300	61.175
35	0.552	0.01311	61.235	0.580	0.01384	64.690
40	0.554	0.01316	61.369	0.582	0.01389	64.819
45	0.572	0.01363	63.206	0.604	0.0144644	67.08088

Table C.4 Dissolution Profile of Prednisone in Run 1 at Position 2

Time (min)	Standard System			Testing System		
	UV Absorbance	C (mg/mL)	m_D/m_T (%)	UV Absorbance	C (mg/mL)	m_D/m_T (%)
0	0.081	0.00081	4.071	0.076	0.00068	3.418
5	0.235	0.00483	23.766	0.254	0.00533	26.182
10	0.345	0.00771	37.538	0.403	0.00922	44.840
15	0.430	0.00992	47.946	0.488	0.01144	55.242
20	0.480	0.01123	53.915	0.557	0.01324	63.487
25	0.533	0.01261	60.096	0.598	0.01431	68.248
30	0.577	0.01376	65.089	0.643	0.01548	73.350
35	0.607	0.01454	68.382	0.683	0.01653	77.758
40	0.648	0.01561	72.790	0.708	0.01718	80.401
45	0.666	0.01608	74.611	0.718	0.01744	81.362

Table C.5 Dissolution Profile of Prednisone in Run 2 at Position 2

Time (min)	Standard System			Testing System		
	UV Absorbance	C (mg/mL)	m_D/m_T (%)	UV Absorbance	C (mg/mL)	m_D/m_T (%)
0	0.141	0.00238	11.901	0.082	0.00084	4.201
5	0.264	0.00559	27.631	0.251	0.00525	25.814
10	0.371	0.00838	41.030	0.379	0.00859	41.841
15	0.431	0.00995	48.372	0.462	0.01076	52.001
20	0.522	0.01232	59.270	0.524	0.01238	59.409
25	0.546	0.01295	62.042	0.584	0.01394	66.406
30	0.584	0.01394	66.351	0.615	0.01475	69.900
35	0.614	0.01473	69.651	0.643	0.01548	72.965
40	0.641	0.01543	72.531	0.667	0.01611	75.507
45	0.664	0.01603	74.900	0.700	0.01697	78.938

Table C.6 Dissolution Profile of Prednisone in Run 3 at Position 2

Time (min)	Standard System			Testing System		
	UV Absorbance	C (mg/mL)	m_D/m_T (%)	UV Absorbance	C (mg/mL)	m_D/m_T (%)
0	0.090	0.00105	5.245	0.106	0.00147	7.333
5	0.253	0.00530	26.091	0.295	0.00640	31.504
10	0.330	0.00731	35.729	0.409	0.00938	45.776
15	0.414	0.00951	46.017	0.555	0.01319	63.664
20	0.495	0.01162	55.711	0.578	0.01379	66.380
25	0.540	0.01279	60.949	0.607	0.01454	69.735
30	0.584	0.01394	65.941	0.639	0.01538	73.351
35	0.622	0.01493	70.131	0.666	0.01608	76.310
40	0.659	0.01590	74.096	0.687	0.01663	78.530
45	0.682	0.01650	76.449	0.712	0.01728	81.113

Table C.7 Dissolution Profile of Prednisone in Run 1 at Position 3

Time (min)	Standard System			Testing System		
	UV Absorbance	C (mg/mL)	m_D/m_T (%)	UV Absorbance	C (mg/mL)	m_D/m_T (%)
0	0.088	0.00100	4.984	0.112	0.00162	8.116
5	0.283	0.00609	29.923	0.268	0.00569	28.067
10	0.418	0.00961	46.825	0.408	0.00935	45.598
15	0.514	0.01212	58.577	0.485	0.01136	55.021
20	0.565	0.01345	64.660	0.545	0.01292	62.189
25	0.618	0.01483	70.833	0.628	0.01509	71.889
30	0.661	0.01595	75.705	0.649	0.01564	74.229
35	0.690	0.01671	78.878	0.686	0.01661	78.302
40	0.708	0.01718	80.758	0.707	0.01715	80.510
45	0.736	0.01791	83.652	0.726	0.01765	82.438

Table C.8 Dissolution Profile of Prednisone in Run 2 at Position 3

Time (min)	Standard System			Testing System		
	UV Absorbance	C (mg/mL)	m_D/m_T (%)	UV Absorbance	C (mg/mL)	m_D/m_T (%)
0	0.090	0.00105	5.245	0.087	0.00097	4.853
5	0.238	0.00491	24.173	0.310	0.00679	33.373
10	0.359	0.00807	39.324	0.429	0.00990	48.269
15	0.459	0.01068	51.570	0.528	0.01248	60.389
20	0.529	0.01251	59.938	0.589	0.01407	67.673
25	0.576	0.01373	65.406	0.648	0.01561	74.549
30	0.621	0.01491	70.5089	0.669	0.01616	76.890
35	0.676	0.01634	76.601	0.700	0.01697	80.291
40	0.684	0.01655	77.375	0.716	0.01739	81.954
45	0.716	0.01738	80.692	0.735	0.01789	83.887

Table C.9 Dissolution Profile of Prednisone in Run 3 at Position3

Time (min)	Standard System			Testing System		
	UV Absorbance	C (mg/mL)	m_D/m_T (%)	UV Absorbance	C (mg/mL)	m_D/m_T (%)
0	0.09	0.00105	5.245	0.084	0.00089	4.462
5	0.294	0.00637	31.334	0.279	0.00598	29.401
10	0.386	0.00877	42.849	0.409	0.00937	45.677
15	0.474	0.01107	53.624	0.539	0.01277	61.599
20	0.557	0.01324	63.554	0.554	0.01316	63.356
25	0.555	0.01319	63.267	0.607	0.01454	69.532
30	0.581	0.01386	66.199	0.64	0.01540	73.258
35	0.616	0.01478	70.065	0.674	0.01629	76.999
40	0.647	0.01559	73.387	0.69	0.01671	78.663
45	0.661	0.01595	74.794	0.716	0.01739	81.348

Table C.10 Dissolution Profile of Prednisone in Run 1 at Position 4

Time (min)	Standard System			Testing System		
	UV Absorbance	C (mg/mL)	m_D/m_T (%)	UV Absorbance	C (mg/mL)	m_D/m_T (%)
0	0.100	0.00131	6.550	0.094	0.00115	5.767
5	0.190	0.00366	18.060	0.246	0.00512	25.206
10	0.313	0.00687	33.465	0.389	0.00885	43.113
15	0.412	0.00945	45.592	0.476	0.01112	53.763
20	0.491	0.01151	55.043	0.528	0.01248	59.969
25	0.538	0.01274	60.512	0.570	0.01358	64.853
30	0.573	0.01365	64.468	0.609	0.01459	69.271
35	0.609	0.01459	68.432	0.637	0.01532	72.339
40	0.625	0.01501	70.095	0.653	0.01574	74.007
45	0.651	0.01569	72.778	0.673	0.01626	76.054

Table C.11 Dissolution Profile of Prednisone in Run 2 at Position 4

Time (min)	Standard System			Testing System		
	UV Absorbance	C (mg/mL)	m_D/m_T (%)	UV Absorbance	C (mg/mL)	m_D/m_T (%)
0	0.101	0.00134	6.681	0.111	0.00160	7.986
5	0.212	0.00423	20.876	0.279	0.00598	29.471
10	0.352	0.00789	38.41	0.413	0.00948	46.25
15	0.438	0.01013	48.939	0.494	0.01159	56.163
20	0.501	0.01178	56.468	0.548	0.01300	62.61
25	0.54	0.01279	61	0.596	0.01426	68.2
30	0.583	0.01392	65.879	0.63	0.01514	72.043
35	0.612	0.01467	69.06	0.658	0.01587	75.112
40	0.638	0.01535	71.824	0.686	0.01661	78.096
45	0.664	0.01603	74.507	0.699	0.01694	79.389

Table C.12 Dissolution Profile of Prednisone in Run 3 at Position 4

Time (min)	Standard System			Testing System		
	UV Absorbance	C (mg/mL)	m_D/m_T (%)	UV Absorbance	C (mg/mL)	m_D/m_T (%)
0	0.105	0.00144	7.203	0.088	0.00100	4.984
5	0.257	0.00541	26.642	0.292	0.00632	31.074
10	0.398	0.00909	44.298	0.436	0.01008	49.103
15	0.478	0.01118	54.089	0.515	0.01214	58.768
20	0.541	0.01282	61.617	0.570	0.01358	65.333
25	0.572	0.01363	65.208	0.609	0.01460	69.862
30	0.599	0.01433	68.250	0.639	0.01538	73.245
35	0.626	0.01504	71.212	0.676	0.01634	77.325
40	0.644	0.01551	73.106	0.695	0.01684	79.320
45	0.678	0.01640	76.655	0.712	0.01728	81.041

Table C.13 Dissolution Profile of Prednisone in Run 1 at Position 5

Time (min)	Standard System			Testing System		
	UV Absorbance	Concentration (mg/mL)	m_D/m_T (%)	UV Absorbance	Concentration (mg/mL)	m_D/m_T (%)
0	0.141	0.00238	11.901	0.109	0.00155	7.725
5	0.264	0.00559	27.631	0.309	0.00677	33.303
10	0.371	0.00838	41.030	0.438	0.01013	49.453
15	0.431	0.00995	48.372	0.503	0.01183	57.403
20	0.522	0.01232	59.270	0.570	0.01358	65.412
25	0.546	0.01295	62.042	0.619	0.01486	71.117
30	0.584	0.01394	66.351	0.659	0.01590	75.648
35	0.614	0.01473	69.651	0.696	0.01687	79.723
40	0.641	0.01543	72.531	0.719	0.01747	82.152
45	0.664	0.01603	74.900	0.739	0.01799	84.189

Table C.14 Dissolution Profile of Prednisone in Run 2 at Position 5

Time (min)	Standard System			Testing System		
	UV Absorbance	C (mg/mL)	m_D/m_T (%)	UV Absorbance	C (mg/mL)	m_D/m_T (%)
0	0.089	0.00102	5.115	0.095	0.00118	5.898
5	0.203	0.00400	19.694	0.257	0.00541	26.616
10	0.355	0.00797	38.731	0.403	0.00922	44.898
15	0.430	0.00992	47.909	0.445	0.01032	50.026
20	0.487	0.01141	54.718	0.550	0.01306	62.602
25	0.505	0.01188	56.786	0.552	0.01311	62.783
30	0.532	0.01259	59.834	0.595	0.01423	67.666
35	0.560	0.01332	62.915	0.645	0.01554	73.208
40	0.615	0.01475	68.870	0.672	0.01624	76.079
45	0.645	0.01554	71.983	0.701	0.01700	79.080

Table C.15 Dissolution Profile of Prednisone in Run 3 at Position 5

Time (min)	Standard System			Testing System		
	UV Absorbance	C (mg/mL)	m_D/m_T (%)	UV Absorbance	C (mg/mL)	m_D/m_T (%)
0	0.098	0.00126	6.289	0.100	0.00131	6.550
5	0.238	0.00491	24.194	0.224	0.00455	22.408
10	0.359	0.00807	39.345	0.365	0.00823	40.066
15	0.414	0.00951	46.072	0.476	0.01112	53.661
20	0.457	0.01063	51.205	0.530	0.01253	60.106
25	0.495	0.01162	55.630	0.587	0.01402	66.749
30	0.523	0.01235	58.796	0.630	0.01514	71.620
35	0.548	0.01300	61.543	0.676	0.01634	76.701
40	0.582	0.01389	65.200	0.703	0.01705	79.560
45	0.605	0.01449	67.577	0.729	0.01773	82.229

Table C.16 Dissolution Profile of Prednisone in Run 1 at Position 6

Time (min)	Standard System			Testing System		
	UV Absorbance	C (mg/mL)	m_D/m_T (%)	UV Absorbance	C (mg/mL)	m_D/m_T (%)
0	0.108	0.00152	7.594	0.100	0.00131	6.550
5	0.312	0.00684	33.684	0.305	0.00666	32.767
10	0.447	0.01037	50.586	0.454	0.01055	51.423
15	0.515	0.01214	58.902	0.541	0.01282	62.069
20	0.608	0.01457	70.032	0.600	0.01436	69.112
25	0.624	0.01499	71.855	0.649	0.01564	74.814
30	0.675	0.01632	77.650	0.684	0.01655	78.765
35	0.715	0.01736	82.060	0.715	0.01736	82.164
40	0.726	0.01765	83.171	0.741	0.01804	84.922
45	0.760	0.01854	86.708	0.819	0.02008	93.163

Table C.17 Dissolution Profile of Prednisone in Run 2 at Position 6

Time (min)	Standard System			Testing System		
	UV Absorbance	C (mg/mL)	m_D/m_T (%)	UV Absorbance	C (mg/mL)	m_D/m_T (%)
0	0.148	0.00256	12.814	0.125	0.00196	9.813
5	0.311	0.00682	33.660	0.368	0.00831	40.890
10	0.440	0.01018	49.813	0.458	0.01065	52.152
15	0.523	0.01235	59.972	0.552	0.01311	63.661
20	0.570	0.01358	65.579	0.617	0.01480	71.427
25	0.618	0.01483	71.171	0.660	0.01593	76.426
30	0.672	0.01624	77.313	0.682	0.01650	78.888
35	0.695	0.01684	79.816	0.712	0.01728	82.183
40	0.716	0.01739	82.031	0.749	0.01825	86.154
45	0.733	0.01783	83.752	0.750	0.01828	86.159

Table C.18 Dissolution Profile of Prednisone in Run 3 at Position 6

Time (min)	Standard System			Testing System		
	UV Absorbance	C (mg/mL)	m_D/m_T (%)	UV Absorbance	C (mg/mL)	m_D/m_T (%)
0	0.089	0.00102	5.115	0.089	0.00102	5.115
5	0.300	0.00653	32.099	0.315	0.00692	34.018
10	0.433	0.01000	48.751	0.461	0.01073	52.297
15	0.513	0.01209	58.539	0.561	0.01334	64.536
20	0.562	0.01337	64.384	0.592	0.01415	68.215
25	0.607	0.01454	69.620	0.667	0.01611	76.973
30	0.642	0.01546	73.577	0.672	0.01624	77.476
35	0.686	0.01661	78.441	0.686	0.01661	78.972
40	0.704	0.01707	80.323	0.714	0.01734	81.961
45	0.739	0.01799	83.967	0.739	0.01799	84.542

Table C.19 Dissolution Profile of Prednisone in Run 1 at Position 7

Time (min)	Standard System			Testing System		
	UV Absorbance	C (mg/mL)	m_D/m_T (%)	UV Absorbance	C (mg/mL)	m_D/m_T (%)
0	0.088	0.00100	4.984	0.096	0.00121	6.028
5	0.292	0.00632	31.074	0.294	0.00637	31.350
10	0.427	0.00985	47.976	0.414	0.00951	46.373
15	0.535	0.01266	61.199	0.510	0.01201	58.127
20	0.592	0.01415	68.000	0.572	0.01363	65.532
25	0.635	0.01527	72.995	0.614	0.01473	70.413
30	0.675	0.01632	77.522	0.651	0.01569	74.597
35	0.702	0.01702	80.470	0.679	0.01642	77.663
40	0.722	0.01754	82.570	0.695	0.01684	79.328
45	0.747	0.01820	85.142	0.096	0.01721	80.728

Table C.20 Dissolution Profile of Prednisone in Run 2 at Position 7

Time (min)	Standard System			Testing System		
	UV Absorbance	C (mg/mL)	m_D/m_T (%)	UV Absorbance	C (mg/mL)	m_D/m_T (%)
0	0.126	0.00199	9.943	0.093	0.00113	5.637
5	0.287	0.00619	30.533	0.315	0.00692	34.028
10	0.403	0.00922	45.057	0.441	0.01021	49.802
15	0.497	0.01167	56.568	0.545	0.01293	62.534
20	0.553	0.01313	63.255	0.565	0.01345	64.894
25	0.600	0.01436	68.727	0.604	0.01446	69.428
30	0.643	0.01548	73.604	0.643	0.01548	73.849
35	0.689	0.01668	78.690	0.673	0.01627	77.144
40	0.709	0.01721	80.788	0.699	0.01694	79.911
45	0.727	0.01768	82.610	0.093	0.01775	83.132

Table C.21 Dissolution Profile of Prednisone in Run 3 at Position 7

Time (min)	Standard System			Testing System		
	UV Absorbance	C (mg/mL)	m_D/m_T (%)	UV Absorbance	C (mg/mL)	m_D/m_T (%)
0	0.129	0.00207	10.335	0.102	0.00136	6.811
5	0.319	0.00703	34.634	0.299	0.00650	32.005
10	0.417	0.00958	46.901	0.445	0.01032	50.286
15	0.535	0.01266	61.356	0.539	0.01277	61.791
20	0.555	0.01319	63.718	0.559	0.01329	64.151
25	0.645	0.01554	74.244	0.625	0.01501	71.857
30	0.706	0.01713	81.181	0.626	0.01504	71.908
35	0.728	0.01770	83.561	0.680	0.01645	77.903
40	0.733	0.01783	84.010	0.695	0.01684	79.460
45	0.753	0.01835	86.047	0.102	0.01700	80.007

Table C.22 Dissolution Profile of Prednisone in Run 1 at Position 8

Time (min)	Standard System			Testing System		
	UV Absorbance	C (mg/mL)	m_D/m_T (%)	UV Absorbance	C (mg/mL)	m_D/m_T (%)
0	0.107	0.00149	7.464	0.087	0.00097	4.854
5	0.266	0.00564	27.798	0.268	0.00570	28.002
10	0.436	0.01008	49.087	0.427	0.00985	47.912
15	0.476	0.01112	53.968	0.500	0.01175	56.840
20	0.536	0.01269	61.138	0.549	0.01303	62.685
25	0.571	0.01360	65.203	0.596	0.01426	68.156
30	0.600	0.01436	68.477	0.634	0.01525	72.458
35	0.625	0.01501	71.216	0.654	0.01577	74.627
40	0.650	0.01567	73.880	0.677	0.01637	77.063
45	0.668	0.01614	75.717	0.700	0.01697	79.429

Table C.23 Dissolution Profile of Prednisone in Run 2 at Position 8

Time (min)	Standard System			Testing System		
	UV Absorbance	C (mg/mL)	m_D/m_T (%)	UV Absorbance	C (mg/mL)	m_D/m_T (%)
0	0.112	0.00162	8.116	0.090	0.00105	5.245
5	0.283	0.00609	29.985	0.309	0.00677	33.253
10	0.406	0.00930	45.386	0.408	0.00935	45.644
15	0.479	0.01120	54.319	0.473	0.01105	53.596
20	0.538	0.01274	61.368	0.520	0.01227	59.206
25	0.572	0.01363	65.315	0.566	0.01347	64.566
30	0.592	0.01415	67.555	0.606	0.01452	69.103
35	0.636	0.01530	72.429	0.629	0.01512	71.615
40	0.662	0.01598	75.198	0.652	0.01572	74.057
45	0.678	0.01640	76.816	0.676	0.01634	76.534

Table C.24 Dissolution Profile of Prednisone in Run 3 at Position 8

Time (min)	Standard System			Testing System		
	UV Absorbance	C (mg/mL)	m_D/m_T (%)	UV Absorbance	C (mg/mL)	m_D/m_T (%)
0	0.106	0.00147	7.333	0.093	0.00113	5.637
5	0.273	0.00583	28.691	0.291	0.00630	30.959
10	0.386	0.00878	42.839	0.400	0.00914	44.604
15	0.455	0.01058	51.282	0.473	0.01105	53.537
20	0.501	0.01178	56.773	0.527	0.01246	59.986
25	0.546	0.01295	62.016	0.573	0.01366	65.343
30	0.583	0.01392	66.210	0.612	0.01467	69.763
35	0.607	0.01454	68.836	0.646	0.01556	73.507
40	0.633	0.01522	71.609	0.666	0.01608	75.614
45	0.660	0.01593	74.408	0.692	0.01676	78.300

Table C.25 Dissolution Profile of Prednisone in Run 1 at Position 9

Time (min)	Standard System			Testing System		
	UV Absorbance	C (mg/mL)	m_D/m_T (%)	UV Absorbance	C (mg/mL)	m_D/m_T (%)
0	0.106	0.00147	7.333	0.085	0.00092	4.593
5	0.285	0.00614	30.225	0.306	0.00669	32.856
10	0.381	0.00864	42.243	0.413	0.00948	46.250
15	0.442	0.01024	49.706	0.493	0.01157	56.040
20	0.496	0.01165	56.160	0.553	0.01313	63.208
25	0.538	0.01274	61.051	0.592	0.01415	67.739
30	0.569	0.01355	64.558	0.622	0.01493	71.124
35	0.591	0.01413	66.963	0.653	0.01574	74.532
40	0.615	0.01475	69.521	0.676	0.01634	76.970
45	0.636	0.01530	71.684	0.692	0.01676	78.587

Table C.26 Dissolution Profile of Prednisone in Run 2 at Position 9

Time (min)	Standard System			Testing System		
	UV Absorbance	C (mg/mL)	m_D/m_T (%)	UV Absorbance	C (mg/mL)	m_D/m_T (%)
0	0.102	0.00136	6.811	0.085	0.00092	4.593
5	0.289	0.00624	30.726	0.277	0.00593	29.147
10	0.390	0.00888	43.370	0.423	0.00974	47.428
15	0.463	0.01078	52.304	0.505	0.01188	57.462
20	0.520	0.01227	59.115	0.565	0.01345	64.627
25	0.569	0.01355	64.826	0.611	0.01465	69.977
30	0.597	0.01428	67.983	0.649	0.01564	74.276
35	0.625	0.01501	71.056	0.678	0.01640	77.452
40	0.641	0.01543	72.730	0.711	0.01726	80.979
45	0.663	0.01600	74.996	0.725	0.01762	82.371

Table C.27 Dissolution Profile of Prednisone in Run 3 at Position 9

Time (min)	Standard System			Testing System		
	UV Absorbance	C (mg/mL)	m_D/m_T (%)	UV Absorbance	C (mg/mL)	m_D/m_T (%)
0	0.095	0.00118	5.898	0.088	0.00100	4.984
5	0.295	0.00640	31.476	0.292	0.00632	31.074
10	0.395	0.00901	43.993	0.433	0.01000	48.727
15	0.450	0.01045	50.719	0.512	0.01206	58.393
20	0.494	0.01159	55.971	0.553	0.01313	63.277
25	0.530	0.01253	60.160	0.596	0.01426	68.279
30	0.575	0.01371	65.277	0.629	0.01512	72.009
35	0.597	0.01428	67.681	0.659	0.01590	75.304
40	0.614	0.01473	69.470	0.681	0.01647	77.632
45	0.632	0.01520	71.313	0.700	0.01697	79.571

REFERENCES

Bai G, Armenante P.M., Plank R.V., Gentzler M., Ford, K., Harmon P., 2007. Hydrodynamic investigation of USP dissolution test apparatus II. J. Pharm. Sci. 96, 2327–2349.

Bai, G., Armenante, P.M., 2009. Hydrodynamic, mass transfer, and dissolution effects induced by tablet location during dissolution testing. J. Pharm. Sci. 98, 1511–1531.

Baxter, J.L., Kukura, J., Muzzio, F.J., 2005. Hydrodynamics-induced Variability in the USP Apparatus II Dissolution Test. Int. J. Pharm. 292, 17-28.

Cohen, J.L., Hubert, B.B., Leeson, L.J., Rhodes, C.T., Robinson, J.R., Roseman, T.J., Shelter, E., 1990. The Development of USP Dissolution and Drug Release Standards. Pharm. Res. 7, 983-987.

Costa, P., Lobo, J.M.S., 2001. Modeling and comparison of dissolution profiles. Eur. J. Pharm. Sci. 13(2), 123-133.

Dantec Dynamics Inc FlowMap, 2000. PIV Installation & User's guide.

Division of Drug Analysis, Food and Drug Administration, 1995. Dissolution Test Performance Standard #2.

Dunnett, C.W., Sobel, M., 1954. A Bivariate Generalization of Student's T-Distribution, with Tables for Certain Special Cases. Biometrika, 41, 153-169.

Gray,V., 2003. Dissolution Testing Using Fiber Optics—A Regulatory Perspective. Dissol. Technol. 10 (4), 33–36.

Inman, G.W., 2003. Quantitative Assessment of Probe and Spectrometer Performance for a Multi-Channel CCD-based Fiber Optic Dissolution Testing System. Dissol. Technol. 10 (4), 26–32.

Inman, G.W., Wethington, E. Baughman, K. Horton, M., 2001. System Optimization for in Situ Fiber-Optic Dissolution testing. Pharm. Technol. 10 (4), 92–100.

Josefson, M., Johansson, E., Torstensson, A., 1988. Optical fiber spectrometry in turbid solutions by multivariate calibration applied to tablet dissolution testing. Anal. Chem. 60, 2666-2671.

Martin, C.A., 2003. Evaluating the utility of fiber optic analysis for dissolution testing of drug products. Dissol. Technol. 10, 37–40.

Mirza, T., Liu, Q., Vivilecchia, R., Joshi, Y., 2009. Comprehensive Validation Scheme for In Situ Fiber Optics Dissolution Method for Pharmaceutical Drug Product Testing. J. Pharm. Sci. 98 (3), 1086-1094.

Moore, T.W., 1996. Dissolution Testing: A Fast, Efficient Procedure for Degassing Dissolution Medium. Dissol. Technol. 3, 3-5.

Liu, L., Fitzgerald, G., Embry, M., Cantu, R., Pack, B., 2008. Technical Evaluation of a Fiber-Optic Probe Dissolution System. Dissol. Technol. 15(1), 10-20.

Lu. X., Lozano, R., Shah, P., 2003. In-Situ Dissolution Testing Using Different UV Fiber Optic Probes and Instruments. Dissol. Technol. 10, 6-15.

Schatz, C., Ulmschneider, M., Altermatt, R., Marrer, S., 2000. Reader's response: Hollow Shaft Sampling with Fiber Optics. Dissol. Technol. 7(2), 6-13.

United States Pharmacopeia, 2007.USP Prednisone Tablets RS, Lot P0E203 Certificate.

United States Pharmacopeia, 2008. General Chapter <711> Dissolution. USP 31- NF 26.